Development of a Controlled Rectifier for Variable Power Factor using Pulse Width Modulation

Author:

Ratul Das

Student No.: F1015062243

A thesis submitted in partial fulfillment of the requirements for the degree of

Master of Science in Electrical and Electronic Engineering

Department of Electrical and Electronic Engineering

Bangladesh University of Engineering and Technology

July, 2017

CERTIFICATION

The thesis titled "**DEVELOPMENT OF A CONTROLLED RECTIFIER FOR VARIABLE POWER FACTOR USING PULSE WIDTH MODULATION**" submitted by Ratul Das, Student No. F1015062243, session October, 2015, has been accepted as satisfactory in partial fulfillment of the required degree of MASTER OF SCIENCE IN ELECTRICAL AND ELECTRONIC ENGINEERING on July 05, 2017.

Board of Examiners

1. Harun Rashid
Dr. A. B. M. Harun-ur Rashid
Professor — Chairman(Supervisor)
Department of EEE, BUET, Dhaka.

2. ______________________
Dr. Quazi Deen Mohd Khosru
Professor and Head — Member(Ex-officio)
Department of EEE, BUET, Dhaka.

3. ______________________
Dr. Mohammad Jahangir Alam
Professor — Member
Department of EEE, BUET, Dhaka.

4. ______________________
Dr. Tapan Kumar Chakraborty
Professor and Director, IEERD — Member(External)
Department of EEE, University of Asia Pacific,
74/A Green Road,
Dhaka 1215, Bangladesh.

Declaration of Authorship

I, Ratul Das, declare that this thesis titled, "Development of a Controlled Rectifier for Variable Power Factor Operation using Pulse Width Modulation" and the work presented in it are my own. I confirm that:

- This work was done wholly or mainly while in candidature for a research degree at this University.
- Where any part of this thesis has previously been submitted for a degree or any other qualification at this University or any other institution, this has been clearly stated.
- Where I have consulted the published work of others, this is always clearly attributed.
- Where I have quoted from the work of others, the source is always given. With the exception of such quotations, this thesis is entirely my own work.
- I have acknowledged all main sources of help.
- Where the thesis is based on work done by myself jointly with others, I have made clear exactly what was done by others and what I have contributed myself.

Signed: রাতুল দাস

Date: 05/07/2017

"Anyone who has never made a mistake has never tried anything new. The important thing is not to stop questioning. Curiosity has its own reason for existing. "

Albert Einstein (1879-1955)

"Why do we fall? So that we can learn to pick ourselves up. "

Batman Begins The Movie (2005)

Abstract

Generally uncontrolled rectifier is made of diodes and controlled rectifiers are made of thyristors. Both these types of rectifiers distorts the input current in a way that the shapes of the current are nonsinusoidal. These distortion of the current increases the harmonic terms. In other words, there remains total harmonic distortion or THD in the current. These THD not only degrades the power factor but also degrades the power quality of the grid. In recent years, these THD have become significant because of the increase of use of rectifier based electrical and electronic devices. To eliminate the THD, Space Vector Pulse Width Modulated(SVPWM) rectifier has been proposed over conventional rectifiers. But the pulse generation is very complex for this kind of rectifier. This thesis analyzes the SVPWM rectifier and proposes a new hybrid scheme to generate real time PWM patterns. Because of the new scheme the rectifier will be a fully functional device which will draw sinusoidal input current in phase with input voltage. By modifying the timing of the pulses, the pulses can be lagged or lead from the original time. By thus, the device is also capable of drawing leading or lagging current. This capability gives the devices functionality as a reactive power compensator at some extents. The goal of this thesis is to develop a prototype of the rectifier. At first, simulation will be done in MATLAB Simulink. After that microcontroller and Look Up Table(LUT) based hybrid circuit to generate real time PWM patterns will be interfaced with proper switches to conduct the work.

Acknowledgements

At first, I would like to thank my supervisor Dr. Harun-ur Rashid for the continuous support for my M.Sc. study and thesis work. His enthusiasm, immense knowledge and motivation have influenced me in every aspect of my research. He also managed the required facilities to conduct the hardware work. Without his help and inspiration it was impossible to complete the work in time.

I would also like to thank Engineer Rabiul Alam, CEO, Energypac Engineering Ltd., Tejgaon, Dhaka to allow me to use his industry resources. My several visit to his factory have improved my knowledge about Industrial Electronics and Drives.

I am very much grateful to my undergraduate thesis supervisor Dr. Kazi Mujibur Rahman for guidelines for research. It was him who taught me the very basics of practical works. His wise comments have also guided me in the present work.

I would also like to thank Dr. Anwarul Abedin and Mr. Gobinda Saha, senior researchers in my group whose supports and suggestions have guided me throughout this work.

My thanks also goes to Mr. Afzal Hossain and Mr. Shariful Islam whose cumulative little helps are beyond measurement.

And at last, I would like to thank my classmate and wife Baishakhi Biswas who has always encouraged me no matter how deep in trouble I was. Her feedback and comments were also very important to conduct this work. …

Contents

List of Figures

List of Tables

Chapter 1

Introduction

1.1 Background

Power electronic converters are very common in almost all electronic and electrical devices. This converters are mainly of three types: DC-AC converters or inverters, AC-DC converters or rectifiers and AC-AC converters. Almost all electronic and a major portion of electrical devices run by DC. These devices operate in all ranges of voltages from micro-levels to kilo-levels. Depending on the applications, rectifiers have uses in Aerospace Applications [1], Industry Applications [2], Battery Charging Applications [3] etc. So, rectifiers are of special interests of researches so that the technology can be more sophisticated to meet the power, current and other important constraints of the devices. Moreover, with the invention of modern switching devices, high voltage DC transmission is also possible and it is advantageous in some cases [4, 5].

But, rectifiers are non-linear devices which generate harmonic voltages and currents. The non-linear operation causes highly distorted input currents. The harmonics generated not only disturbs other electrical devices throughout the power distribution system, but also, degrades the power factor of the rectifier which by turns, derives reactive power from generators of the system and forces to increase Volt-Ampere rating of the generators, transformers and distribution system line. Recently, with emergence of battery powered electric vehicle, the use of rectifiers have been heavily increased throughout the world and also in Bangladesh. These Battery charging rectifiers are degrading the power quality due to the non-linearity[6].

The Space Vector Pulse Width Modulated Rectifier presented in this thesis can draw sinusoidal input current with input power factor. By thus it ensures safety of other devices connected to the system and minimum Volt-Ampere ratings of components of the system. Moreover, it has flexibility to have a leading or lagging power factor which gives it the ability to compensate reactive power of the system in some extents. In other words, presented rectifier in this thesis has the ability to act as resistive, capacitive and inductive load according to instructions and so, it is a ideal load which can also improve the condition of the power distribution system.

1.2 Literature Review

Inductors followed by uncontrolled rectifier and a capacitor in parallel to the load already shows a power factor greater than 0.9 with THD around 30% [7, 8]. Power Factor Correction (PFC) rectifiers only targets a slight improvement of PF(>0.99)[9]. The requirements of an ideal Active PFC Rectifiers are sinusoidal input current with THD<5%, linear load behaviour, fault tolerance, unidirectional power flow and reduced EMI emission [9]. With the progress of Semiconductor Device Physics, new types of switches are being invented which can operate in different quadrants [10] and thus new topologies are being proposed to convert AC to DC voltage [9, 11] which cover the mentioned characteristics.

Replacing the diode switches of uncontrolled rectifier with switches of first and second quadrants, active six switch Buck type rectifier has been proposed [12]. But, the switching frequency of such switches are relatively low(less than 10 KHz)[13]. Basically a rectifier is a inverter seen from the input side. Based on that view, all the proposed PWM techniques for inverters[14, 15, 16, 17, 18, 19, 20, 21] can be used to control the Buck type rectifier [22].
Real time PWM pattern generation for converters (inverters and rectifiers) is a big challenge. Few literatures have discussed the pulse generation techniques in details for academic purpose. Generally the PWM pulses are generated by DSP processor or FPGA which have the capability of high computing[23, 24].
Muhammad Quamruzzaman and Kazi Mujibur Rahman presented a new hybrid scheme to generate real time pulses to be implemented with Voltage Source Inverters[25]. This hybrid scheme generated Sine Pulse Width Modulated(SPWM) pulses with the help of a microprocessor and external memory. The microprocessor used a real time pulse generation algorithm. This type of scheme has not been found in literature for the case of rectifiers.
A variable PF rectifier has been proposed based on Space Vector PWM which is able to pull lagging, leading or synchronized current from three phase power system [26]. A DSP processor with minimum flexibility controls the total system. Based on the programming the system can operate at a particular power factor and output voltage at a particular operation. The main advantage of this system is control by full software operation.This kind of system can be used as reactive power compensator for the grid [27] also.
In this work, the proposed software controlled SVPWM rectifier[26] has been implemented in the hybrid scheme[25] described for inverters. The Phase Locked Loop for synchronization has been made by following and customizing this work [28].

1.3 Objective and Expected Result of the thesis

The goals of this research is to investigate feasibility of a rectifier to compensate VAR as well supplying real power to the load. In this purpose a simple and cost effective micro-controller based circuit will be built to implement space vector pulse width modulation. The circuit will have the capability to regulate the output voltage. Sinusoidal current from the input will be ensured by the SVPWM. By making the current leading or lagging from the input voltage, the power factor will be varied. The possible outcomes of this research are as follows:

- A hardware prototype of rectifier with unity PF and flexibility of VAR compensation.
- A circuit to generate SVPWM pulses in synchronization with the power system.
- Gate driving circuits for the switches of the rectifier.

At first, simulation will be conveyed to develop the theoretical model and verify it. After that, Hardware circuits will be built to be matched with the simulation results.

1.4 Thesis Outline

This work has been described in the next four chapters. Chapter two includes the basics of PWM rectifier and theoretical analysis for SVPWM rectifier. Using the expressions and equations of chapter two a Simulink model have been simulated in chapter 3. Based on the findings of chapter two and three, a hardware version of the rectifier has been built and the details have been included in chapter 4. Chapter 5 summarizes this dissertation and states possible future developments in this research.

Chapter 2

Space Vector Pulse Width Modulated Rectifier

2.1 Concept of PWM Rectifier

The circuit operation of a six switch PWM rectifier is very complex. Before going into deep of the control scheme, it is required to understand the complex behavior of such a circuit. In this purpose, the operation of a six switch rectifier is explained by comparing with a Buck DC-DC converter. At the first of the chapter, the simple operation of Buck converter is presented. Based on the concept and with the help of uncontrolled rectifier, the PWM rectifier is explained.

2.1.1 Overview of a Buck DC-DC Converter

Buck converter can be called as the very basic circuit of Power Electronics. Its work is to convert a DC voltage level to another level which is lower. A typical Buck converter(Figure 2.1) consists of a SPDT switch and L-C filter. The SPDT switch can be replaced with two SPST switches. In real circuits, Two SPST switches are generally used. For, asynchronus operation, one transistor/MOSFET and one diode are used to realize the SPST switches whether two transistor/MOSFETs are required for synchronus operation [10].
When SPDT switch in Figure 2.1 is in position 1, the inductor is connected with the input voltage source, V_{in} and when the switch is in position 2, the inductor is connected with ground. In a certain period of time switching between position 1 and both occurred and this operation is repeated continuously. So, the voltage waveshape at the inductor's end or V_x is a pulse train. If the switch continues to stay at position 1 and 2 same time for every repeating period, the average of the pulse train is always constant. The voltage at V_x is filtered with the L-C filter and the output voltage is obtained as the average voltage of V_x. The voltage shapes of V_{in}, V_{out} and V_x are shown in Figure 2.2.

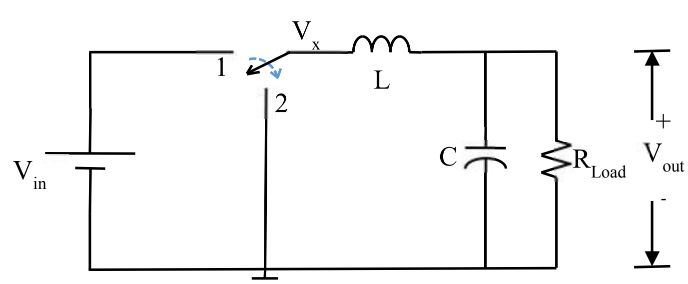

FIGURE 2.1: A typical Buck Converter

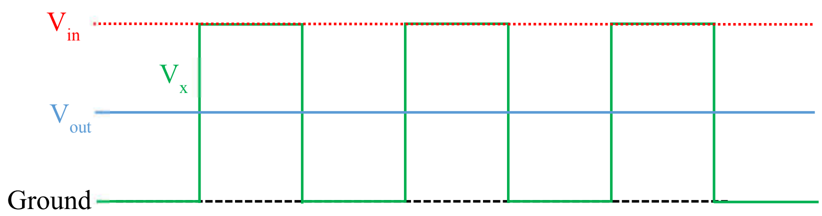

FIGURE 2.2: Wave shape of input voltage, output voltage and node voltage of a Buck converter

To understand the operation the operation of PWM rectifier, the current direction in Buck converter in the switching positions are needed to be clearly understood. As an inductor opposes the change of current, current flowing through it is almost constant. This constant current comes from the input voltage source when the switch is in position 1 and stores energy in the inductor, this energy forces the current to be continuous and flowing through the inductor when the switch is in position 2(Figure 2.3 and 2.4). Switching position 2 is called free whiling operation of Buck converter.
It is apparent from the above discussion that Buck converter's output voltage is the average voltage of the node prior to the filter and output current is supplied from the input source as well as from the free whiling operation of inductor.

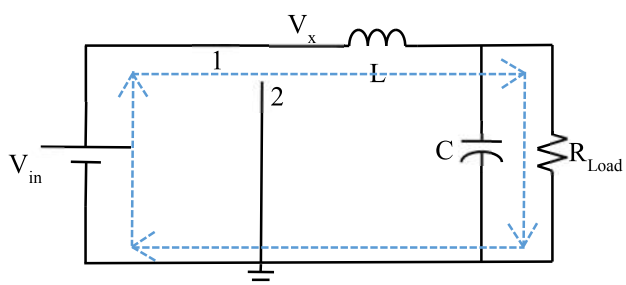

FIGURE 2.3: Current direction through inductor at switch position 1

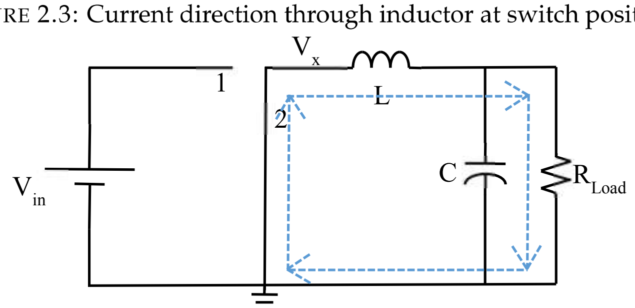

FIGURE 2.4: Current direction through inductor at switch position 2

2.1.2 Three Phase Uncontrolled rectifier

Three phases of the power supply system are sine waves of voltages and they are shifted sequentially by 120°. For full wave rectification they are connected with six diodes (Figure 2.5). At a particular time, the output voltage V_{out} stems from two different phases which have the highest positive voltage difference. The resultant wave shape of V_out is shown with different phase to phase voltage for a particular period in Figure 2.6. But the phase current shape is not sinusoidal like the phase voltage. This results in a THD greater than the specified range and thus worsening the PF(Figure 2.7).

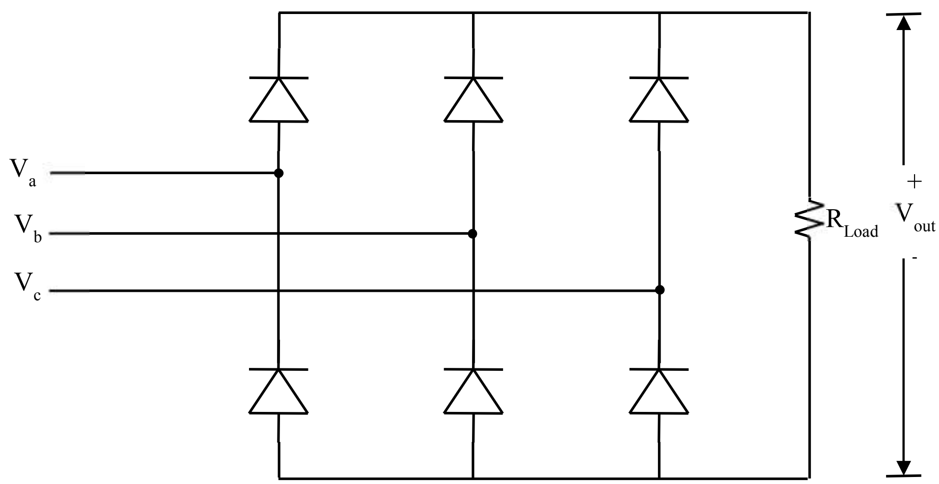

FIGURE 2.5: Diode Rectifier

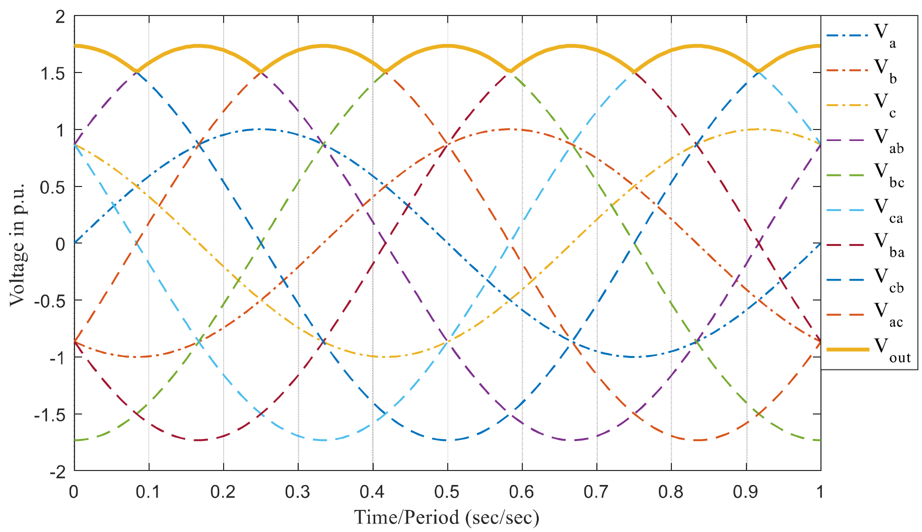

FIGURE 2.6: Wave shapes of Uncontrolled Rectifier

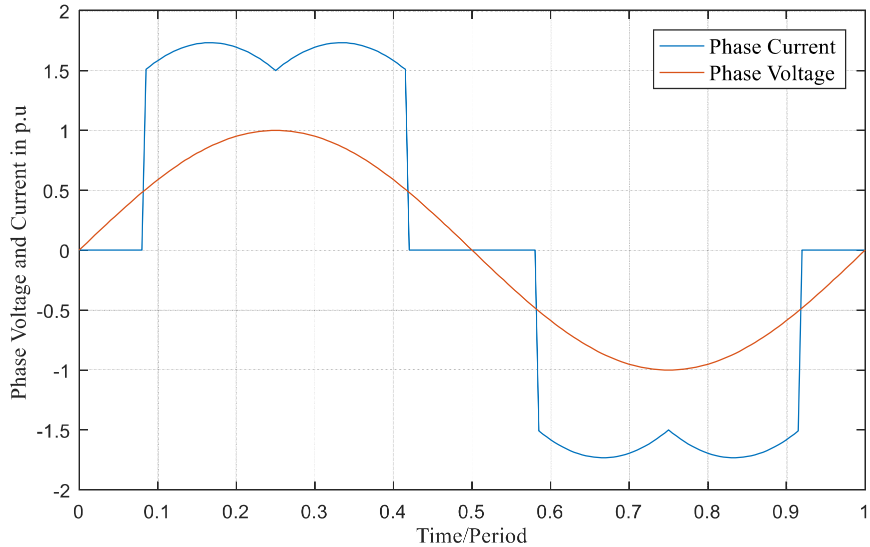

FIGURE 2.7: Wave shapes of Phase Voltage and Phase Current

2.1.3 Three phase PWM rectifier

The output of an uncontrolled rectifier can be connected with a Buck converter to control the output by Pulse Width Modulation(Figure 2.8). But, this will not ensure a sinusoidal wave shape of the input phase current (Figure 2.9).
To make the phase current sinusoidal or directly proportional to the phase voltages, the switching should be done according to the magnitude of the phase voltages. Observation of the phase voltages (Figure 2.10) reveals that

$$V_a + V_b + V_c = 0 \tag{2.1}$$

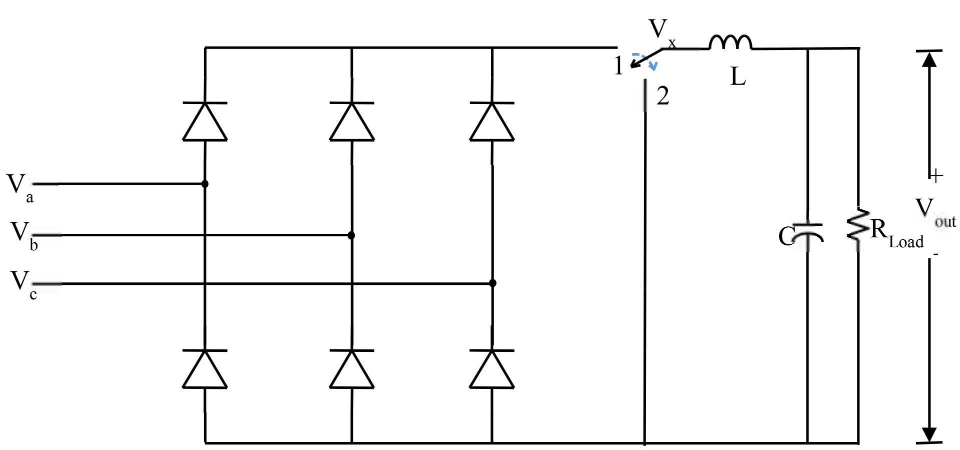

FIGURE 2.8: Uncontrolled rectifier followed by a Buck Converter

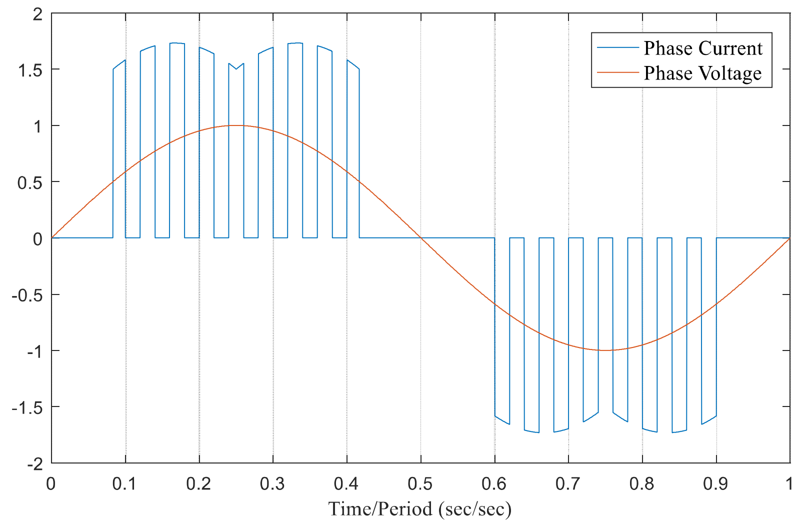

FIGURE 2.9: Phase Voltage and Phase Current of an Uncontrolled rectifier followed by a Buck Converter

If at a particular time, one of the phase voltages is positive and the other two phase are negative, then current should come from the positive phase and enter into the negative two phases. And if two of the phase voltages are positive and other one is negative then load current will come from the positive phases and go back to the negative phase.
The diode switches of uncontrolled rectifier should be replaced with controllable switches in this purpose. To a get a DC voltage, a filter should be added after the three legs of the switches. The total structure is shown in Figure 2.11. The switches are numbered according to conventional way.
If at a particular time, current should come from phase a and go back to phase b and c. Then, switch 1, switch 6 and switch 2 should be controlled carefully so that the system can be forced to follow the said operation. Here is a point to be noted that, due to the inductor effect of the load side, the load current will be nearly constant. And this system will always take constant current from the total three phase system when connected. So, sinusoidal current output is not actually possible from this structure. Rather, a constant magnitude of current which has a average sinusoidal magnitude is possible by this structure. The trick is switches should be kept closed according to their relevant phase magnitude. However, in discussing example, switch 6 and 2 should never be closed together. Rather keeping the switch 1 closed, switch 6 and 2 should be closed according to their phase magnitude. And thus the load will take a average sinusoidal phase current from the system. So, in a particular period, switch position 4 should be kept close when switch 1 is closed and switch 6 and 2 is open. Vx will be the average of two line voltage V_{ab} and V_{ac}. From the concept of Buck converter, it is evident that the system will need a free whiling operation. This operation system is valid for all other phase orientation with valid switch operations. This example is illustrated in Figure 2.12, 2.13 and 2.14.

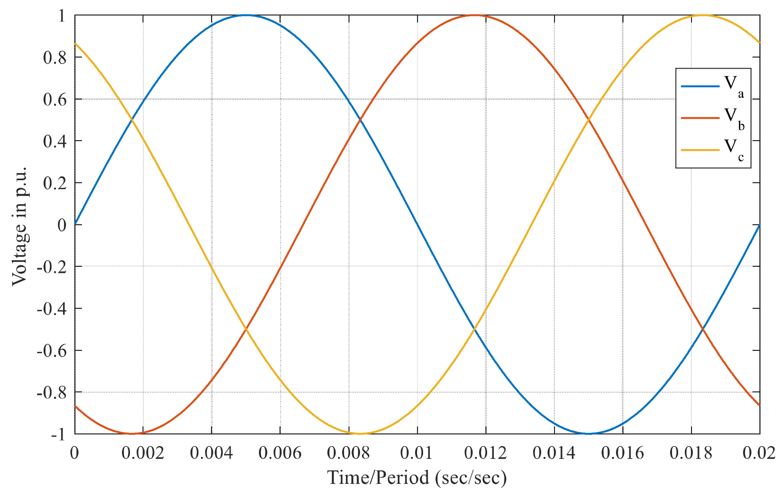

FIGURE 2.10: Phase Voltage of a Three Phase System

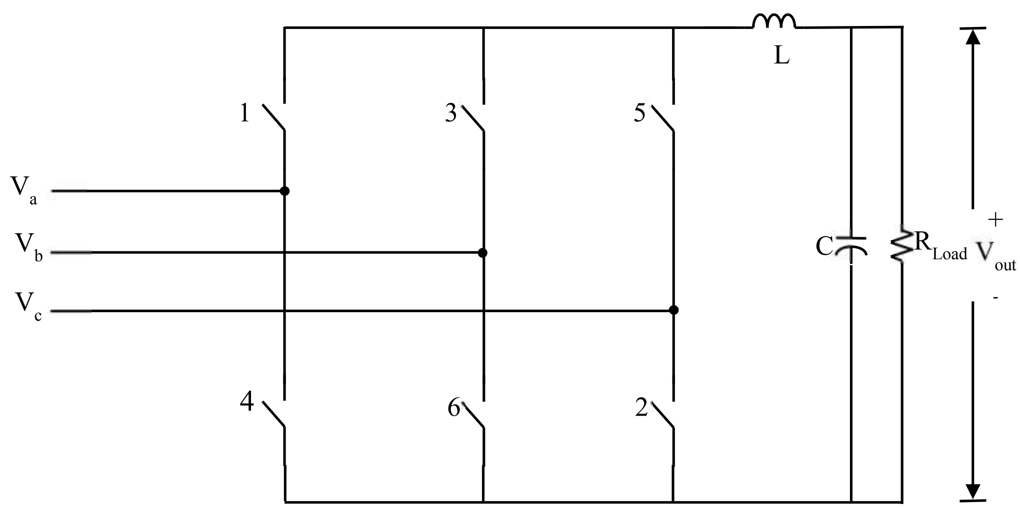

FIGURE 2.11: Structure of a Three Phase PWM rectifier

In summary, when a upper switch is fully on, all the lower switches should be turned on sequentially and according to the magnitude and vice versa. The current shape resultant to this kind of PWM system varies according to the modulation technique. The resultant current wave shape of SVPWM rectifier will be shown later in this thesis.
However, the resultant constant magnitude average sinusoidal current can be filtered (Figure 2.15) and turned into total sinusoidal wave shape although current filtering is very difficult.

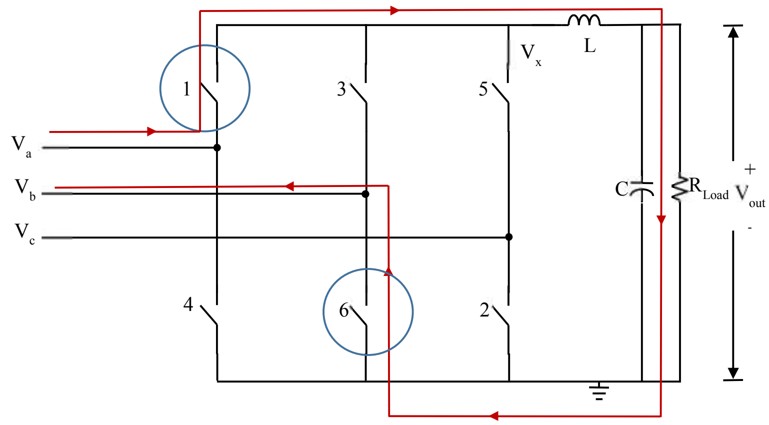

FIGURE 2.12: Current is allowed to go from phase a to phase b by closing switch 1 and 6(Condition: $V_{ab} > 0$ and $V_{ac} < 0$)

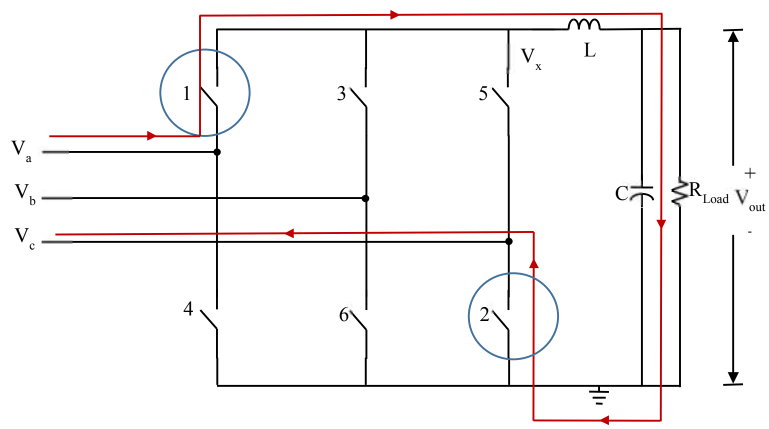

FIGURE 2.13: Current is allowed to go from phase b to phase c by closing switch 1 and 2

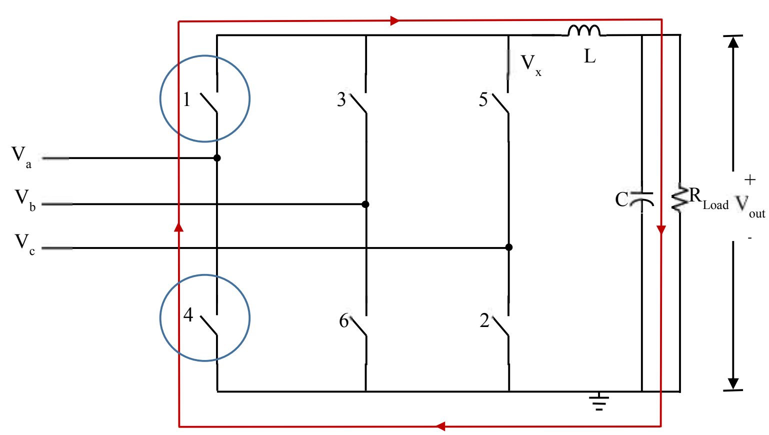

FIGURE 2.14: Current is allowed to wheel freely by closing switch 1 and 4

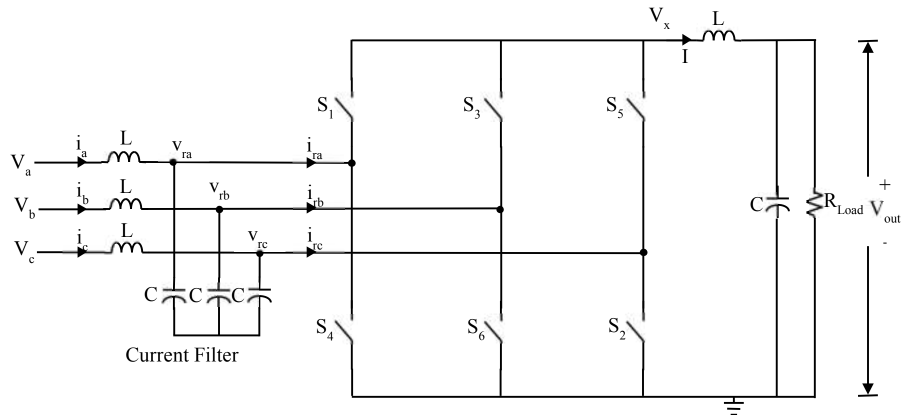

FIGURE 2.15: Total PWM Rectifier Structure with Current Filter

2.2 Space Vector PWM Rectifier

This section contains theoretical and mathematical analysis of a Space Vector PWM Rectifier in order to calculate the switching functions. The analysis has been done with the help of the work of Kwon et al[26].

2.2.1 Space Vector of three phases

Three phase voltages of power system are shifted by 120°. It is very difficult to keep track of all the voltages and change switching conditions according to them. So, the voltages are converted to Space Vector domain.

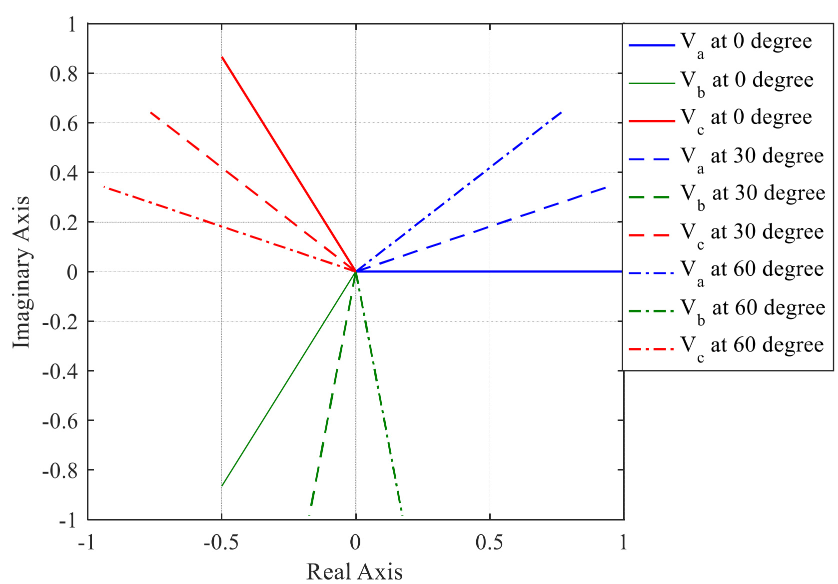

FIGURE 2.16: Change of Three Phase Voltages

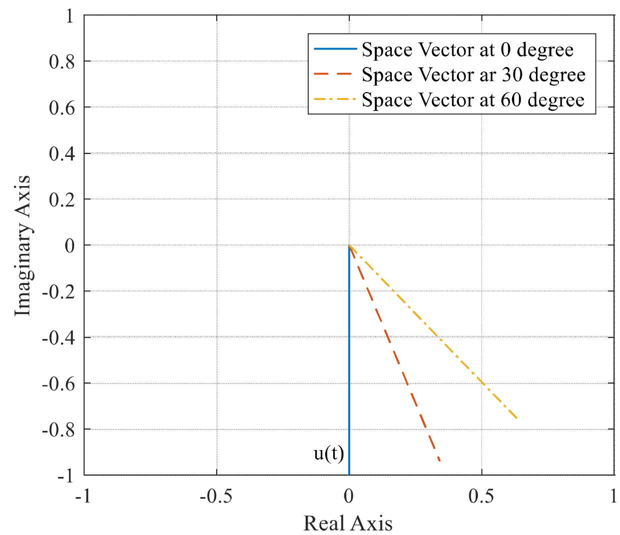

FIGURE 2.17: Change of Space Vector of Voltages

Any three functions of time that satisfy

$$V_a(t) + V_b(t) + V_c(t) = 0 \tag{2.2}$$

can be represented in a two-dimensional space where coordinates are chosen so that the vector $[V_a\ 0\ 0]^T$ is placed along the horizontal axis, the vector $[0\ V_b\ 0]^T$ is by $120°$ and the vector $[0\ 0\ V_c]^T$ is by additional $120°$. Then the space vector is given by,

$$u(t) = \frac{2}{3}(V_a + V_b e^{\frac{2}{3}j\pi} + V_c e^{-\frac{2}{3}j\pi}) \tag{2.3}$$

where,

$$u(t) = u_x + ju_y \tag{2.4}$$

and $\frac{2}{3}$ is a scaling factor.
In simple, space vector representation of phase voltages at a particular is a complex number in Argand plane. As the phase voltages are changing over time, the complex number also changes. The change of the phase voltages and the resultant space vector is shown in Figure 2.16 and 2.17.
The conversion formula from phase voltages to space vector is

$$\begin{bmatrix} u_x \\ u_y \end{bmatrix} = \frac{2}{3}\begin{bmatrix} 1 & \frac{-1}{2} & \frac{-1}{2} \\ 0 & \sqrt{3}/2 & -\sqrt{3}/2 \end{bmatrix}\begin{bmatrix} V_a \\ V_b \\ V_c \end{bmatrix} \tag{2.5}$$

This is the formula for abc to alpha-beta conversion. It is clear from the Figure 2.16 and 2.17 that only keeping track of this space vector, it is possible to get clear idea of the phase voltages and changing switching states according to them.

TABLE 2.1: Switch Combinations of the PWM rectifier with current link

	I_1	I_2	I_3	I_4	I_5	I_6	I_7	I_8	I_9
S_1	1	0	0	0	0	1	1	0	0
S_2	1	1	0	0	0	0	0	0	1
S_3	0	1	1	0	0	0	0	1	0
S_4	0	0	1	1	0	0	1	0	0
S_5	0	0	0	1	1	0	0	0	1
S_6	0	0	0	0	1	1	0	1	0
i_a	I	0	-I	-I	0	I	0	0	0
i_b	0	I	I	0	-I	-I	0	0	0
i_c	-I	-I	0	I	I	0	0	0	0

2.2.2 PWM Algorithm

It is evident from the previous discussion that, only one switch among S1,S3 and S5 and one among S2, S4 and S6 (Figure 2.15) should be on at a particular time. If the switches S1 to S6 have duty cycles d1 to d6, the following relations are satisfied:

$$d_1 + d_3 + d_5 = 1 \tag{2.6}$$

$$d_4 + d_6 + d_2 = 1 \tag{2.7}$$

Now, if the line current of the three phase are i_{ra}, i_{rb} and i_{rc} and the output DC current is I, then the following relations exist among line currents, duty cycles and DC current:

$$i_{ra} = (d_1 - d_4) * I \tag{2.8}$$

$$i_{ra} = (d_3 - d_6) * I \tag{2.9}$$

$$i_{ra} = (d_5 - d_2) * I \tag{2.10}$$

The rectifier can only produce six space vectors ($I1 - I6$) and three zero vectors ($I7 - I9$) shown in Table 2.1. From equation 2.3, the current equations are

$$I_n = \frac{2}{\sqrt(3)} * I * e^{j*(2*n-1)*pi/6} \text{ for } n = 1, 2, ..., 6 \tag{2.11}$$

$$I_n = 0 for \text{ for } n = 7, 8, 9 \tag{2.12}$$

Depending on the space vectors, the space vector plane is divided into six sectors (Figure 2.18). Switching sequence are change at the beginning of every sector.
Given the constraint that only one from the upper and one from the lower switches will be closed at a time, the rectifier is capable of only generating the border vectors of the sectors(I1 to I6) and three zero vectors of the current. If the required output voltage is V_{out} and load is R_{out}, then load current is

$$I = \frac{V_{out}}{R_{load}} \tag{2.13}$$

From Figure 2.18 and 2.1 it is clear that, switches can only generate border vectors of current. It is not actually possible to generate a continuous current vector which will follow exactly the voltage space vector. Rather, steps are taken such that at a particular span of time, the current

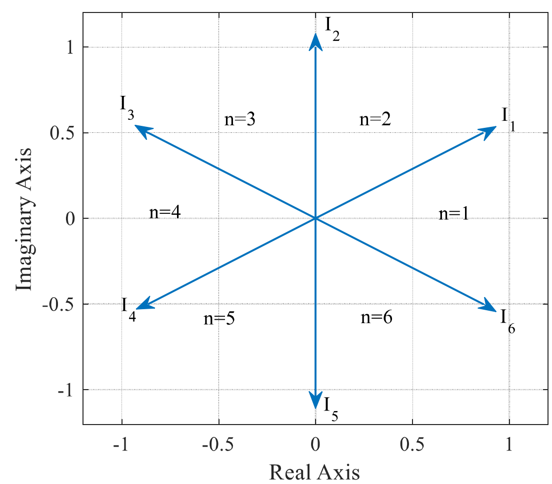

FIGURE 2.18: Sectors in Space Vector Plane

space vector matches with the average voltage space vector of that time in space angle. The magnitude of the current space vector is chosen from the required output current.
The required space vector $i_r(t)$ is modulated as follows:

$$i_r(t) = (T_\alpha I_\alpha + T_\beta I_\beta) \tag{2.14}$$

which is defined as the space vector modulation. This modulation is achieved by using two adjacent vectors I_α and I_β with the appropriate on-time T_α and T_beta. T_s is the period of career frequency. The real and imaginary components are decomposed as

$$i_r(t) = \frac{2}{\sqrt(3)} I((T_\alpha + T_\beta sin60^\circ) + jT_\beta cos30^\circ) \tag{2.15}$$

Figure 2.19also gives

$$i_r(t) = \sqrt(3) I((i_{r\alpha} + i_{r\beta} sin60^\circ) + ji_{r\beta} cos30^\circ) \tag{2.16}$$

where

$$i_{ra} = \frac{2}{\sqrt(3)} |i_r(t)|(sin60^\circ cos\theta_r - cos30^\circ cos\theta_r) = \frac{2}{\sqrt(3)} |i_r(t)| sin(60^\circ - \theta_r) \tag{2.17}$$

$$i_{rb} = \frac{\frac{\sqrt(3)}{2} \frac{2}{\sqrt(3)} |i_r(t)| sin\theta_r}{sin60^\circ} = \frac{2}{\sqrt(3)} |i_r(t)| sin(60^\circ - \theta_r) \tag{2.18}$$

θ_r and $|i_r(t)|$ denote the location and magnitude of the space vector $i_r(t)$. Comparing the equations

$$T_\alpha = \frac{i_r(t)}{I} T_s sin(60 - \theta_r) \tag{2.19}$$

$$T_\beta = \frac{i_r(t)}{I} T_s sin\theta_r \tag{2.20}$$

The on time of the zero vector is

$$T_0 = T_s - T_\alpha - T_\beta \tag{2.21}$$

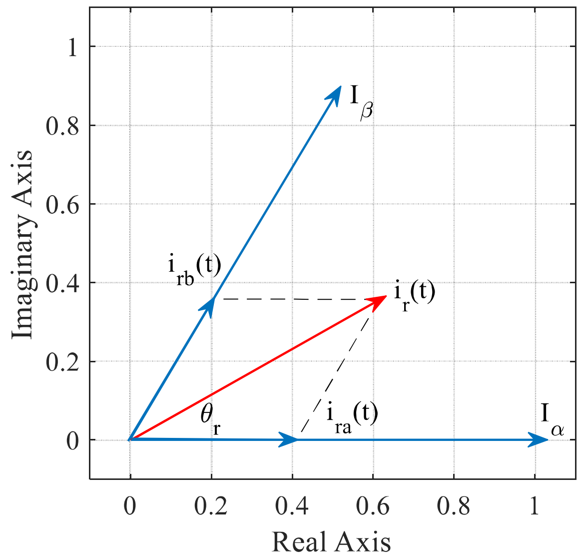

FIGURE 2.19: Current Components

From equations 2.6, 2.7, 2.19, 2.20 and 2.21 switching functions of the switches in the sector n=1 are obtained as follows:

$$d_1 = 1 \tag{2.22}$$

$$d_3 = 0 \tag{2.23}$$

$$d_5 = 0 \tag{2.24}$$

$$d_6 = msin(60^\circ - \theta_r) \tag{2.25}$$

$$d_2 = msin\theta_r \tag{2.26}$$

$$d_4 = 1 - d_6 - d_2 \tag{2.27}$$

where the modulation index $m(0 \leq m \leq 1)$ is defined as

$$m = \frac{i_r(t)}{I} \tag{2.28}$$

Since these switching functions are positive for the full range of θ_r, they can be implemented. The switching function of the switches for all sectors are shown in Table 2.2.

TABLE 2.2: Switching Functions of the Six Switches

	$n=1$	$n=2$	$n=3$	$n=4$	$n=5$	$n=6$
d_1	1	$msin(60° - \theta_r)$	0	1-d_3-d_5	0	$msin\theta_r$
d_2	$msin\theta_r$	1	$msin(60° - \theta_r)$	0	1-d_4-d_6	0
d_3	0	$msin\theta_r$	1	$msin(60° - \theta_r)$	0	1-d_5-d_1
d_4	1-d_6-d_2	0	$msin\theta_r$	1	$msin(60° - \theta_r)$	0
d_5	0	1-d_1-d_3	0	$msin\theta_r$	1	$msin(60° - \theta_r)$
d_6	$msin(60° - \theta_r)$	0	1-d_2-d_4	0	$msin\theta_r$	1

Chapter 3

Simulation of Space Vector Pulse Width Modulated Three Phase Rectifier

3.1 Switch Realization

Switch realization means selection of proper switches to operate a system. There are four quadrants of operation for switches [22]. Based on the operation, switches operating in one, two or even four quadrants are selected for a system. In a six switch PWM rectifier, every switch needs to behave like a diode but the switch must have the option to be controlled. So, The switch must be working in second quadrant of switching. Instead of a diode, a MOSFET can be used as a switch as it is a current bi-directional switch, and one of its working quadrant is second quadrant. But, Due to the fabrication process, there is always a anti-parallel diode built in within a MOSFET. And this might result a current flow int he reverse direction when the MOSFET is OFF. To overcome this problem, a diode in series with a MOSFET can be used to replace the diodes of an uncontrolled rectifier to make it a controlled rectifier.

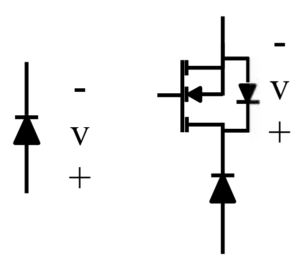

FIGURE 3.1: Switch Realization

3.2 Pulse generation by MATLAB

The calculation to generate the six gate pulses are done in MATLAB in purpose of using them to simulate the system in Simulink. The procedure to generate the pulses are enlisted below:
1. The phase voltages of power system is calculated for a period.
2. The alpha-beta transformation of phase voltages is performed. This transformation represents the space-vector representation of phase voltages.
3. Carrier frequency is selected as $1500Hz$, which is 30 times of the line frequency. So, the entire period is divided is 30 equal time-lengths. Each time-length is the period of carrier.
4. The values of the space vector at the mid-times of the carrier-periods are assumed as the average value of the space vector in the period.

5. The position of the space vector determines the sector of operation.
6. The modulation index, m is varied and the values $msin(\theta_r)$,$msin(60° - \theta_r)$ and $1 - msin(\theta_r) - msin(60° - \theta_r)$ changes.
7. The values calculated in step 6 are compared with the carrier which is a sawtooth wave of 1500 Hz.
8. The generated pulses from step 7 are stored as the pwm pattern of the respective switches according to the sector.

The pulses for six switches are shown in Figure 3.2 and 3.3. Pulses have been generated for a period of line voltage. These pulses need to be repeated for every period synchronizing with the system.

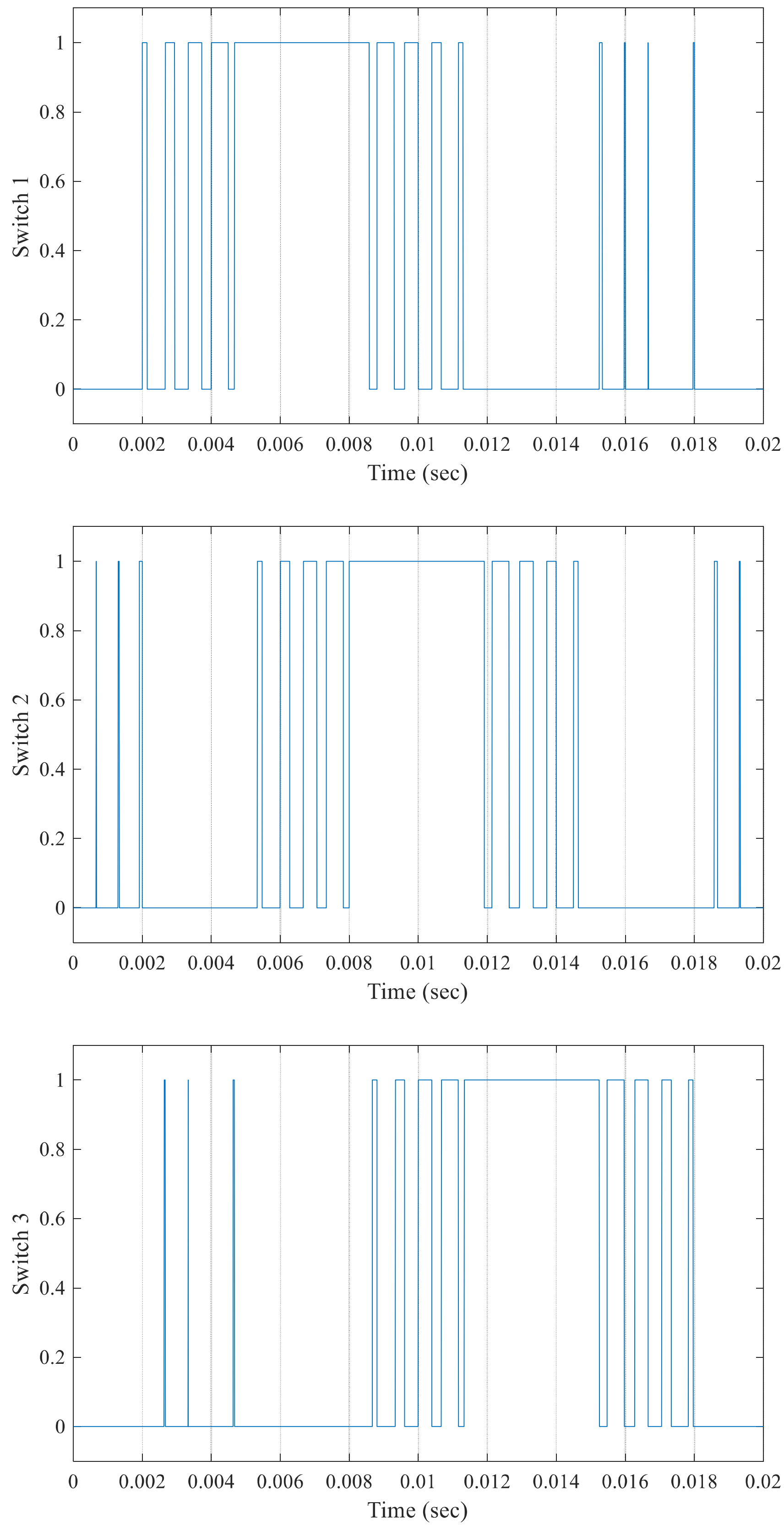

FIGURE 3.2: Gate Pulses generated by MATLAB (Switch 1, 2 and 3)

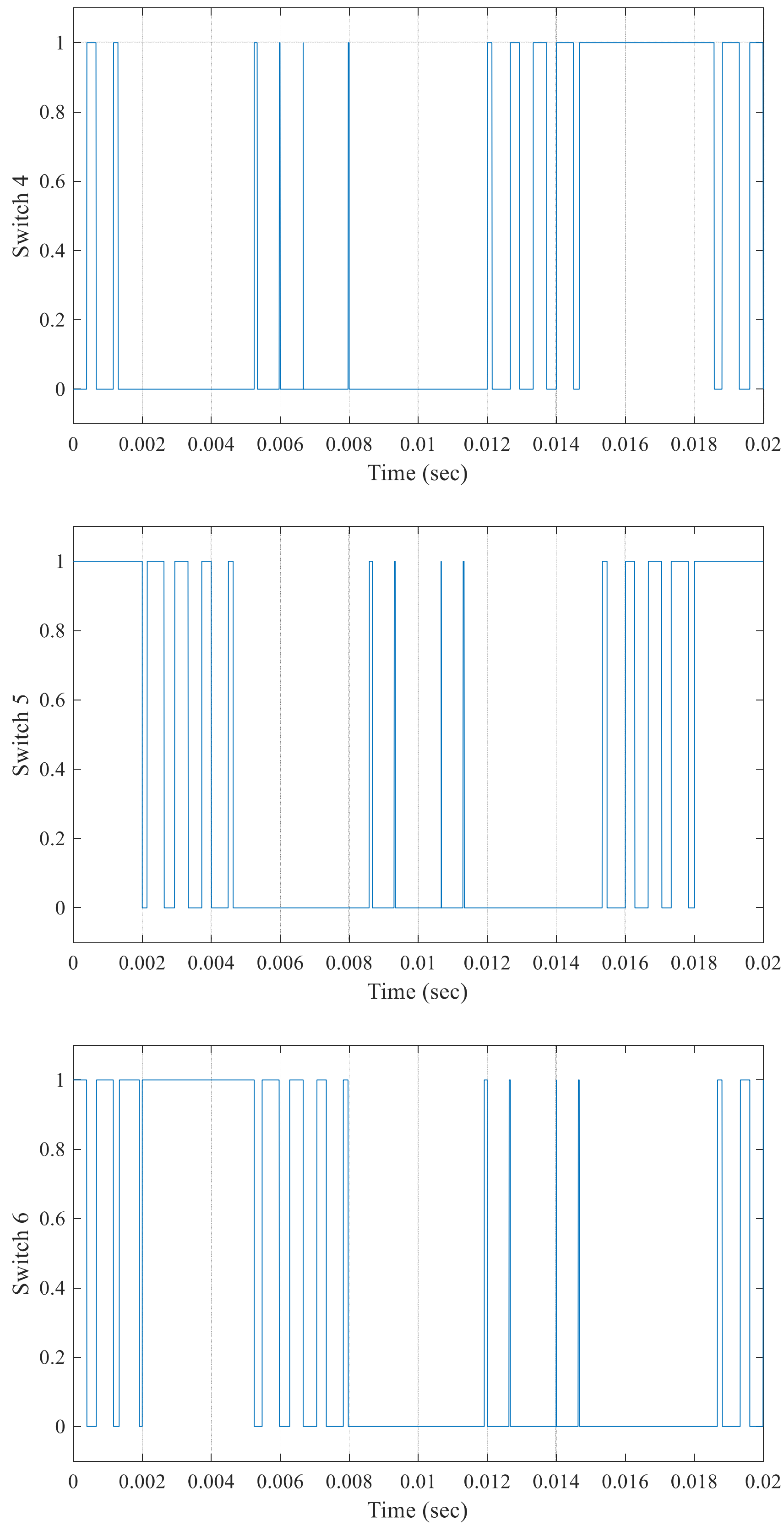

FIGURE 3.3: Gate Pulses generated by MATLAB (Switch 4, 5 and 6)

3.3 Simulation in MATLAB-Simulink

Building the rectifier system in Simulink (Figure 3.4), the generated pulses have been used to drive the system. In practical, a load of 12V-12A rating was intended to connect with the rectifier which will be given power a three phase system(Amplitude of the phase voltage is 30V). That's why a load of resistance 1Ω was connected with the system. The filter in the load side has inductance $100mH$ and capacitance $4700uF$. The input current filter consists of $40mH$ inductor and a $47uF$ capacitor in each phase. A zero-crossing detector followed by a PLL ensured the synchronization.

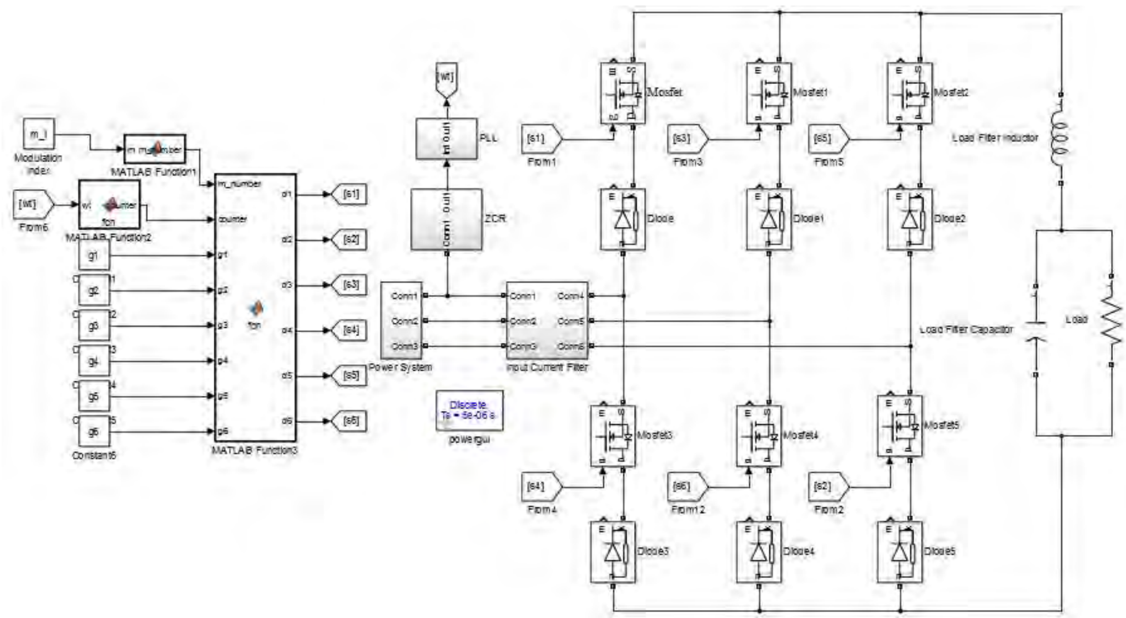

FIGURE 3.4: Block diagram of controlled rectifier in Simulink

3.3.1 Simulation

To understand the effect of filtering, the system was simulated without the current filter at first. After that, the filter was included and the system was simulated again. Input voltages and resultant input currents were observed.

At first the system was simulated without any current filter at the input side. The modulation index was selected as 0.25, 0.5, 0.75 and 1.0. The pulses were made lagging or leading to understand the effect of firing angle change.

After that the input current filter was introduced in the system and the system was simulated with the same modulation index change and pulse angle change. The resultant current with and without current filter for modulation index 0.50 and for angles of pulses $-36°$, $0°$ and $36°$ respectively are shown in Figure **??** to Figure 3.10. The characteristics of the system have been observed for four different modulation indexes and 15 different pulse angles. They have been listed in Table 3.1 to 3.4. The angle of pulses term here is used to describe the difference between the zero crossings of phase a and instructed angle of the current's phase. The pictorial representations of the tables are shown in Figure 3.11 to 3.19.

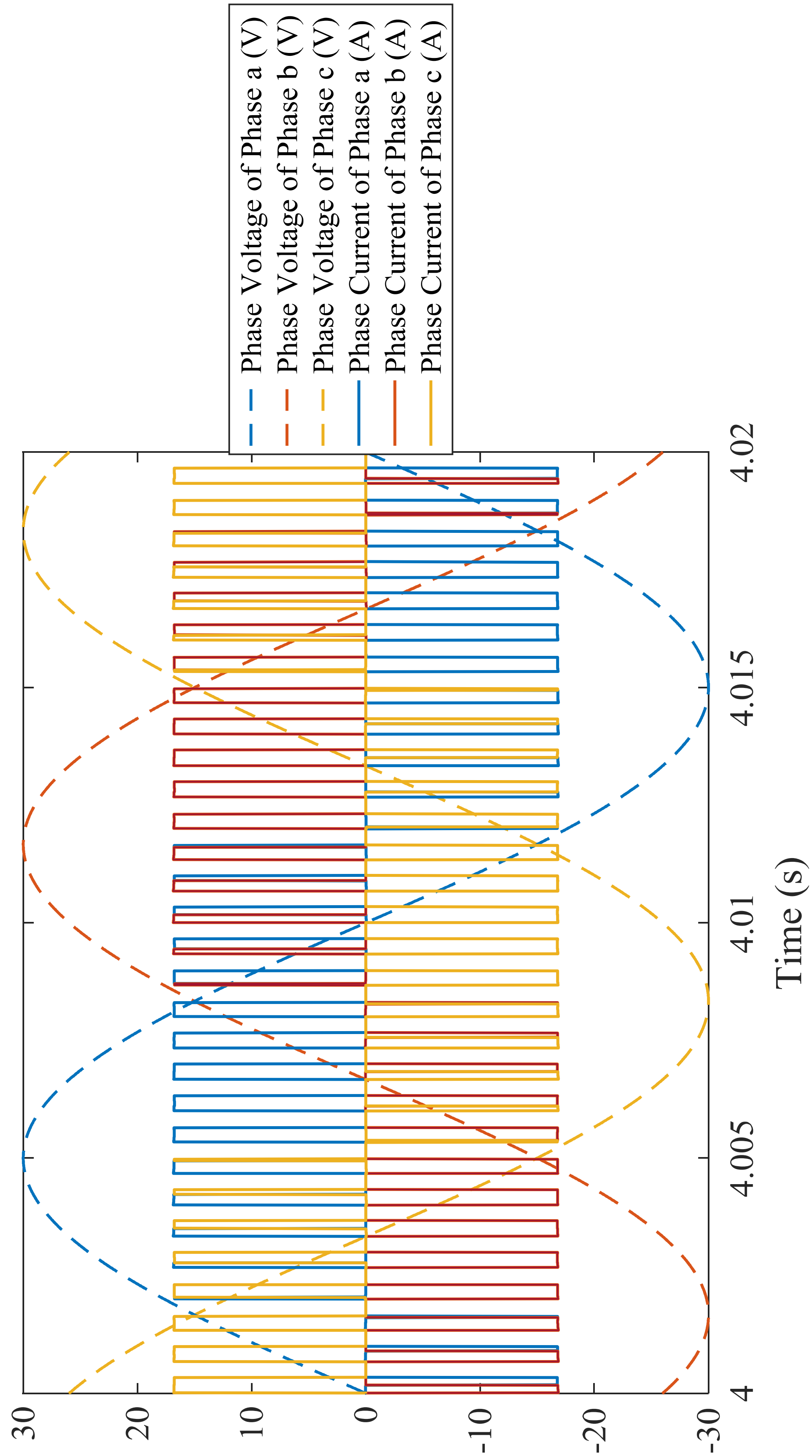

FIGURE 3.5: Voltage and current without current filter at m=0.50 and $\theta_r = 36°$

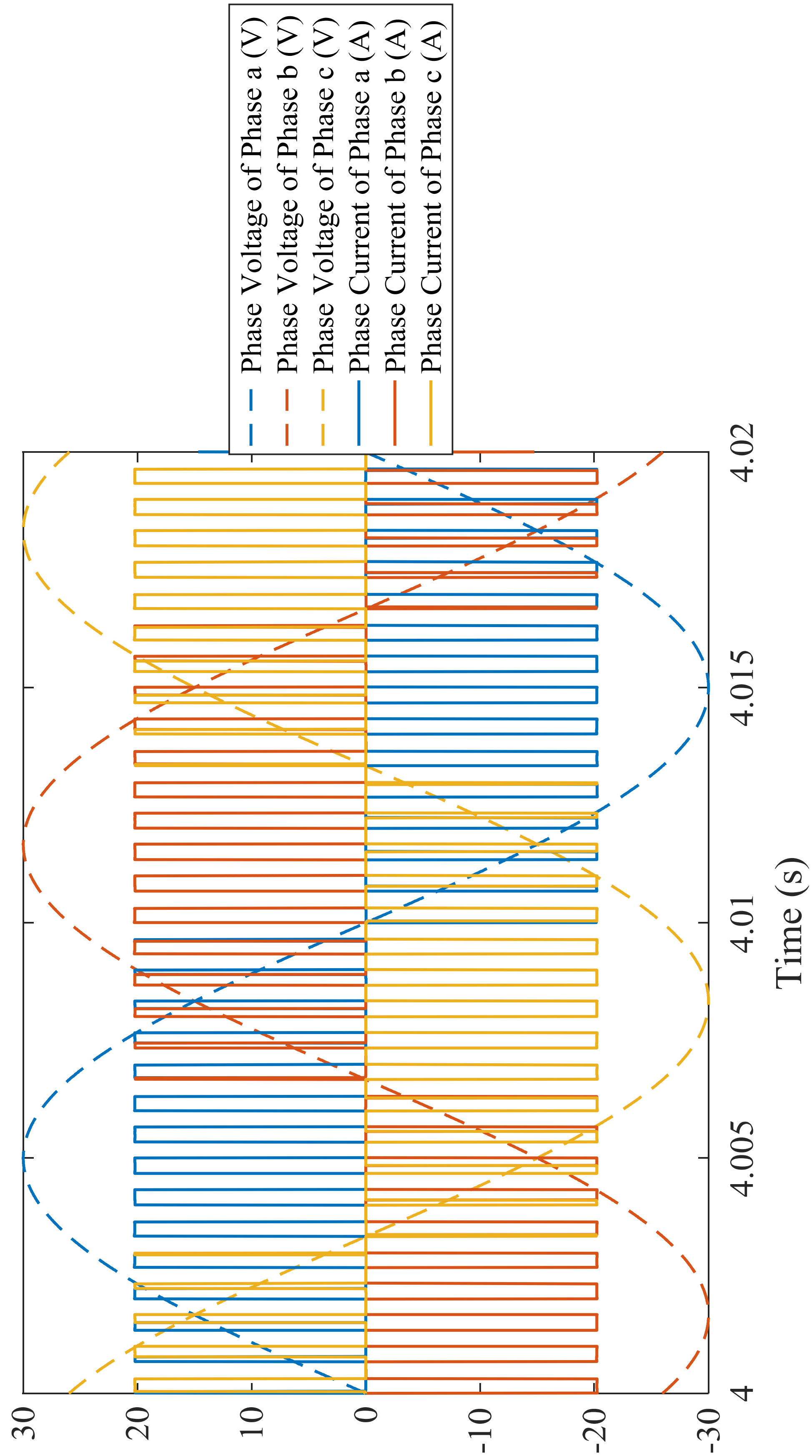

FIGURE 3.6: Voltage and current without current filter at m=0.50 and $\theta_r = 0°$

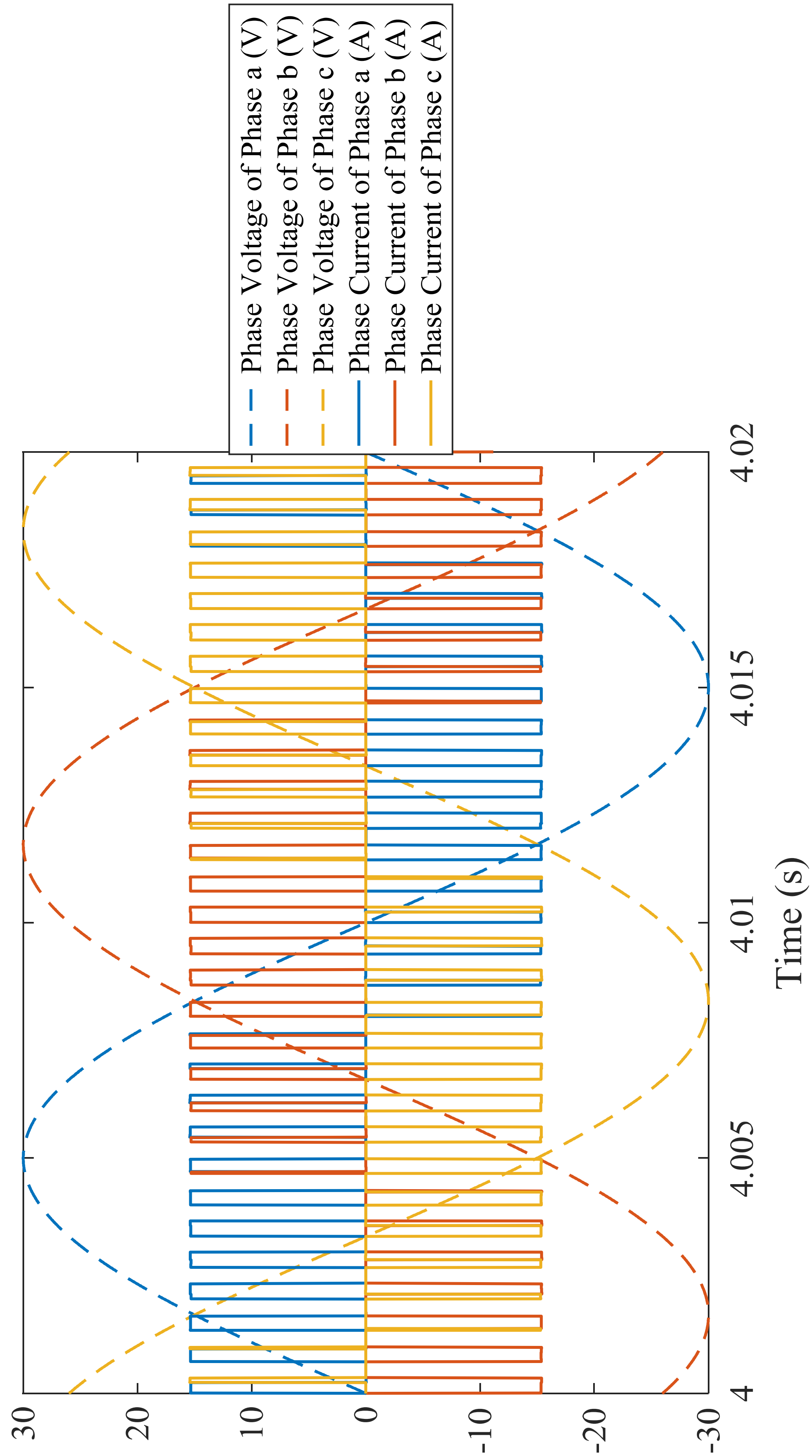

FIGURE 3.7: Voltage and current without current filter at m=0.50 and $\theta_r = -36°$

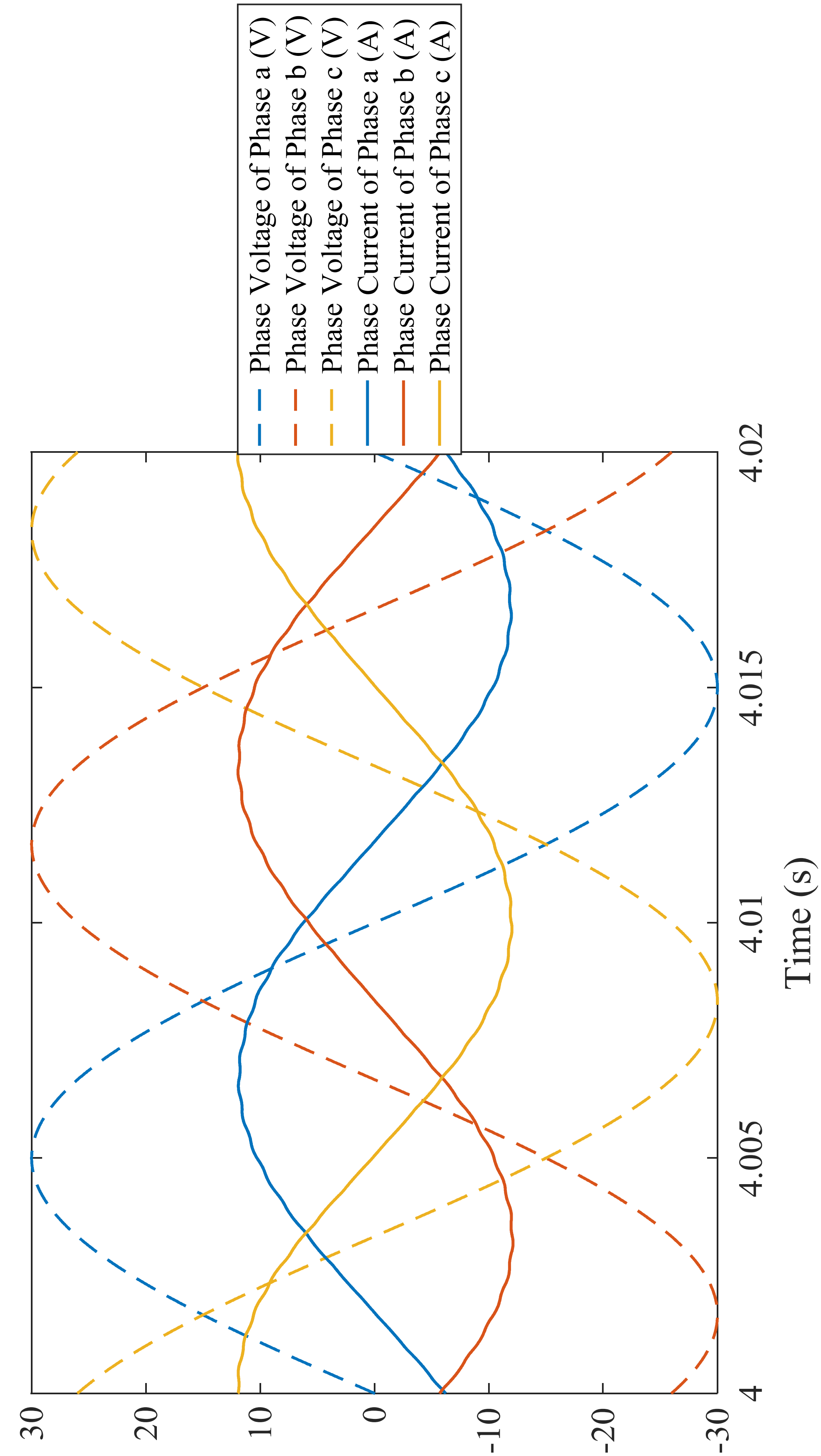

FIGURE 3.8: Voltage and current with current filter at m=0.50 and $\theta_r = 36°$

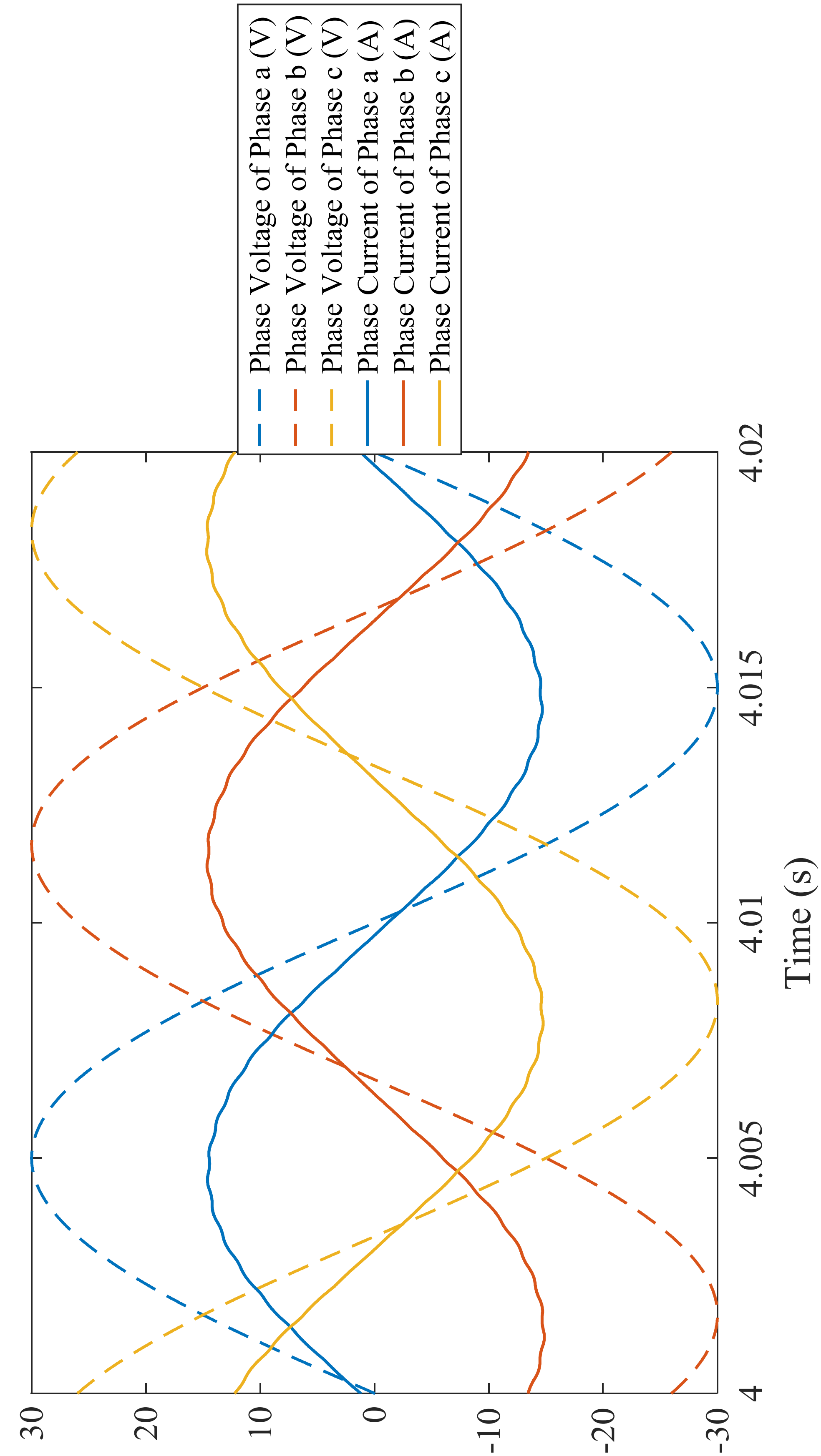

FIGURE 3.9: Voltage and current with current filter at m=0.50 and $\theta_r = 0°$

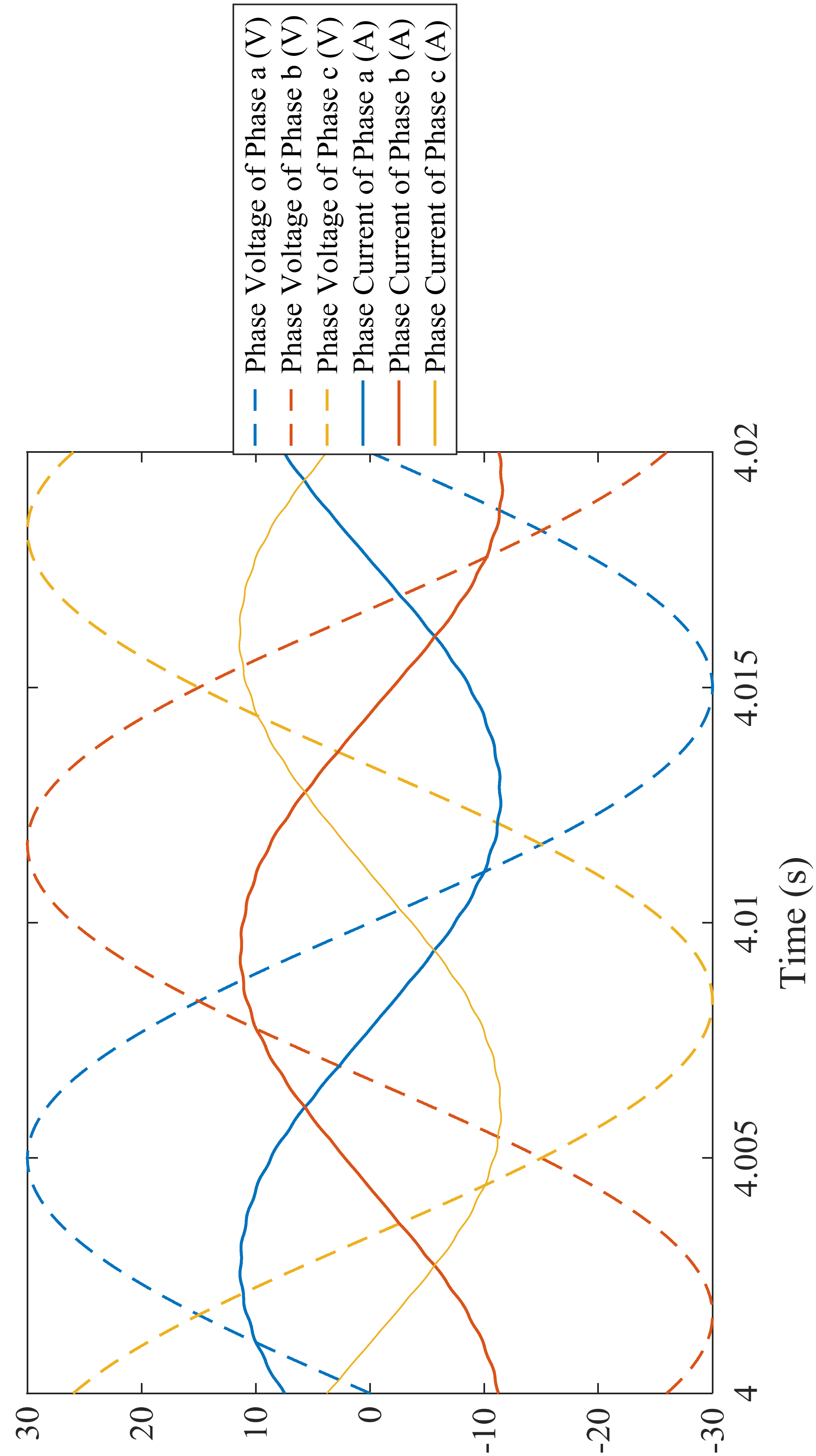

FIGURE 3.10: Voltage and current with current filter at m=0.50 and $\theta_r = -36°$

TABLE 3.1: Characteristics of the Controlled Rectifier for Modulation Index 0.25

Modulation Index = 0.25									
	Without Current Filter		With Current Filter						
Angle of Pulses	Peak Amplitude of Phase Current (A)	Total Harmonic Distortion of Phase Current (%) (Considering First 50 Harmonics)	Peak Amplitude of Phase Current (A)	Total Harmonic Distortion of Phase Current (%) (Considering First 50 Harmonics)	Angle of the Phase Current (°)	Power Factor	Real Power Consumed, P (W)	Reactive Power Consumed, Q (VAR)	Power Supplied to the Load (W)
-84	0.6269	25.9787	0.2550	1.2380	-74.5200	0.2669	3.0947	-11.1751	0.9749
-72	2.8081	24.6967	0.7045	3.3933	-48.3300	0.6645	19.7078	-22.1658	13.2939
-60	4.7888	24.5132	1.4954	1.8717	-44.4600	0.7136	48.1613	-47.2788	36.7977
-48	6.5486	24.6400	2.1812	1.4455	-33.0300	0.8383	82.5533	-53.6911	67.4858
-36	7.8990	24.4986	2.9033	2.0917	-22.4100	0.9243	116.3492	-48.0516	97.2442
-24	8.8823	24.4089	3.3218	1.5714	-11.8800	0.9785	145.2187	-30.6383	122.2008
-12	9.4176	24.5752	3.5625	1.2913	1.0800	0.9997	160.2703	3.6624	136.8086
0	9.4296	24.4672	3.8235	1.8783	12.3300	0.9768	161.8418	35.5126	137.0518
12	9.0394	24.4002	3.7125	1.4470	23.2200	0.9189	150.3533	64.5471	125.9582
24	8.1291	24.5951	3.4060	1.1898	36.3600	0.8053	123.3642	90.8374	102.4628
36	6.8250	24.5266	3.1106	1.6682	47.7000	0.6729	90.3183	99.2837	72.1600
48	5.2306	24.4880	2.5051	1.2855	58.6800	0.5198	56.1583	92.3020	42.5046
60	3.2524	24.7623	1.7705	0.9778	71.6400	0.3150	25.1050	75.6486	16.7606
72	1.1083	25.2955	1.0102	0.8371	82.8000	0.1253	5.4547	43.1795	2.1069
84	0.1986	107.0200	0.5726	0.4329	88.3800	0.0283	0.5508	19.4739	0.0039

TABLE 3.2: Characteristics of the Controlled Rectifier for Modulation Index 0.50

Modulation Index = 0.50									
	Without Current Filter		With Current Filter						
Angle of Pulses	Peak Amplitude of Phase Current (A)	Total Harmonic Distortion of Phase Current (%) (Considering First 50 Harmonics)	Peak Amplitude of Phase Current (A)	Total Harmonic Distortion of Phase Current (%) (Considering First 50 Harmonics)	Angle of the Phase Current (°)	Power Factor	Real Power Consumed, P (W)	Reactive Power Consumed, Q (VAR)	Power Supplied to the Load (W)
-84	2.0338	104.7165	1.1588	1.4258	-76.4100	0.2349	12.3004	-50.8883	7.5191
-72	6.4645	103.9940	4.3368	0.9156	-66.2400	0.4029	78.0706	-177.3539	62.8674
-60	10.4843	103.8758	7.2466	0.8540	-54.4500	0.5814	187.5188	-262.4214	159.4234
-48	14.0104	103.7986	9.9268	1.0361	-43.3800	0.7268	323.6933	-305.9224	280.3040
-36	16.8667	103.8334	11.9542	0.8412	-30.8700	0.8583	460.7310	-275.4513	402.7997
-24	18.9045	103.7997	13.4845	0.8173	-18.8100	0.9466	573.5883	-195.4399	503.2106
-12	20.0767	103.7421	14.5528	1.0081	-7.5600	0.9913	644.3641	-85.7694	564.9447
0	20.2769	103.7860	14.6748	0.8202	4.9500	0.9962	656.7117	57.1338	574.9280
12	19.5573	103.7588	14.2262	0.7989	17.1000	0.9558	613.7854	188.8947	533.5895
24	17.9278	103.7084	13.2714	0.9871	28.3500	0.8800	519.5703	280.4055	447.1764
36	15.4158	103.7576	11.4264	0.7973	40.9500	0.7553	388.5003	337.1483	329.6710
48	12.2299	103.7335	9.1887	0.7719	53.0100	0.6017	251.0750	333.3243	206.6179
60	8.4358	103.6733	6.5721	0.9414	64.2600	0.4343	125.5644	260.4523	97.5701
72	4.1562	103.6678	3.4802	0.7066	76.7700	0.2289	35.7183	151.9317	23.3386
84	0.2267	101.6110	0.5994	0.3806	87.6600	0.0408	1.0689	26.1591	0.0071

TABLE 3.3: Characteristics of the Controlled Rectifier for Modulation Index 0.75

Modulation Index = 0.75									
	Without Current Filter		With Current Filter						
Angle of Pulses	Peak Amplitude of Phase Current (A)	Total Harmonic Distortion of Phase Current (%) (Considering First 50 Harmonics)	Peak Amplitude of Phase Current (A)	Total Harmonic Distortion of Phase Current (%) (Considering First 50 Harmonics)	Angle of the Phase Current (°)	Power Factor	Real Power Consumed, P (W)	Reactive Power Consumed, Q (VAR)	Power Supplied to the Load (W)
-84	2.8079	71.2694	2.7017	1.0514	-80.8200	0.1595	18.9242	-117.1072	12.7933
-72	9.4252	70.6370	9.2715	0.9648	-70.0200	0.3417	143.9473	-395.9427	115.9977
-60	15.5556	70.5240	15.3845	0.8733	-57.9600	0.5305	368.0216	-588.0749	304.4109
-48	20.9142	70.5211	20.6520	0.8782	-45.9000	0.6959	648.4529	-669.2015	540.8307
-36	25.3228	70.4780	25.1378	0.9249	-34.2000	0.8270	937.7597	-637.3871	785.0311
-24	28.5552	70.4433	28.4050	0.8531	-22.0500	0.9268	1185.9	-480.4653	992.5455
-12	30.4670	70.4674	30.2376	0.8641	-9.9000	0.9851	1344.7	-234.9816	1123.8
0	30.9978	70.4393	30.9237	0.9129	1.7100	0.9995	1390.7	43.4171	1158.1
12	30.0965	70.4172	30.0940	0.8429	13.8600	0.9708	1315.1	324.6820	1088.8
24	27.8356	70.4538	27.7926	0.8536	26.0100	0.8987	1128.3	550.6773	927.3307
36	24.3020	70.4374	24.4073	0.9005	37.7100	0.7911	866.4880	670.0123	702.8710
48	19.6224	70.4238	19.8043	0.8279	49.8600	0.6446	573.9394	680.6499	455.8475
60	14.0694	70.4667	14.2497	0.8309	62.0100	0.4693	302.6655	569.4959	231.5279
72	7.8157	70.4614	8.0934	0.8519	73.7100	0.2805	101.0495	345.7998	69.4438
84	1.1171	70.6700	1.4692	0.5211	85.6800	0.0753	4.8750	64.5350	1.0356

TABLE 3.4: Characteristics of the Controlled Rectifier for Modulation Index 1.00

Modulation Index = 1.00									
	Without Current Filter		With Current Filter						
Angle of Pulses	Peak Amplitude of Phase Current (A)	Total Harmonic Distortion of Phase Current (%) (Considering First 50 Harmonics)	Peak Amplitude of Phase Current (A)	Total Harmonic Distortion of Phase Current (%) (Considering First 50 Harmonics)	Angle of the Phase Current (°)	Power Factor	Real Power Consumed, P (W)	Reactive Power Consumed, Q (VAR)	Power Supplied to the Load (W)
-84	3.1503	45.6025	4.0202	1.1133	-83.1600	0.1191	21.3302	-177.8358	14.5293
-72	11.9383	45.1713	14.7677	1.0297	-71.9100	0.3105	209.4957	-641.3694	162.3307
-60	20.1627	45.1726	24.7583	1.0082	-59.9400	0.5009	564.6767	-975.7539	444.8438
-48	27.4137	45.1082	33.6364	0.9663	-47.7000	0.6730	1023.4	-1124.8	808.3018
-36	33.4077	45.0669	41.0497	1.0006	-36.0900	0.8081	1503.2	-1095.9	1188.1
-24	37.8878	45.1174	46.3921	0.9919	-24.0300	0.9133	1920.8	-856.6394	1518.1
-12	40.6466	45.0718	49.8008	0.9546	-11.7000	0.9792	2205.3	-457.1992	1737.6
0	41.5813	45.0411	50.9999	0.9919	0.1800	0.9999	2305.0	23.9820	1809.2
12	40.5915	45.1009	49.7156	0.9838	11.9700	0.9782	2198.4	466.6120	1718.7
24	37.7836	45.0648	46.3520	0.9461	24.3000	0.9114	1911.9	863.4807	1484.0
36	33.2933	45.0446	40.9378	0.9830	35.9100	0.8099	1493.0	1081.3	1146.4
48	27.2212	45.1142	33.4562	0.9724	47.9700	0.6695	1009.0	1119.6	762.9121
60	19.9482	45.0886	24.6056	0.9283	60.3000	0.4954	552.8601	969.3223	406.0403
72	11.7556	45.0927	14.6313	0.9513	71.8200	0.3120	202.5909	616.9405	138.1716
84	2.9147	45.3589	3.8232	0.8212	83.8800	0.1066	17.7405	165.4613	7.4891

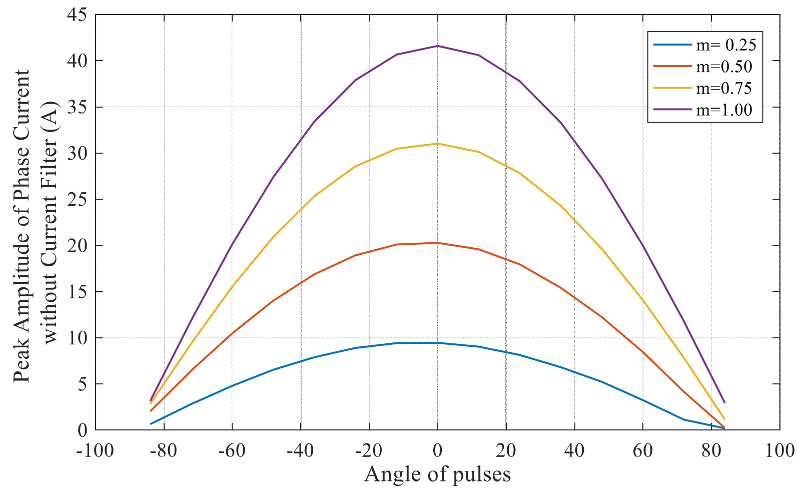

FIGURE 3.11: Peak Amplitude of Phase Current without Current Filter

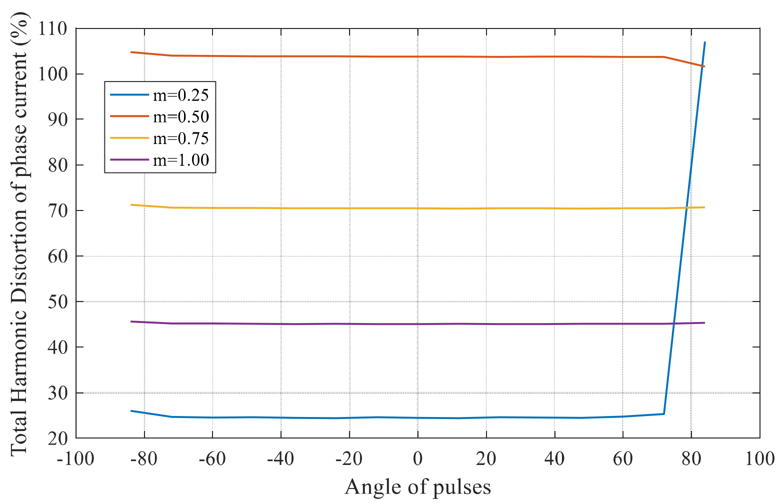

FIGURE 3.12: Total Harmonic Distortion of Phase Current without Current Filter

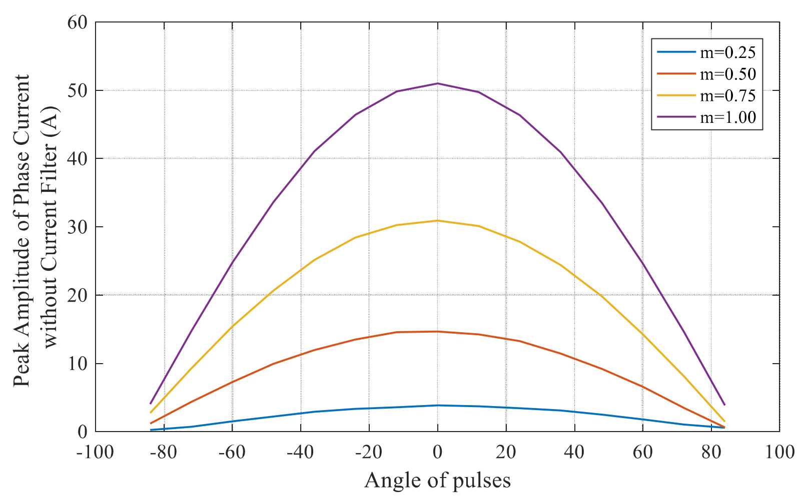

FIGURE 3.13: Peak Amplitude of Phase Current with Current Filter

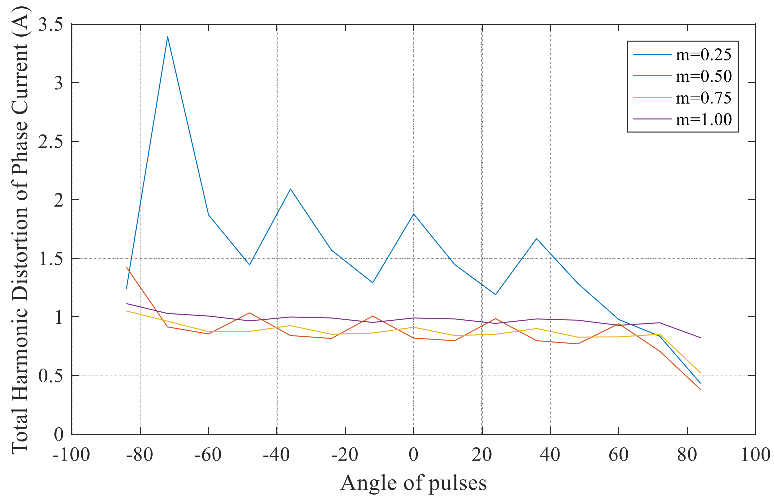

FIGURE 3.14: Total Harmonic Distortion of Phase Current with Current Filter

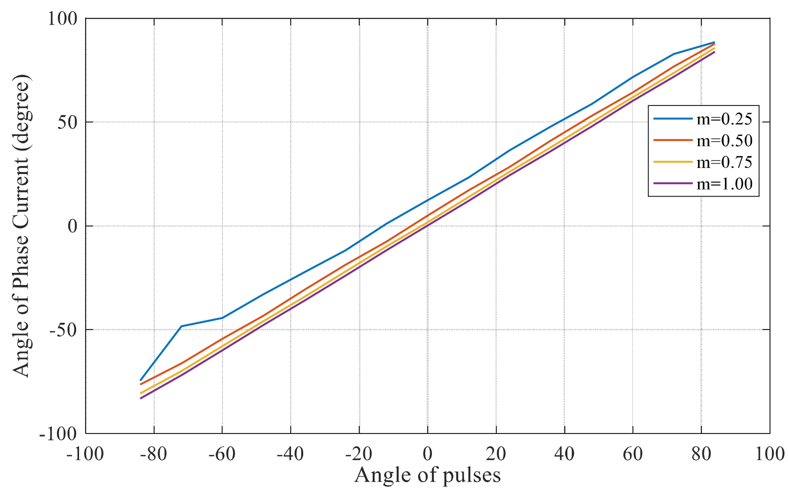

FIGURE 3.15: Angle of Phase Current of Phase Current with Current Filter

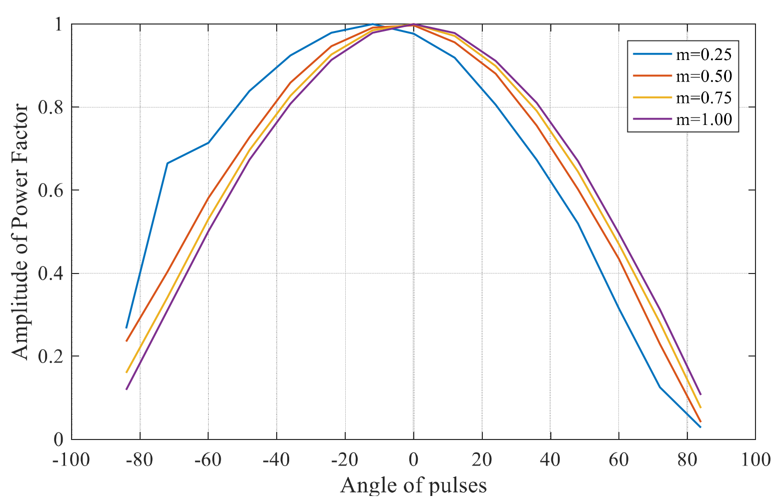

FIGURE 3.16: Power Factor with Current Filter

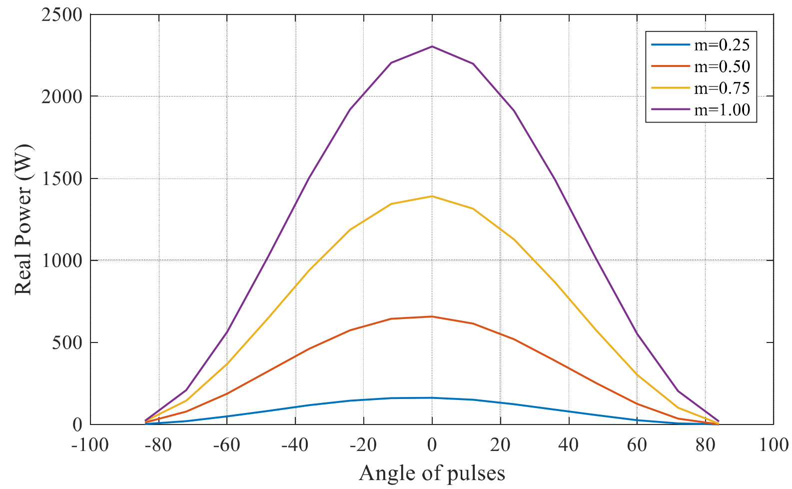

FIGURE 3.17: Real Power with Current Filter

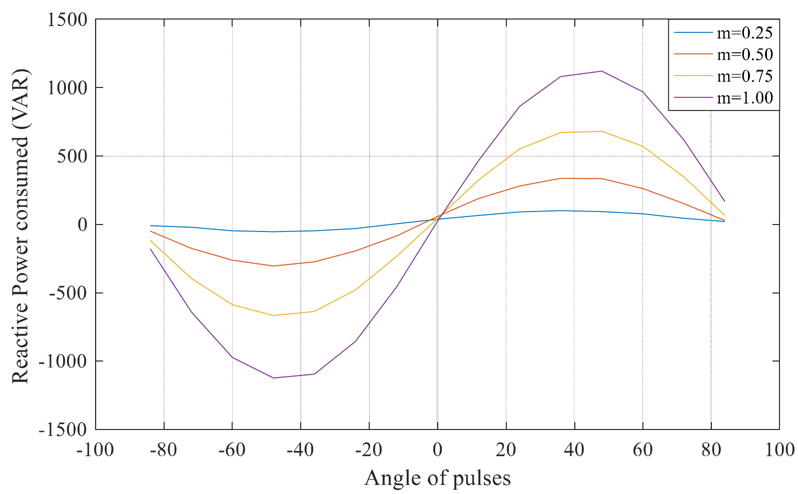

FIGURE 3.18: Reactive Power with Current Filter

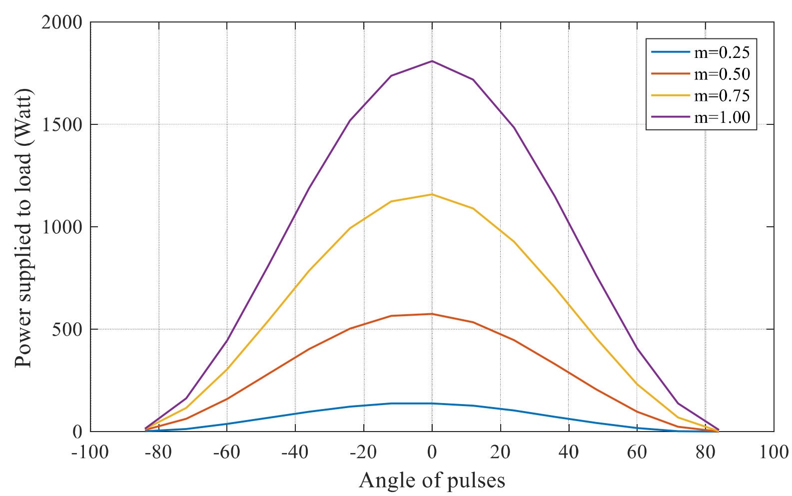

FIGURE 3.19: Power Supplied to load with Current Filter

3.3.2 Simulation at fixed Output Voltage

The intended output of the controlled rectifier is 12 V. Under the above mentioned condition (load value and filter element values), the system was simulated so that the output is 12 V with lagging and leading current drawing from the input side. The figures from **??** to 3.28 shows voltages and currents through different elements of the system for output voltage 12 V with pulse angle $0°$. The system characteristics for all the simalations are listed in 3.5. The pictorial representation of the table has been shown in Figure 3.29 to 3.40.

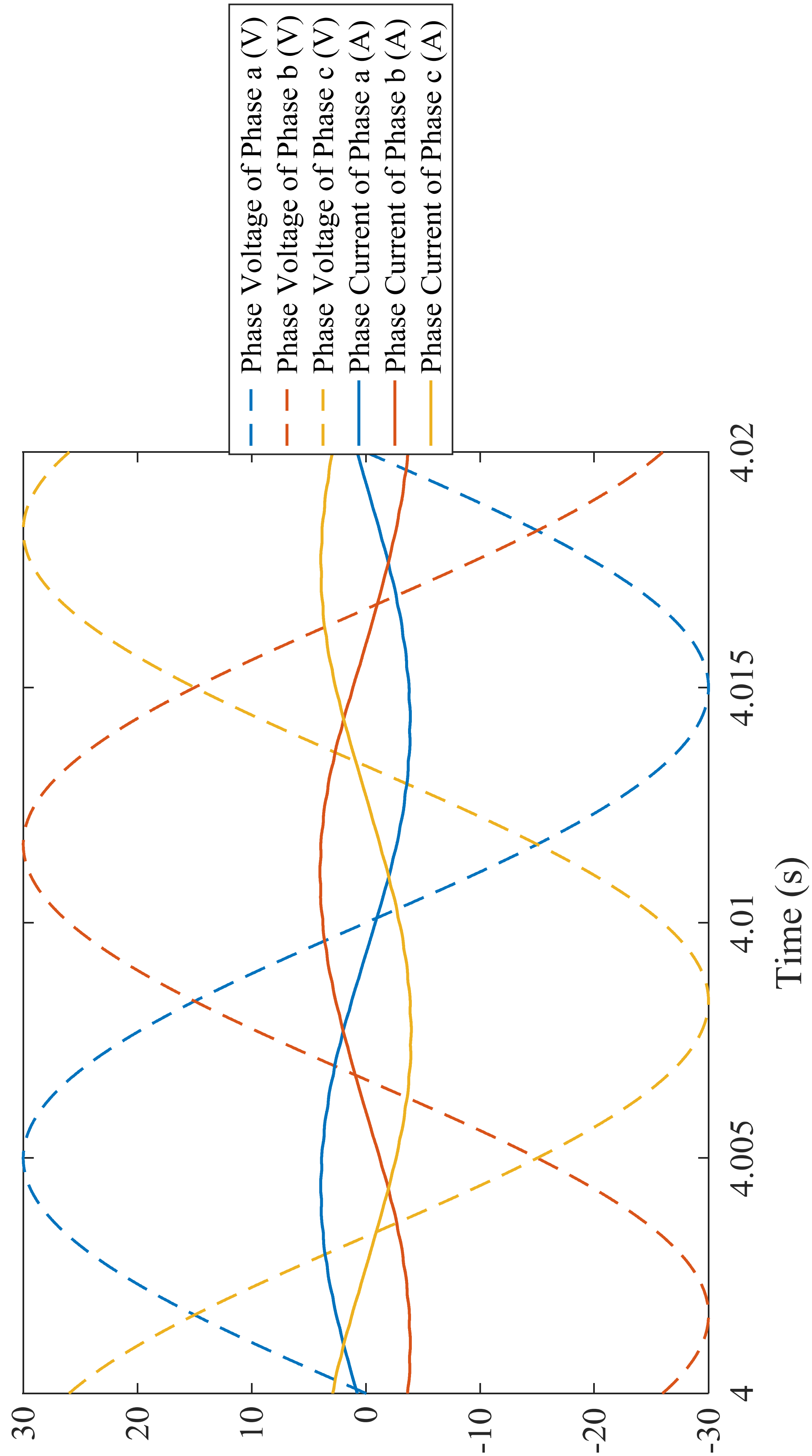

FIGURE 3.20: Voltage and current at output voltage 12V with $\theta_r = 0°$

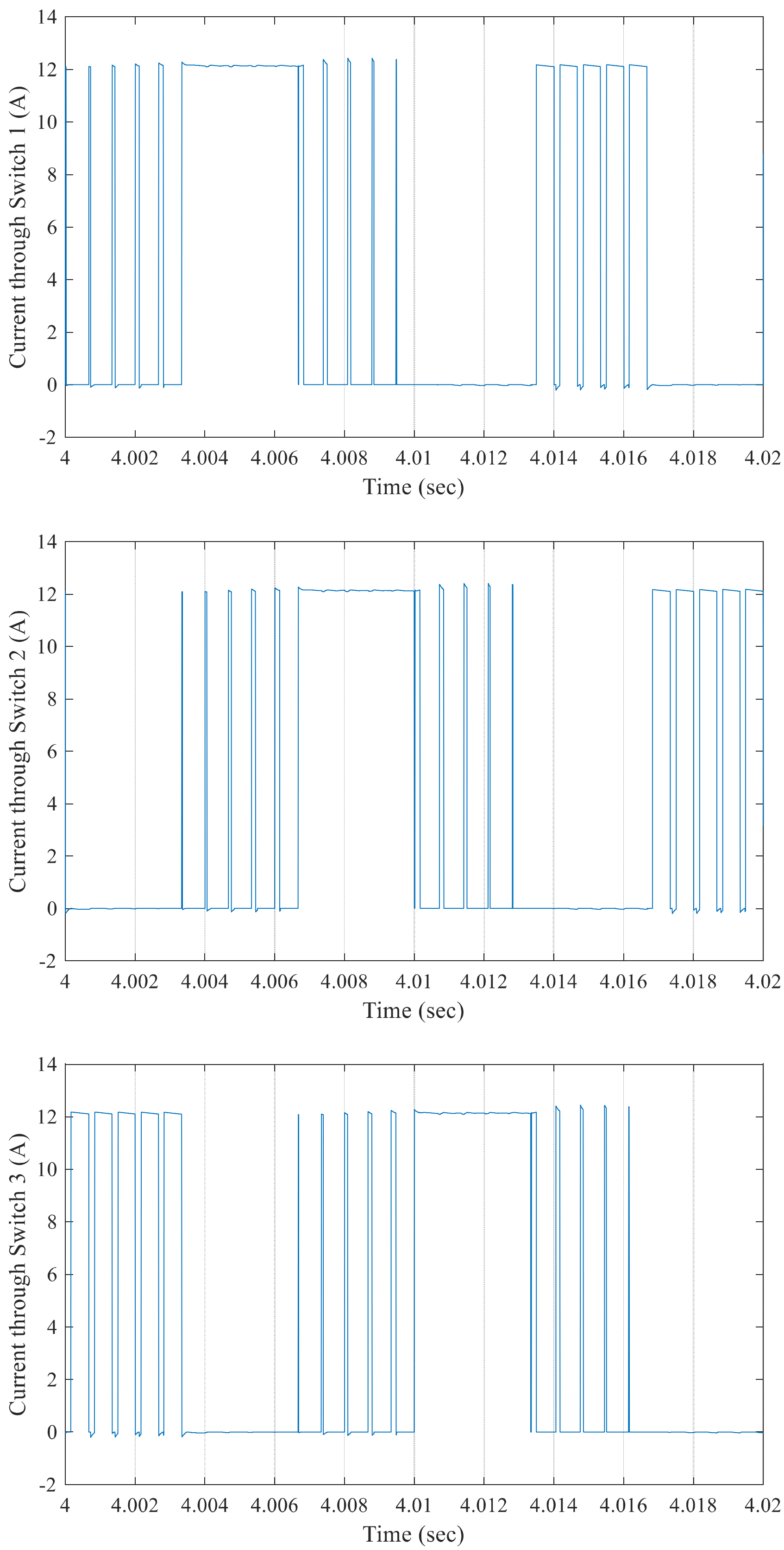

FIGURE 3.21: Current through the switches at output voltage $12V$ with $\theta_r = 0°$ (Switches 1,2 and 3)

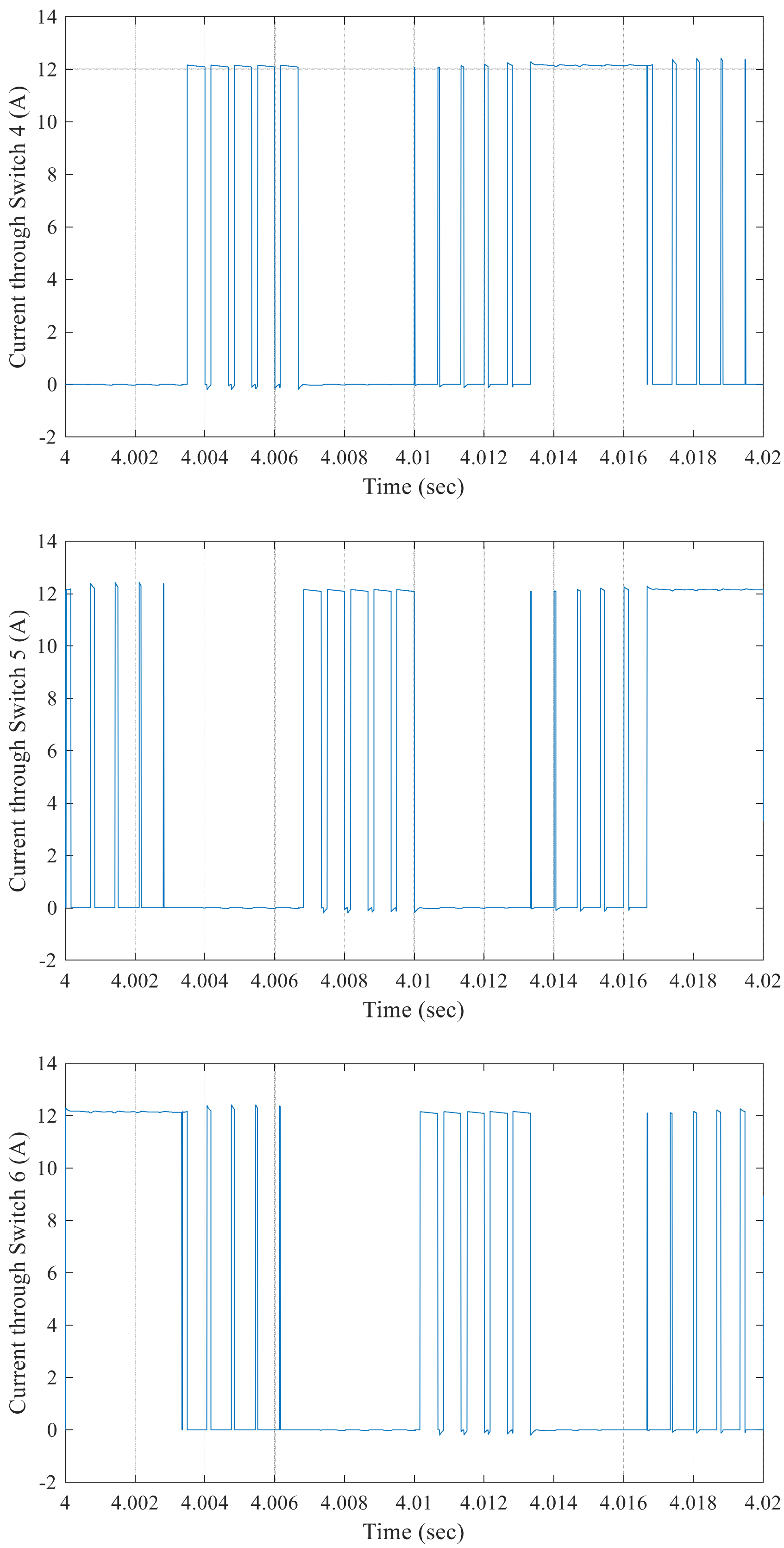

FIGURE 3.22: Current through the switches at output voltage $12V$ with $\theta_r = 0°$ (Switches 4,5 and 6)

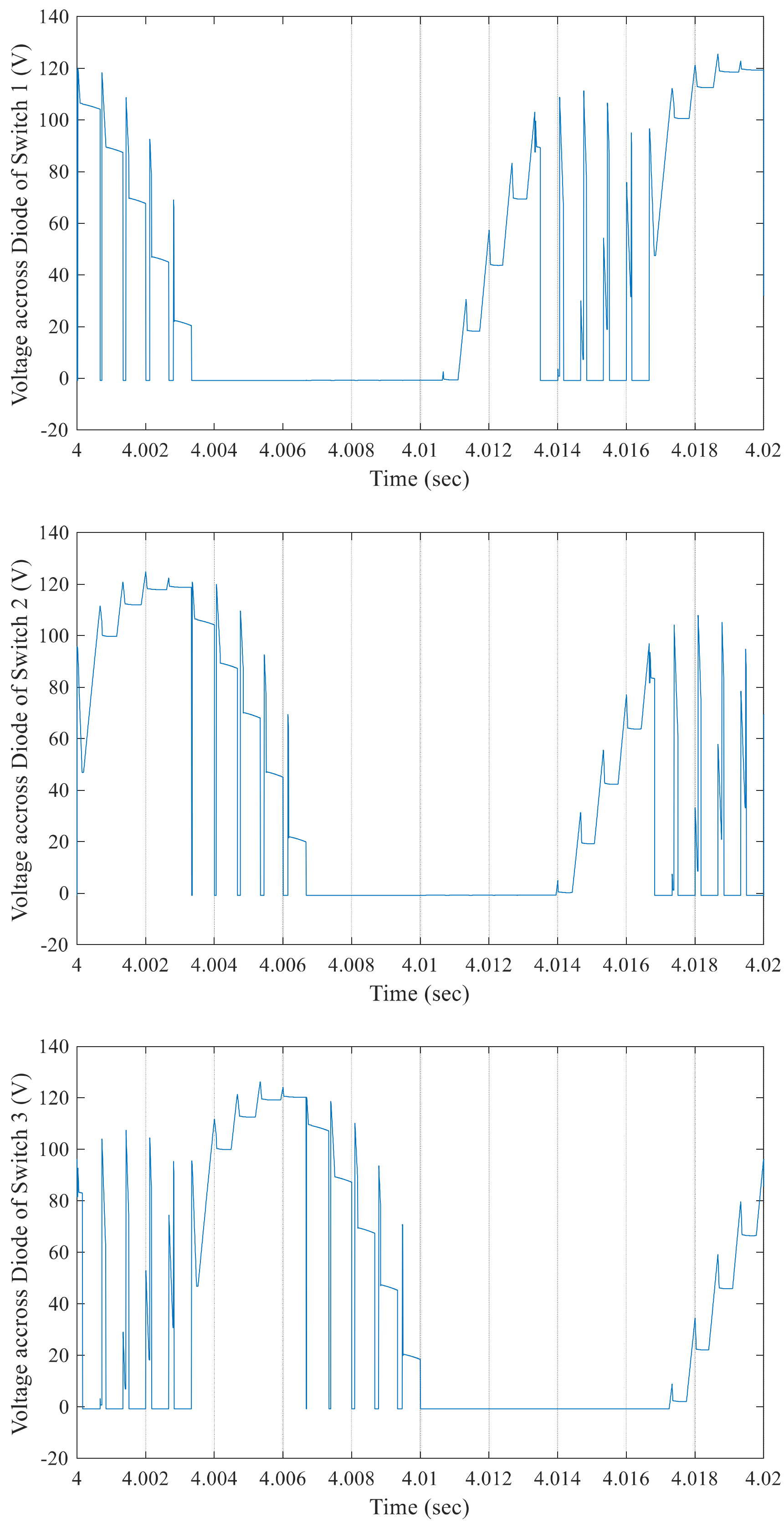

FIGURE 3.23: Current through the switches at output voltage $12V$ with $\theta_r = 0°$ (Switches 1,2 and 3)

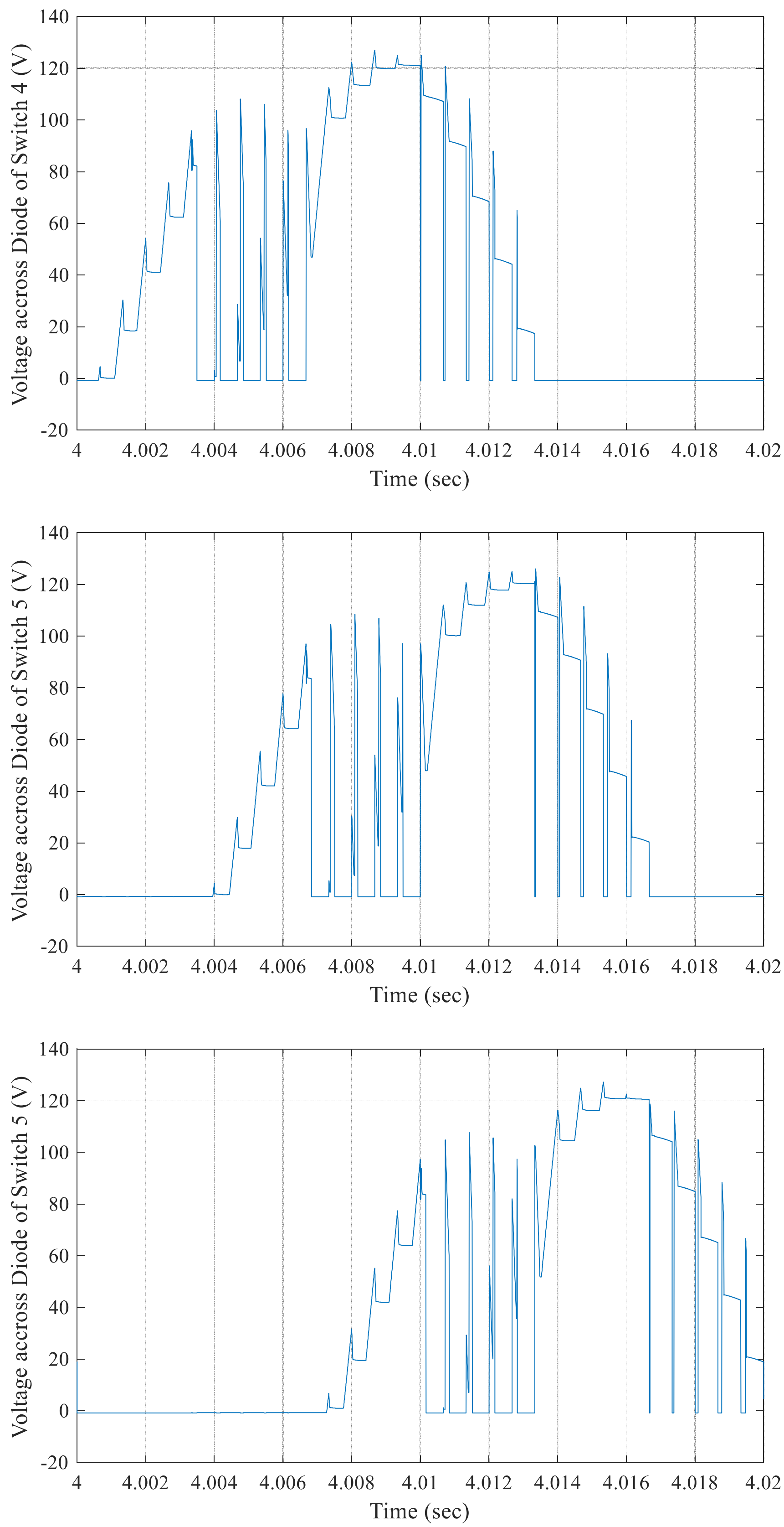

FIGURE 3.24: Current through the switches at output voltage $12V$ with $\theta_r = 0°$ (Switches 4,5 and 6)

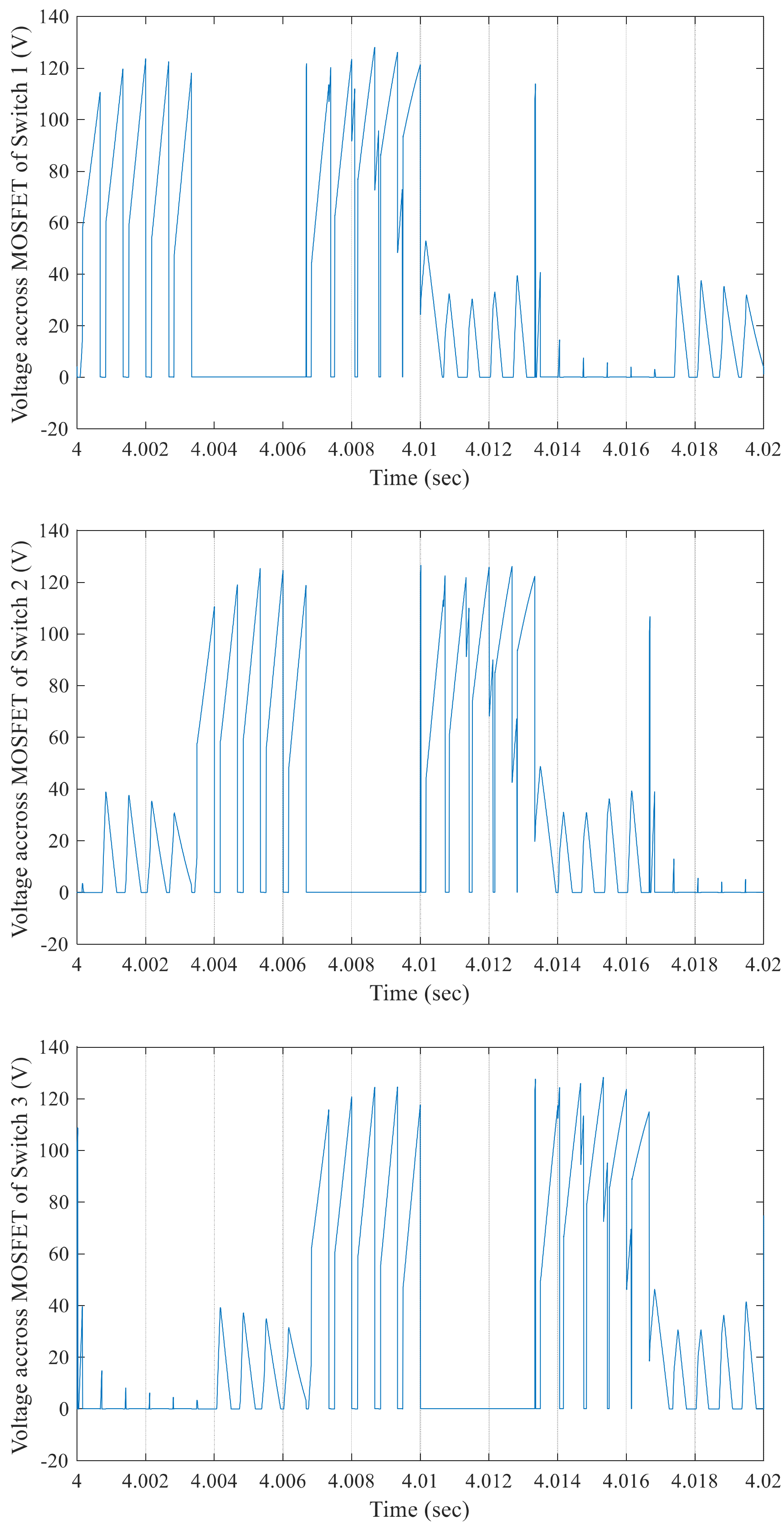

FIGURE 3.25: Voltage across MOSFETs of the switches at output voltage $12V$ with $\theta_r = 0°$ (Switches 1,2 and 3)

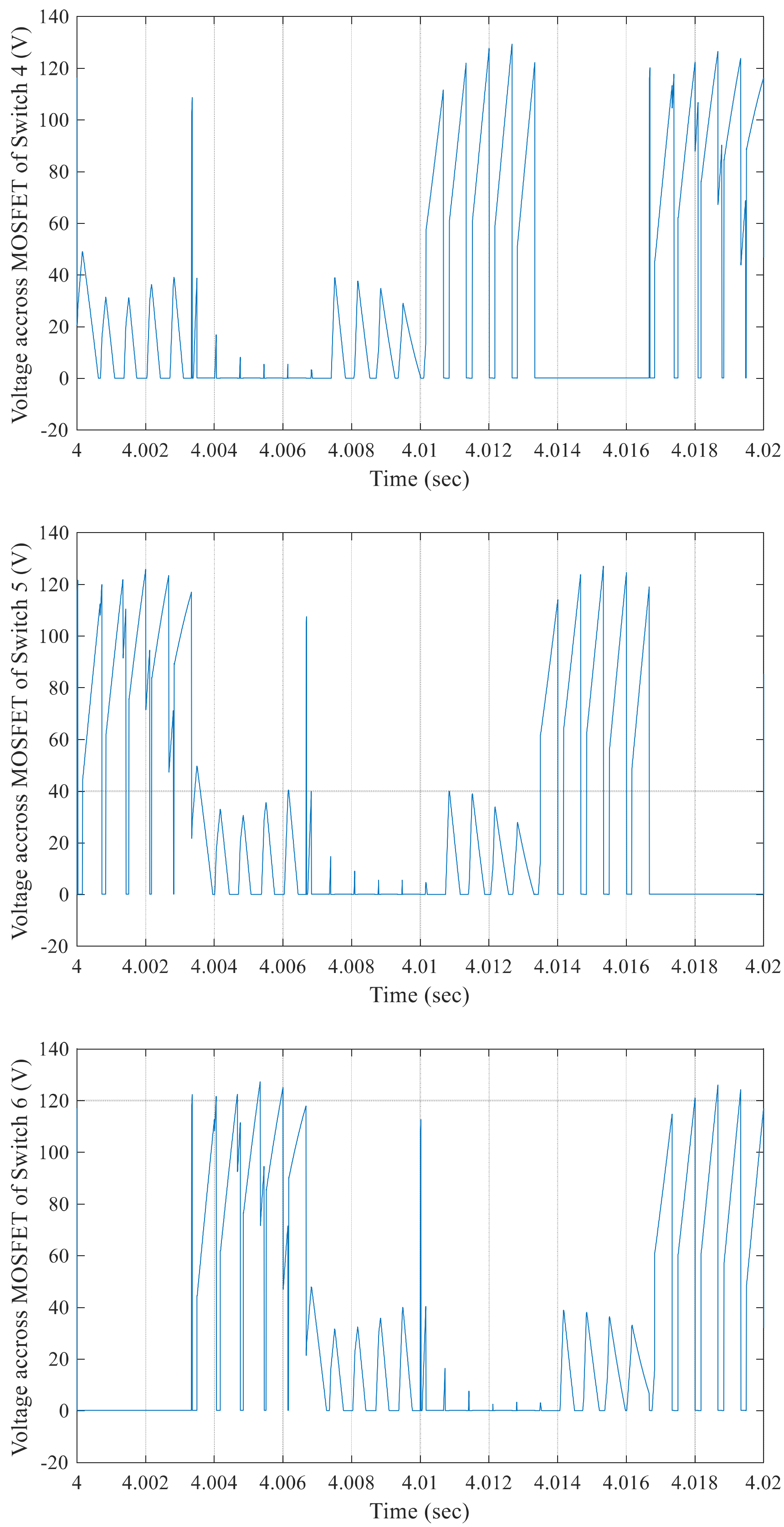

FIGURE 3.26: Voltage across MOSFETs of the switches at output voltage $12V$ with $\theta_r = 0°$ (Switches 4,5 and 6)

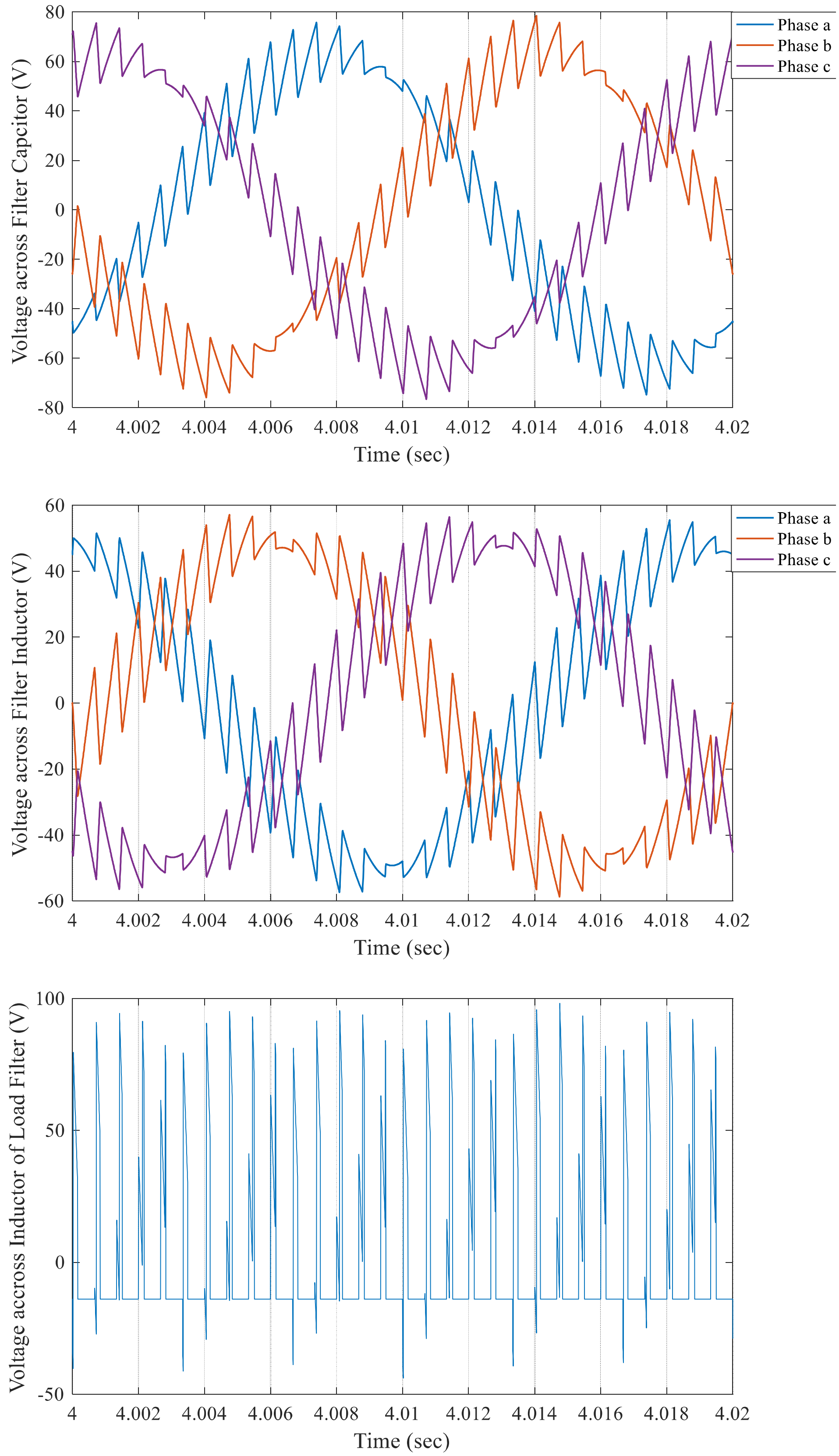

FIGURE 3.27: Voltage across filter elements at output voltage $12V$ with $\theta_r = 0°$

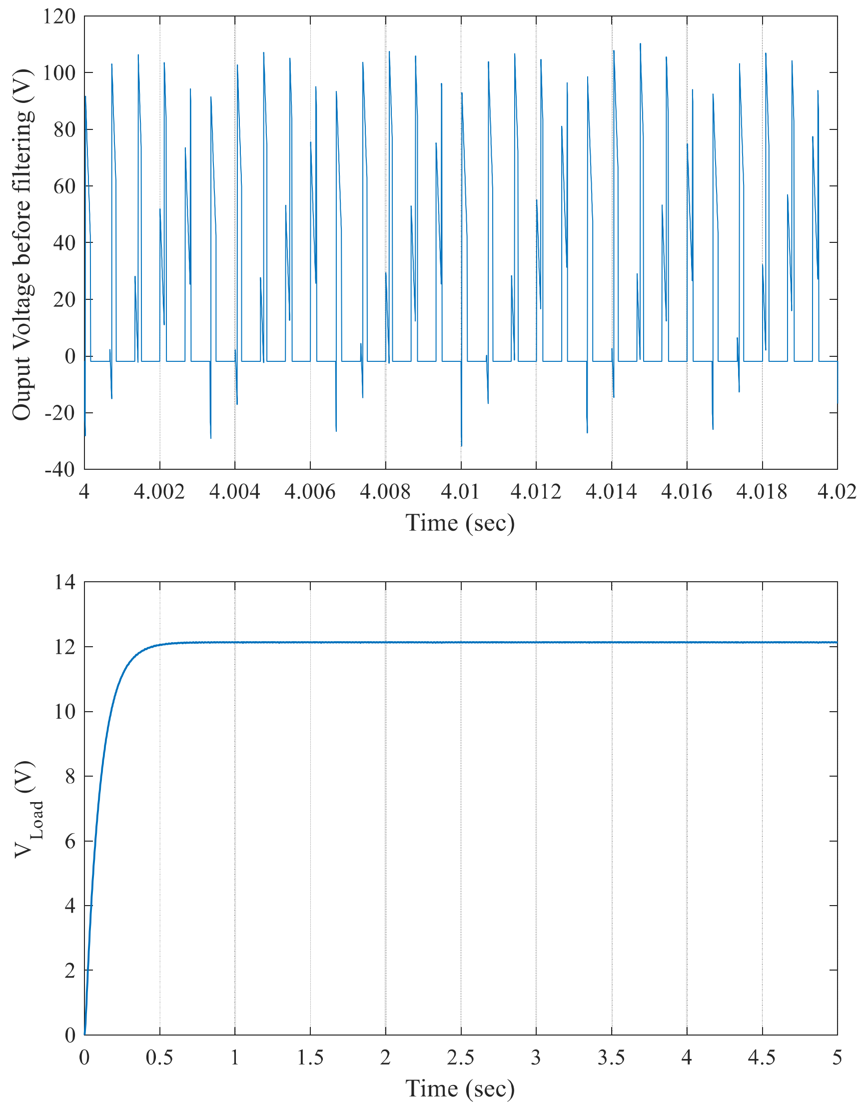

FIGURE 3.28: Output Voltage before and after filtering at output voltage $12V$ with $\theta_r = 0°$

TABLE 3.5: Characteristics of the Controlled Rectifier for Load Voltage 12 V

Firing Angle (°)	Modulation Index	Peak Magnitude of the Phase Current (A)	Total Harmonic Distortion of the Phase Current (%)	Angle of the Phase Current (°)	Power Factor	Real Power, P (W)	Reactive Power, Q (VAR)	Power Supplied to the load (W)	Peak Off Voltage across the MOSFETs (V)	Peak Reverse Voltage across the Diodes (V)	Peak value of the Current through the Switches (A)	Peak Absolute Value of Voltage across Capacitor of the Current Filter (V)
-72	0.8984	12.5236	0.9645	-70.7400	0.3265	185.3440	-536.5348	145.4627	287.7420	285.9032	12.6511	152.9940
-60	0.4766	6.5791	0.8075	-54.2700	0.5811	171.8989	-240.7713	145.9282	141.1139	139.5879	12.4341	80.6494
-48	0.3594	4.9884	1.2293	-39.6000	0.7600	171.6543	-146.7829	146.7001	113.7087	107.4618	12.3847	66.6363
-36	0.3008	4.1724	1.6025	-25.0200	0.9060	169.4912	-79.1638	145.2379	113.3277	108.2101	12.2995	65.6306
-24	0.2734	3.9463	1.4097	-12.0600	0.9778	173.3622	-37.1233	148.2120	118.7874	112.5936	12.4399	67.9423
-12	0.2578	3.8474	1.8350	-0.0900	0.9998	171.4619	-3.1579	146.2145	121.8309	119.2591	12.3664	72.0743
0	0.2578	3.9602	1.6026	11.6100	0.9794	172.5179	35.5564	147.2224	129.3834	127.2519	12.4441	79.4159
12	0.2656	4.1555	1.1374	22.8600	0.9214	171.4300	72.3048	144.9835	141.2758	140.2114	12.3919	84.1242
24	0.2930	4.6713	0.7305	34.2900	0.8262	173.4876	118.3108	146.5763	157.7747	156.1234	12.5009	91.6367
36	0.3398	5.4774	1.1650	43.3800	0.7268	174.9860	165.3842	146.3696	186.0263	184.4173	12.5788	106.3924
48	0.4219	6.7697	0.9847	53.1000	0.6004	179.1630	238.6409	146.7295	223.3348	221.7820	12.7033	123.0160

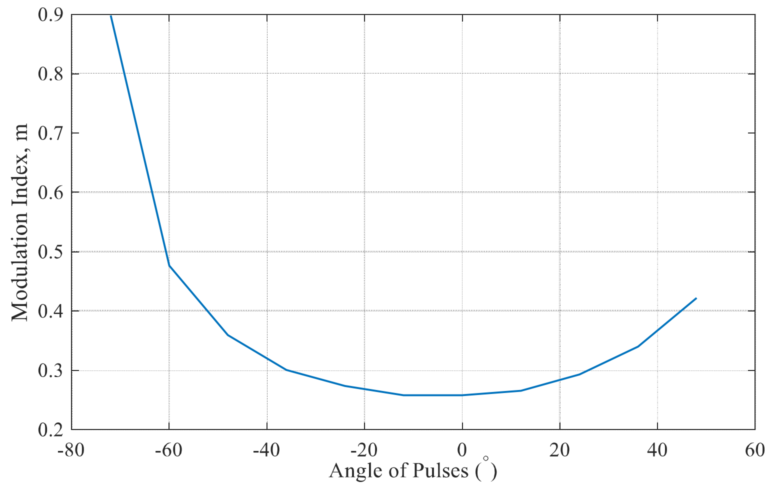

FIGURE 3.29: Modulation Indexes for Different Firing Angles at Load Voltage $12V$

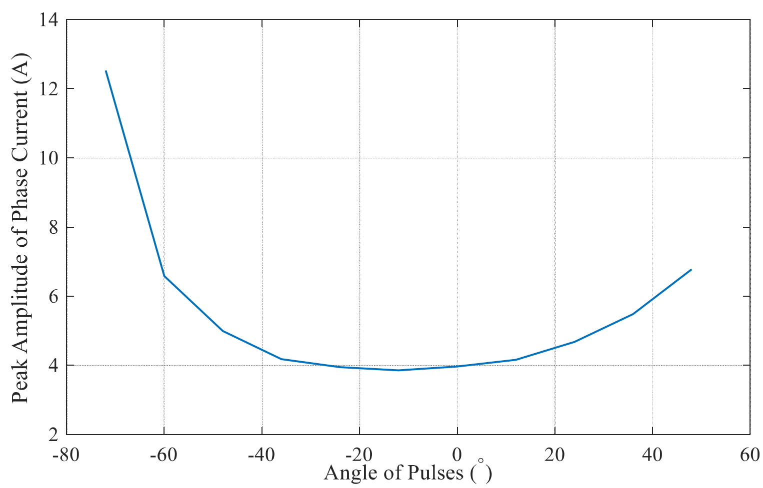

FIGURE 3.30: Peak Amplitude of Phase Current at Load Voltage $12V$

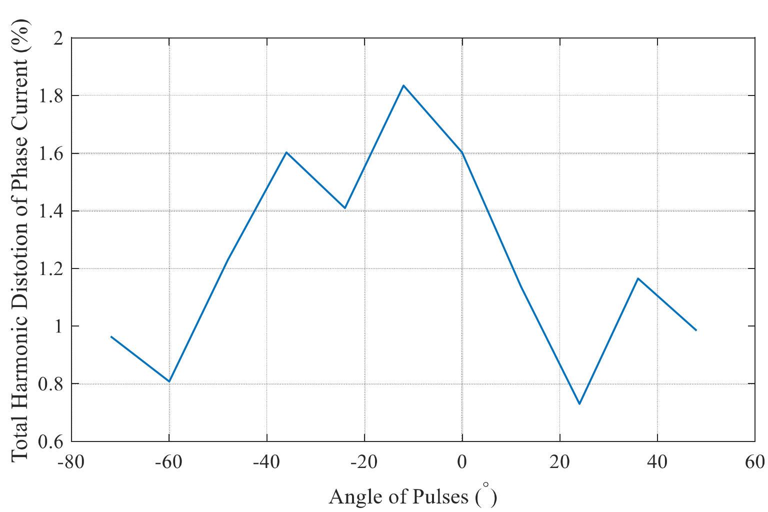

FIGURE 3.31: Total Harmonic Distortion of Phase Current at Load Voltage $12V$

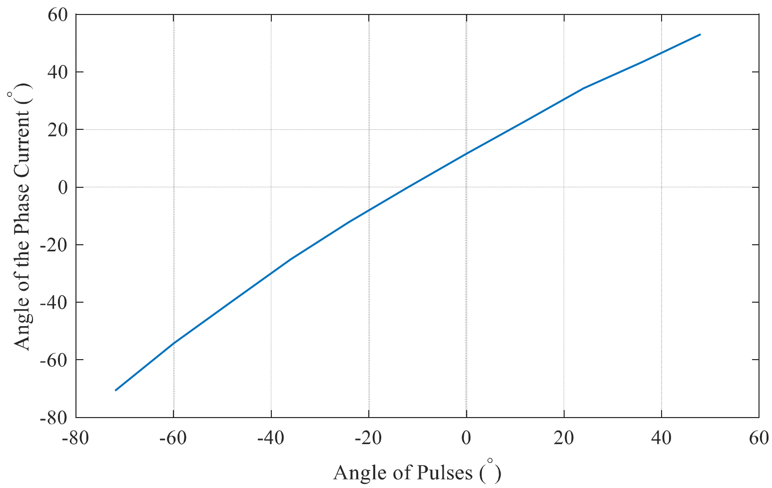

FIGURE 3.32: Angle of the Phase Current at Load Voltage $12V$

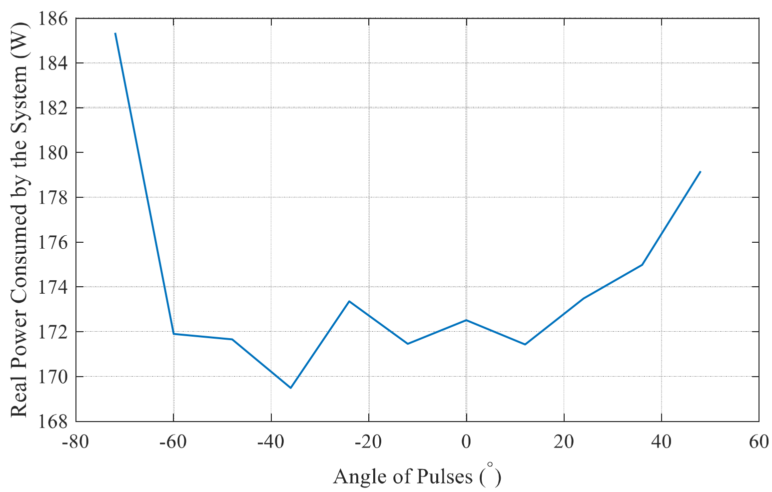

FIGURE 3.33: Real Power Consumed by the System at Load Voltage $12V$

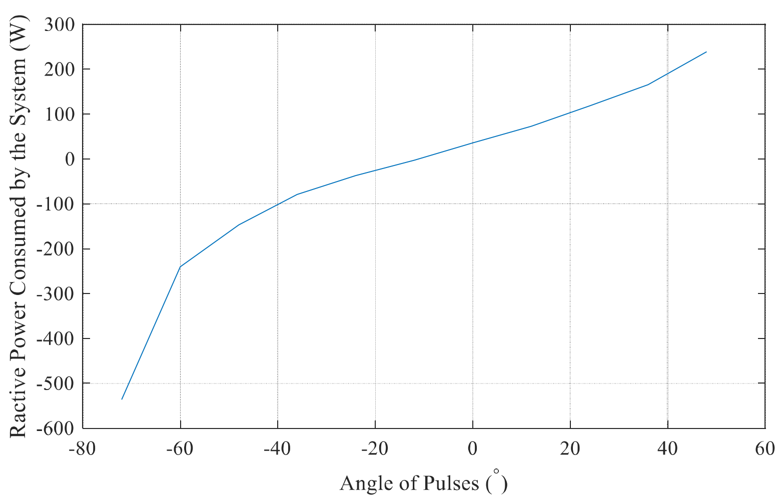

FIGURE 3.34: Reactive Power Consumed by the System at Load Voltage $12V$

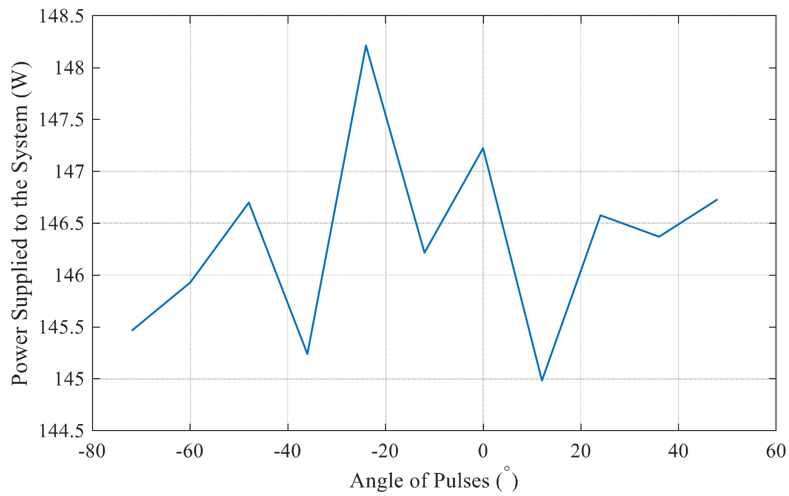

FIGURE 3.35: Real Power Consumed by the System at Load Voltage $12V$

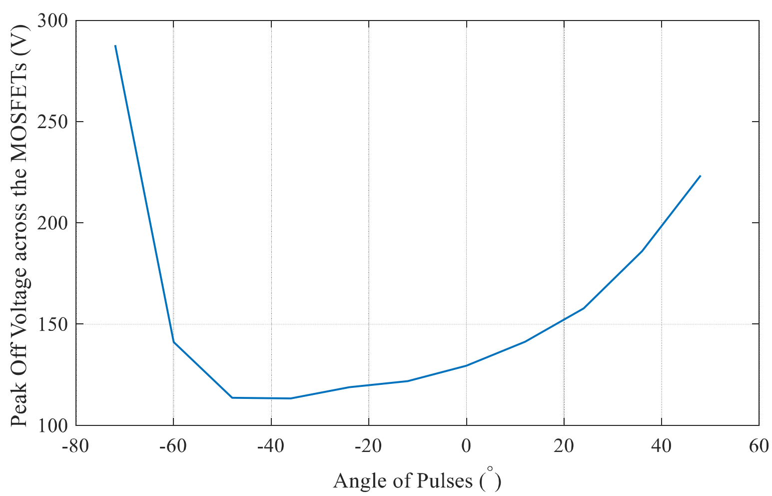

FIGURE 3.36: Reactive Power Consumed by the System at Load Voltage $12V$

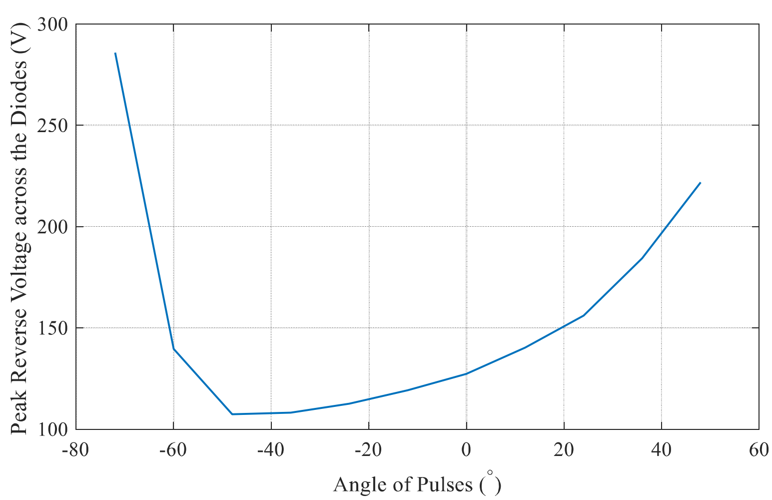

FIGURE 3.37: Real Power Consumed by the System at Load Voltage $12V$

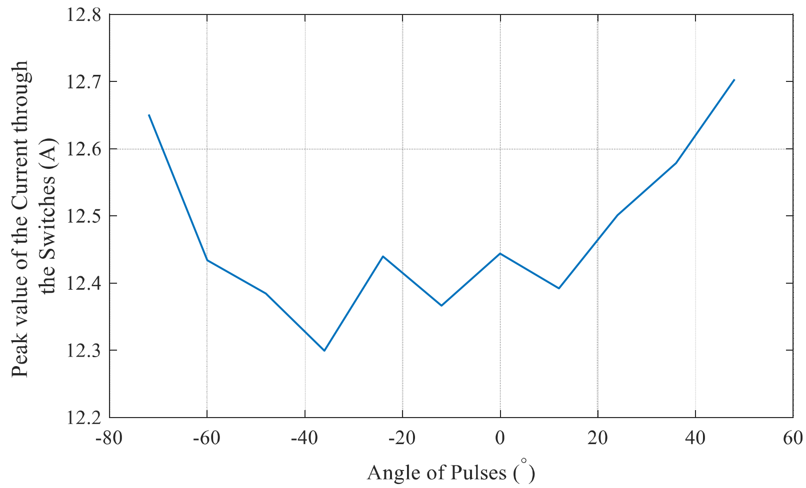

FIGURE 3.38: Reactive Power Consumed by the System at Load Voltage 12V

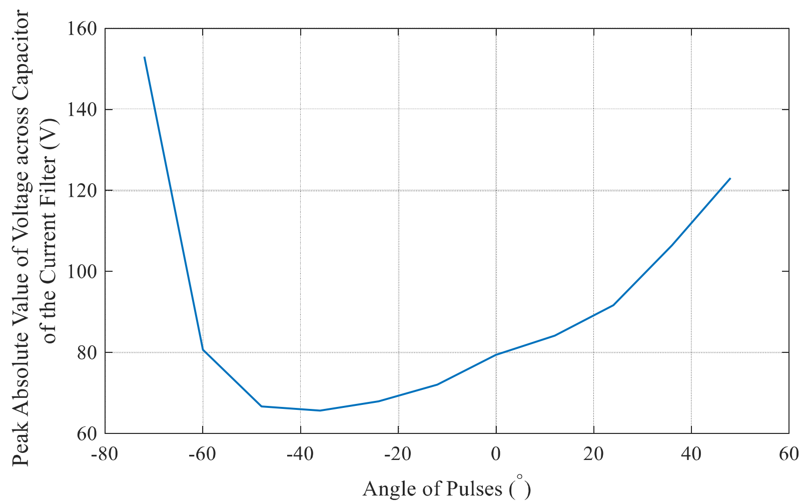

FIGURE 3.39: Peak Absolute Value of Voltage across Capacitor of the Current Filter at Load Voltage 12V

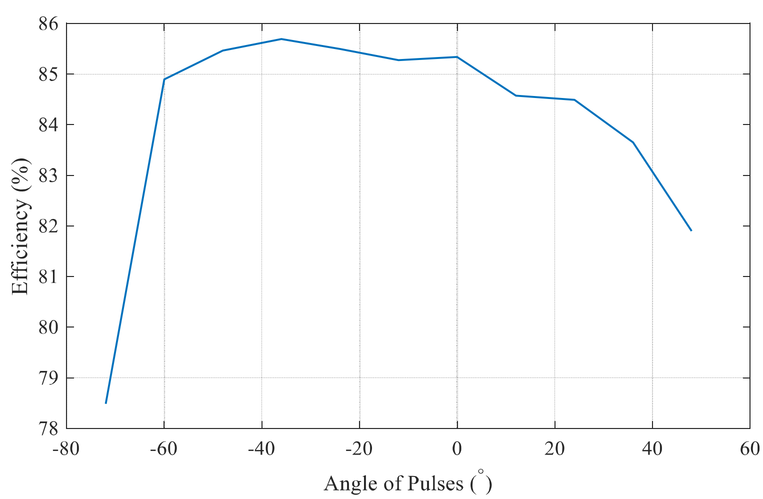

FIGURE 3.40: Efficiency of the system at Load Voltage 12V

Chapter 4

Hardware Implementation of SVPWM Rectifier

The simulated system was totally implemented in hardware. Hardware circuits can be divided into four categories : Phase Locked Loop for Synchronization, PWM Pattern Generation Circuit, Gate Driving circuit and Main Rectifier.

4.1 Phase Locked Loop for Synchronization

A Phase Locked Loop is required to synchronize the pulses with line voltages. That is why, a zero crossing detector circuit needs to detect the zero crossings of phase in terms of square pulses. At first a optocoupler was used to detect the zero crossings of phase a. A transformer was used to downsize the high voltage and then the downsized voltage was sent to the optocoupler. Optocoupler IC 4N25[29] was used in this purpose. A current limiting resistor was added in in series with the secondary side of the transformer and optocoupler's light emitting diode. This resistor selection was done according to the datasheet of IC 4N25 so that current through the light emitting diode was under the maximum value. The npn transistor of the optocoupler was connected to the ground by emitter and to the VDD(5V) by collector via a 1kΩ resistor. By this arrangement, the collector point of the transistor served as an inverted output.

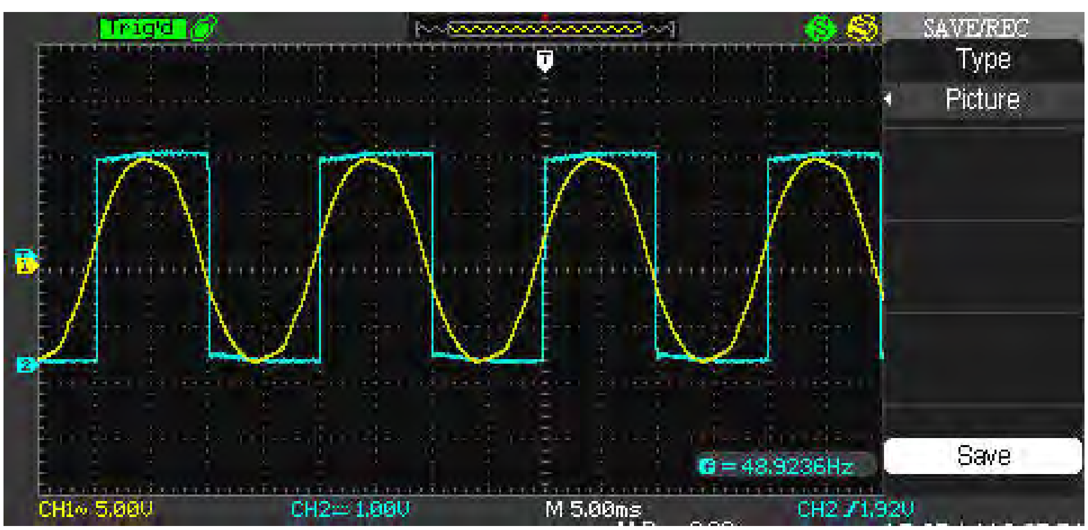

FIGURE 4.1: Zero Crossing Detection by Operation Amplifier(Yellow: Transfomer's Secondary Voltage and Blue: Operational Amplifier's Output)

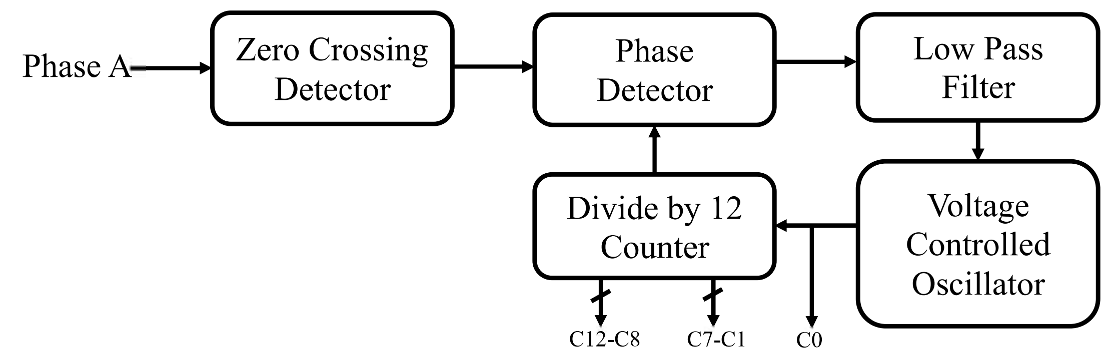

FIGURE 4.2: Phase Locked Loop

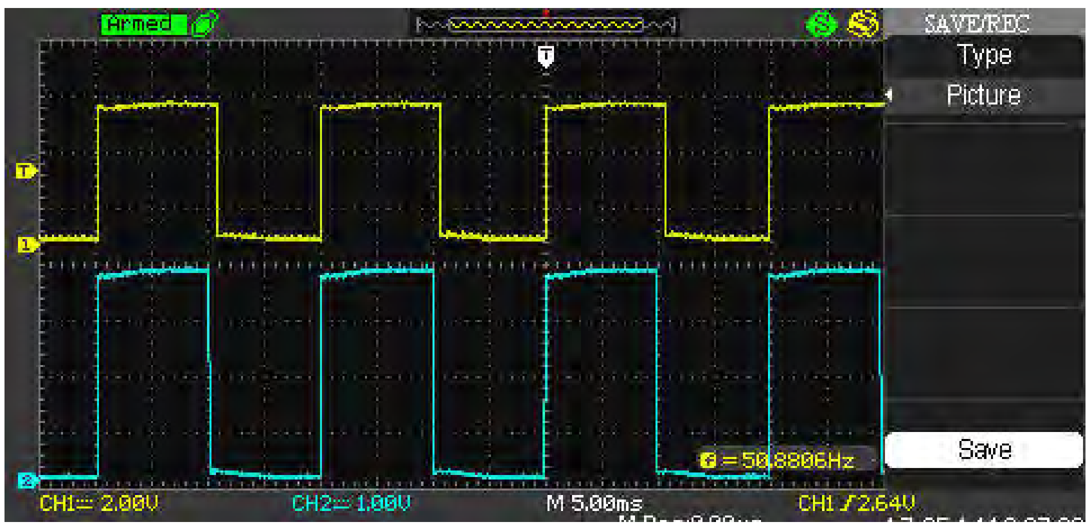

FIGURE 4.3: Synchronization of the Input Signals of the Phase Detector(Yellow: From Counter and Blue: From Comparator)

Another arrangement was also possible in which The resistor is connector between emitter and ground instead of the VDD and collector. And then, the emitter served as a non-inverted output. But the output was not sharp enough to be compatible with the following PLL circuit. That is why, a comparator built with operational amplifier was used to detect the crossings. LM324[30] operational amplifier was selected in this purpose because it can be driven by biasing only by one voltage source which is sufficient tin this application. The downsized voltage waveform of the phase a was further reduced by a voltage divider circuit by two resistors so that the seen input by LM324 was smaller than the biasing voltage. But theoretical values of the resistors did not served as expected. So, the fixing the ground side resistor to 1kΩ, the other one was varied in the ascending order. The lowest resistor which allowed the output with square pulses to the consistent with the input was selected. The detected output with the input has been showed in Figure 4.1.

The output of the comparator served as the input of a Phase Locked Loop System (Figure 4.2). The Phase Locked Loop has been implemented by a PLL IC CD4046[31] and a digital counter IC CD4040[32]. The PLL IC has a built-in voltage controlled oscillator in it whose output serves as the clock of the counter. The highest bit of the counter is sent to the Phase Detector which remains in synchronization with the output of the comparator. Phase detector's

output is passed through a low pass filter and conveyed to the input of the voltage controlled oscillator. The low pass filter was a normal R-C filter. The resistance and capacitance of the filter was chosen according to the datasheet of CD4046[31]. The synchronized signals at the phase detector are shown in Figure 4.3.
For the application purpose, the time period of the line voltage was required to be divided among 30 equal time lengths. The used counter IC CD4040 in the Phase Locked Loop system has 12 outputs. Including the input clock from the voltage controlled oscillator, it has the ability to serve the time division purpose with resolution of 8 bits per time length. To reset the counter some extra logic gates were included in the circuit. Figure 4.4 shows the time division.

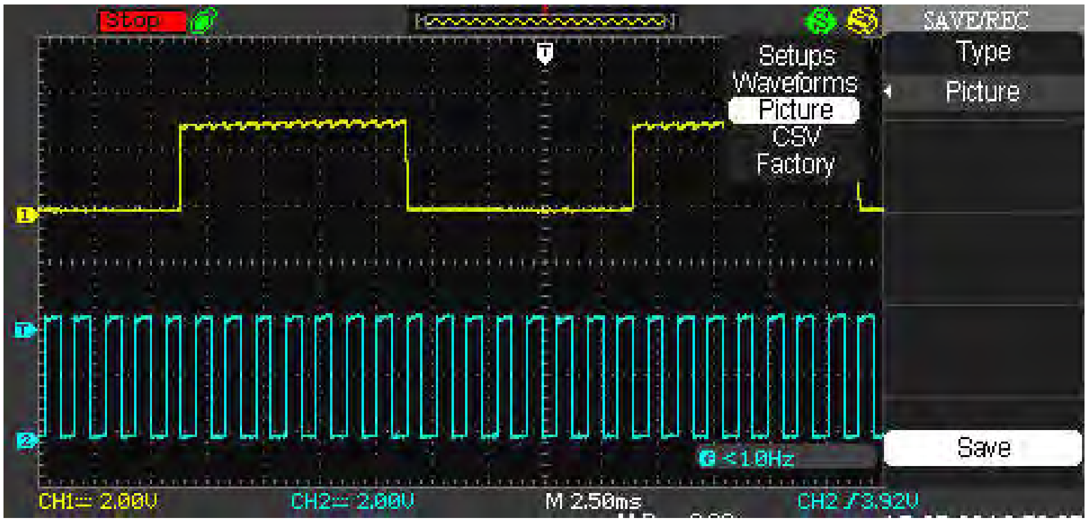

FIGURE 4.4: Division of One Time period into 30 equal timelengths(Yellow: From Zero Crossing Detector and Blue: From Counter C8)

4.2 Pattern Generation Circuit

The pulse generation circuit is basically a memory based circuit. The pulses required for each gate for a faction of time of a period are stored in EEPROMs. These pulses are supplied to the gates of the switches when required. The modulation index and firing angle are determined from two potentiometer's output which respectively control the output voltage and input power factor. These output are read by ADCs of a microcontroller. The microcontroller uses its interrupts to be synchronized with the PLL and ensures that every gate gets its proper signal.
From Figure 4.2, the 12 bit counter in the system, which with its clock actually can give a total 13 bit resolution. With 13 bit resolution a time period can be divided into 8192 equal time lengths. But for the ease of calculation and limitation of hardware, a period was divided into 7680 equal time lengths using 13 bits(30 equal time lengths with 8 bit resolution or 30 multiplied by 256). This arrangements gives advantages with a career frequency 30 times of line frequency with each career period dividing into 256 equal time lengths. The selection of career frequency 30 times of line frequency is advantageous because 30 is a multiple of 6 which is the number of sector. And for this work, memory requirements can be reduced by only storing pulses for only one sector by this kind of time division.

+

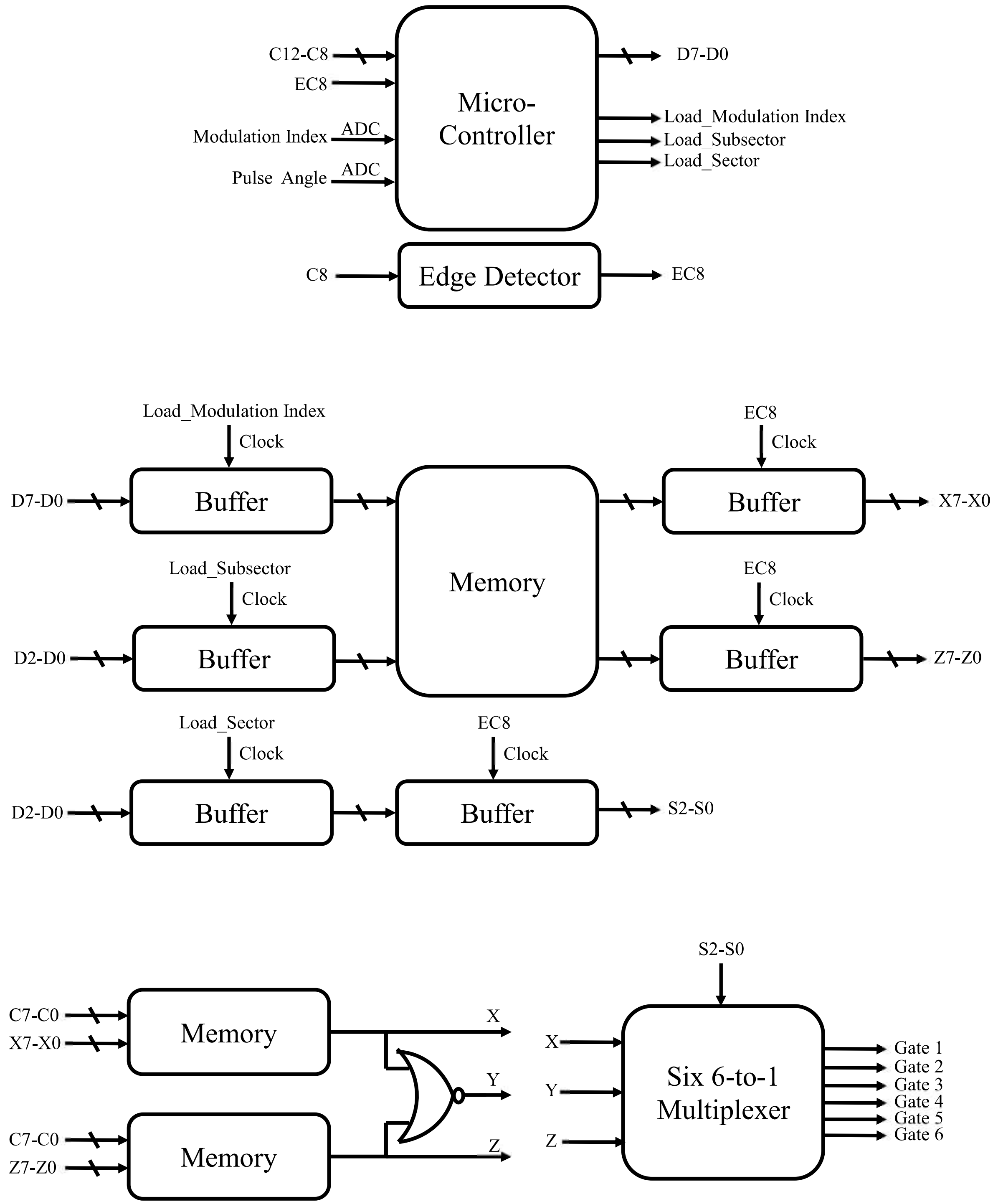

FIGURE 4.5: Pulse Generation Circuit

The C8 of the counter was sent to an edge detection circuit. The edge detection circuit is basically a level to edge converter circuit. The output edges from EC8 were sent to microcontroller to interrupt its normal function. The microcontroller was programmed so that it can be externally interrupted by a rising edge at its interrupt pin. The EC8 were further required as the clock of the second buffer line of Figure 4.5.
The EC8 generates an interrupt in the microcontroller. After each interrupt the microcontroller supplies the pre-calculated modulation index, sector and subsector number respectively through D7-D0. After each time loading the D7-D0 with a particular number, it generates a pulse through the corresponding Load pins(Load Modulation Index, Load Sector, Load Subsector). After completing these, the microcontoller samples the modulation index and firing angles by ADC and calculates it for the next interrupt. It also calculates the current division of the period through C12-C8.
The system generates required duty cycles by modulation index and subsector number. Modulation index was directly obtained deom ADC but the subsector number and sector numbers were calculated from the time division. This task was also done by the microcontroller. The dutycycles were calculated before during the software simulation(Chapter 3). The precalculated dutycycles were stored in the memory units. The edges of C8, EC8 ensures the loading of the duty cycle in the buffers at the right time.
The dutycyles are generated by X7-X0 nd Z7-Z0 pins. These dutycyles are again supplied to memory units containing 1s and 0s which. The memories implement the dutycycles with 256 pulse resolution because of the counter of the PLL. The input dutycyles are all integer numbers less than 256. The memory with X input generated 1s first according to the duty cycles and the rest of the pulses are 0s. The memory with Z input generated 0s first and after that generated 1s according to the number of the dutycycles. The Y pulses are generated by logic synthesis from X and Y pulses. These X, Y And Z pulses are supplied to the proper gates according to the sector number S2-S0. The selection procedure was done by six 6 to 1 multiplexers.
The whole process's pictorial representation has been shown in Figure 4.5. The digital ICs used in this process are 8 bit register 74LS273s[33] as buffer, 64kbytes EPROM 27C512s[34] as memory and 8 to 1 multiplexer 74LS151[35]. A pulse generated by this circuit for gate 1 has been shown in Figure 4.6. The pulse is totally similar to the pulses of Figure 3.2 and 3.3.

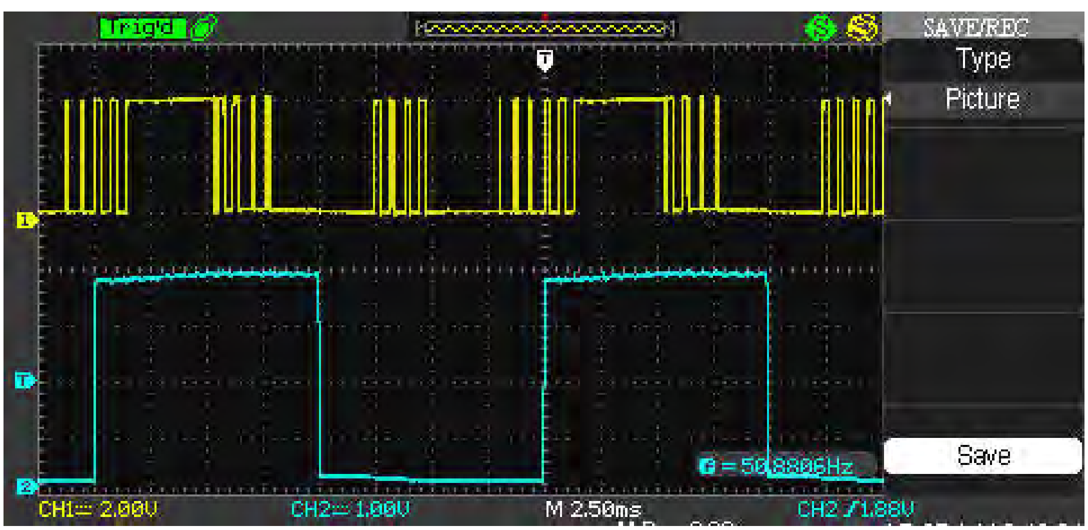

FIGURE 4.6: Generated Pulse for Gate 1(Yellow: Generated Pulse for gate 1 and Blue: Zero Crossing Detector's output)

4.3 Algorithm for Real time Pulse generation

To generate real time pulses, a microcontroller was needed which ensured the proper operation of the circuit. Atmega32A[36] served this purpose. By the Double Buffered scheme described in the previous section, real time PWM pattern generation algorithm is stated below:
1. Enable the golabl interrupt.
2. Set the ISC00 and ISC01 of MCVCR to enable the microcontroller to be interrupted at the rising edge at its INT0 pin.
3. Enable the INT0 pin(Incoming Ec8).
4. Declare B2 of PORTD as output and B0, B1 and B7 as input pins.
5. Set PORTA as input and PORTB as output.
6. Initialize Analog to Digital conversion.
7. Continue to read the modulation index and pulse angle in a loop manner and until a interrupt occurs.
8. If interrupted, then follow the interrupt routine below:
a. Set PORTB(D7-D0) as the modulation index.
b. Give a pulse at B0 of PORTD(Load_modulation index).
c. Set PORTB(D7-D0) as the subsector number.
d. Give a pulse at B1 of PORTD(Load_subsector).
e. Set PORTB(D7-D0) as the sector number.
f. Give a pulse at B7 of PORTD(Load_sector).
g. Read the digital count value by least significant 5 bits of PORTA.
h. Determine the sector and subsector number for the next interrupt.
i. Go to step 7.

4.4 Gate Driving Circuit

The generated pulses by the pulse generation circuit must be supplied to the gates of the MOSFETs with proper magnitude and with proper references. To properly turn on a MOSFET the gate pulses should be with respect to their sources. A typical power MOSFET properly turns on when the magnitude of the applied pulse is much greater than the threshold voltage. The compatible MOSFETs for this application requires gate to source voltage of at least 10 V to turn them on. The maximum gate to source voltage is 20V.
The required voltage source for the pulse generation circuit was 5V. So, that is not suitable to supply required voltage to the MOSFETs. 12V fixed voltage sources would have been perfect for this purpose. At least 4 such sources were required for the six MOSFETs because three of them are tied together by their sources. Unfortunately, four 12V fixed voltage sources for this purpose would have been very costly. Batteries availabe in market become costlier with

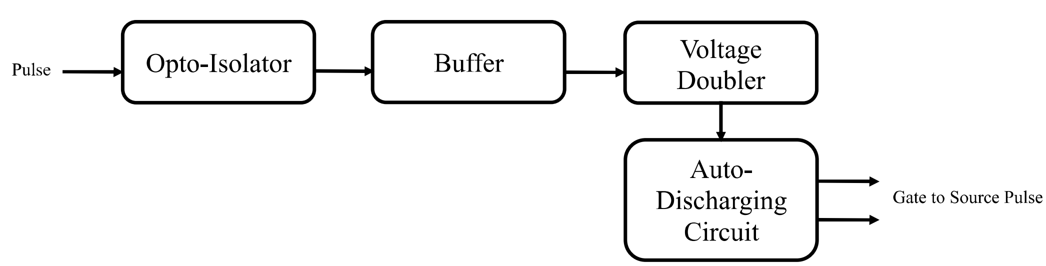

FIGURE 4.7: Block Diagram of Gate Driving Circuit

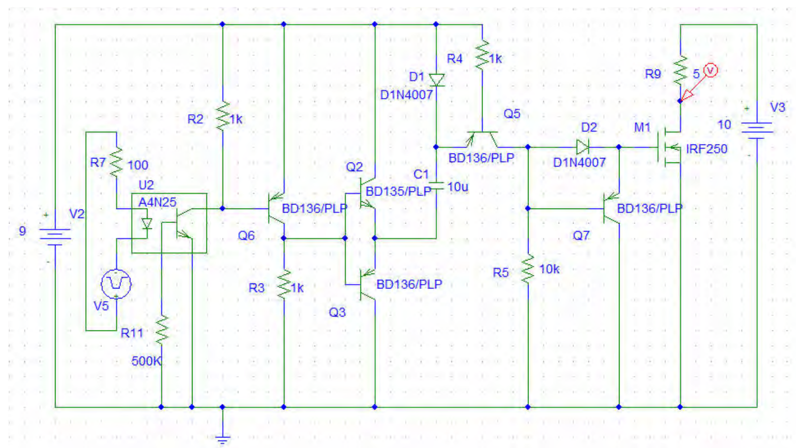

FIGURE 4.8: Practical Gate Driving Circuit

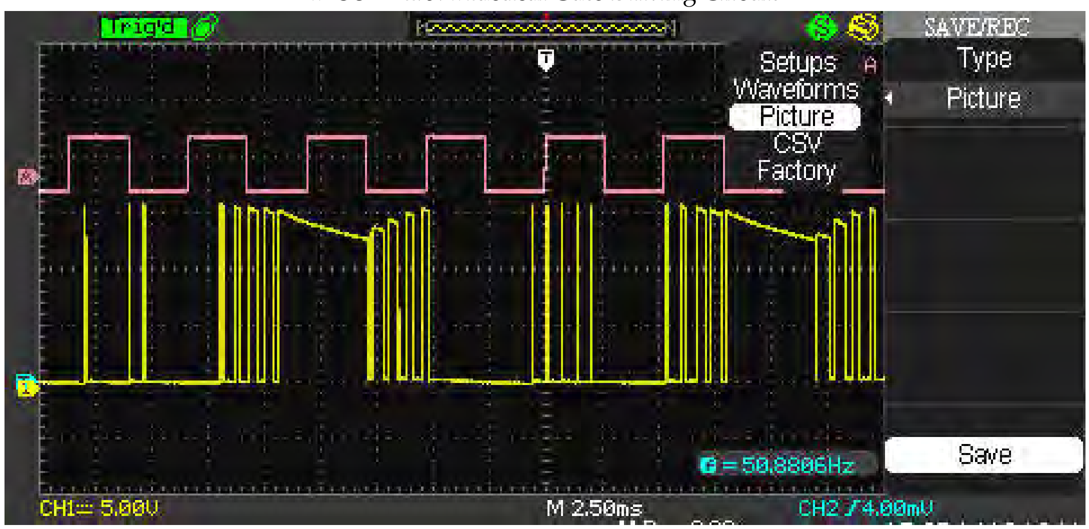

FIGURE 4.9: Pulses Generated by the Gate Driving Circuit(Yellow)(Pink coloured waveshape is a reference from the oscilloscope)

the preciseness and supply voltage by then reduces with time which have a strong possibility to interrupt the normal behaviour of MOSFET. That is why, a proper technique was required which can uninterruptedly supply the required biasing voltage to the MOSFETs. And another important thing here is the isolation. As three sources are tied so there are actually four seperatd nodes which will act as the reference point of the gates of six MOSFETs. And for protection, the reference nodes should be isolated from the ground of the pulse generation circuit.

So, at first, the pulses from pulse generation circuit is isolated by optoisolators. 4N25 ICs[29] were used in this purpose. The opto-isolated outputs are then passed through a buffer circuit and a voltage doubler circuit. These circuits are biased by 9V batteries. These batteries are very low cost and available everywhere. But the 9V voltage is not suitable to turn on a MOSFET when required. That is why, the voltage doubler circuit was used which stored energy when there was no pulse and then whenever the pulses required to be conveyed to the gate, the stored energy adds up with the biasing 9V voltage as series voltage source and doubled the voltage. This procedure ensured lowest possible on resistance of the MOSFET to exist while operation.

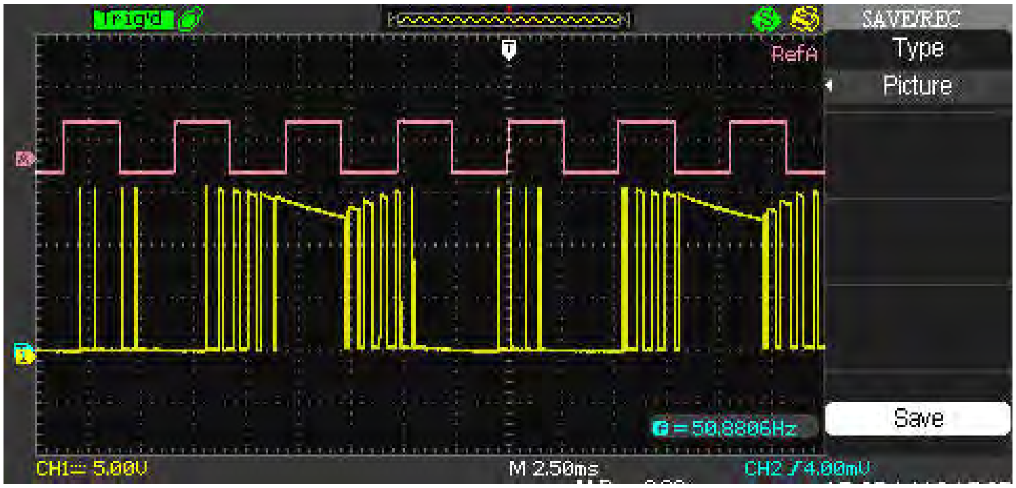

FIGURE 4.10: Effect of Change of Modulation Index: Highest Modulation Index(Pink coloured waveshape is a reference from the oscilloscope)

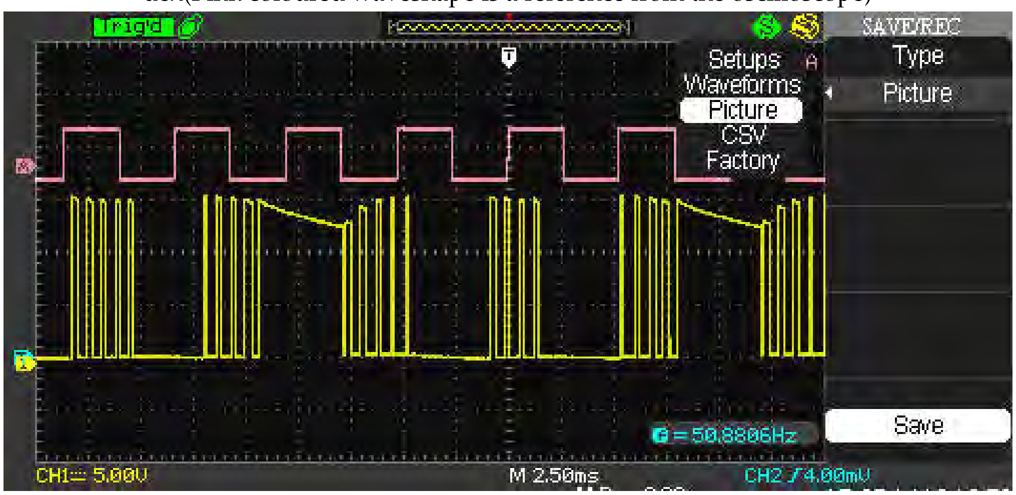

FIGURE 4.11: Effect of Change of Modulation Index: Medium Modulation Index(Pink coloured waveshape is a reference from the oscilloscope)

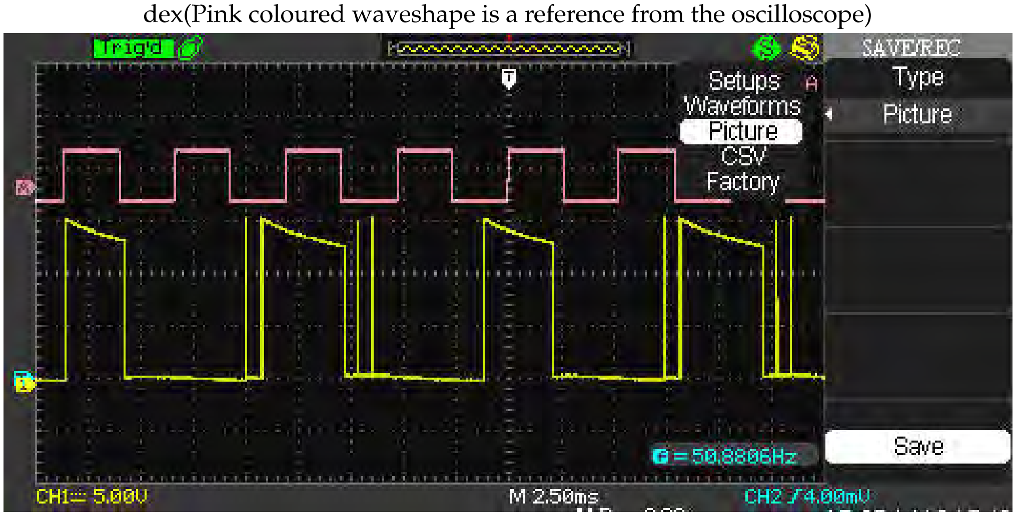

FIGURE 4.12: Effect of Change of Modulation Index: Lowest Modulation Index(Pink coloured waveshape is a reference from the oscilloscope)

When a MOSFET should be turned off, not only removing the applied voltage is enough to turning it off. There is a stray capacitor between MOSFET's gate and source. This capacitor become charged during the pulse voltage. When ever the MOSFET should be turned off, it is required to pull the charges out of the capacitor to pull down the gate to source voltage less than the threshold voltage. An extra mechanism was added with the help of a pnp transistor between MOSFET's gate and source so that the stray capacitor's charge did not stay in it during the off-time. This mechanism could have been replaced with high resistance between the gate and source. But, that would have resulted an increased off time.
The practical gate driving circuit built is shown in the schematic diagram of Figure 4.8. The circuit was built with mainly optocoupler 4N25[29], npn transistor BD135[37], pnp transistor[37] and diode 1N4007[38]. The figure of shown for a single MOSFET and a simple circuit. In the application of the three phase controlled rectifier six such circuit was required to drive the MOSFETs. The pulse generated by the gate driving circuit has been shown in Figure 4.9. The pulses had magnitude fluctuation caused by the voltage reduction of the capacitor by discharging to generate the pulses.
One feature of the pulse generation circuit was to control the pulse angle and modulation index to change the magnitude and phase of the current. This was performed by analog to digital conversion by the microcontroller. The microconytoller was programmed to regulate the phase angle from $-36°$ to $36°$ at $12°$ step. The modulation index change results can be observed Figures 4.10, 4.11 and 4.12. The change of the phase angle over the pulse for gate 1 can be observed from Figure 4.13 to 4.19.

4.5 Rectifier Circuit

The main rectifier circuit was comparatively easy to build in respect to the pulse generation and gate driving circuits. Following Figure 3.4, the MOSFETs and diodes were placed and connected through wires with sufficient thickness so that a large amount of current can flow. Application and regulation for unit power factor suggest that a large amount of current depending on the capacitor of the current filter should be pulled by the rectifier. That is why, the MOSFETs and diodes were also needed to be capable of conducting large current without heat dissipation. In other words, the on resistances of both the MOSFETs and diodes should have

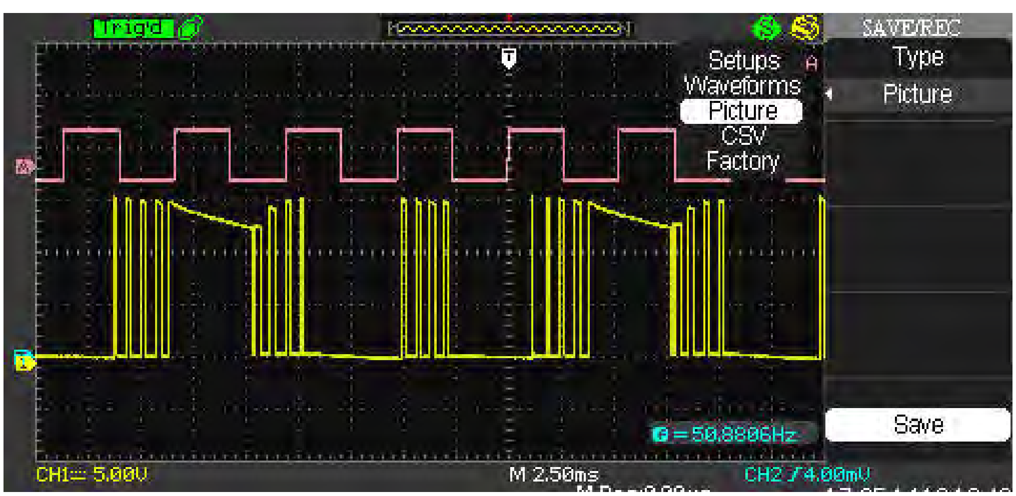

FIGURE 4.13: Effect of Change of Pulse Angle: Pulse Angle=$-36°$(Pink coloured waveshape is a reference from the oscilloscope)

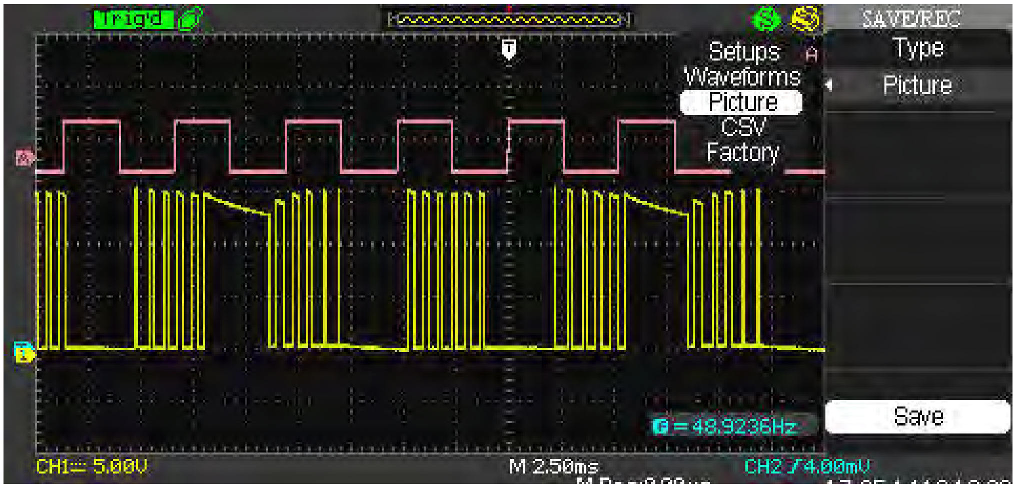

FIGURE 4.14: Effect of Change of Pulse Angle: Pulse Angle=−24°(Pink coloured waveshape is a reference from the oscilloscope)

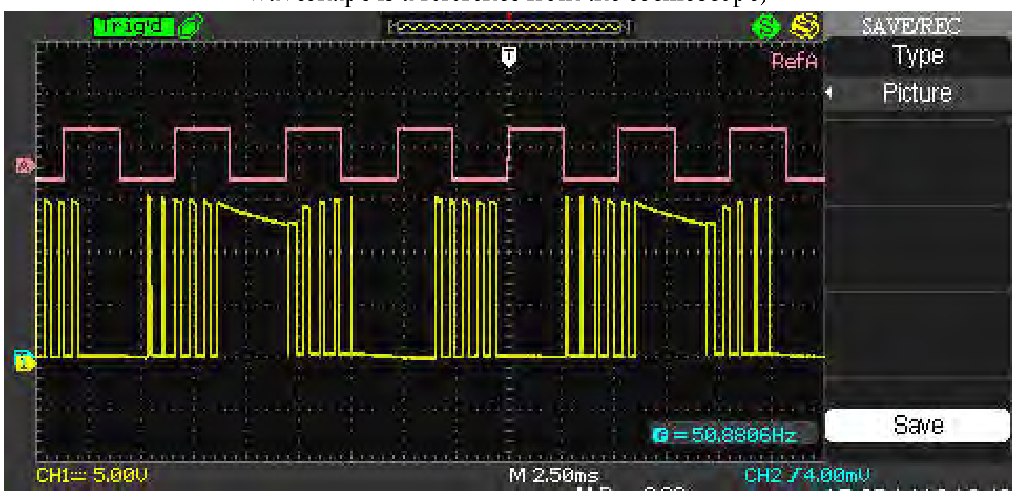

FIGURE 4.15: Effect of Change of Pulse Angle: Pulse Angle=−12°(Pink coloured waveshape is a reference from the oscilloscope)

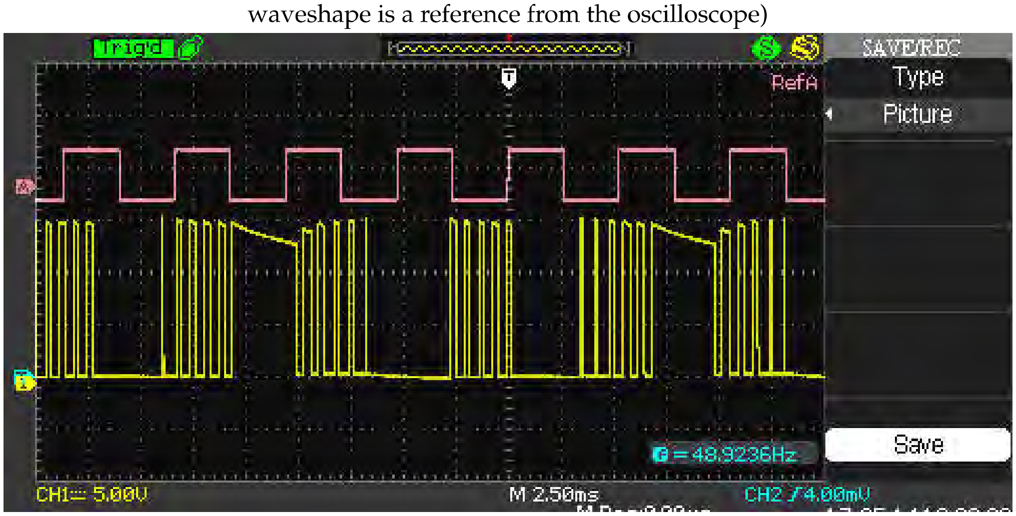

FIGURE 4.16: Effect of Change of Pulse Angle: Pulse Angle=0°(Pink coloured waveshape is a reference from the oscilloscope)

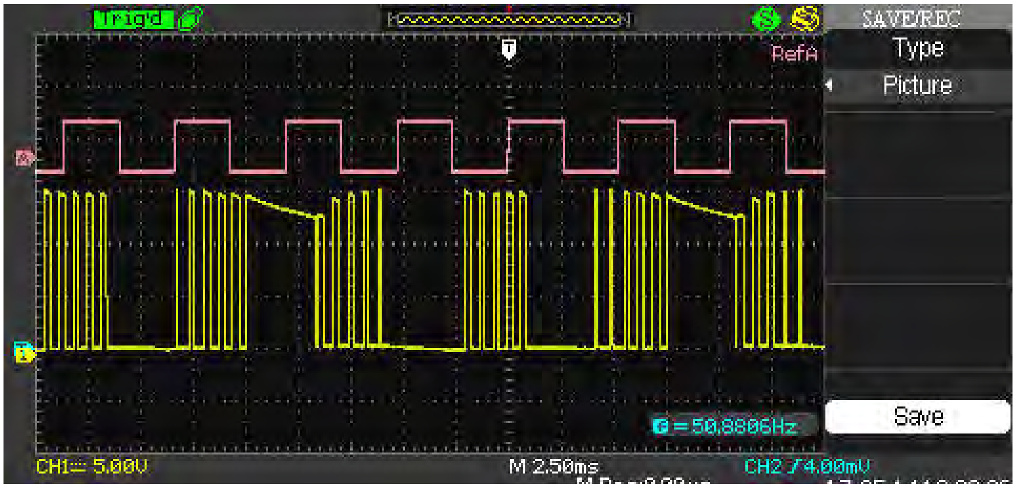

FIGURE 4.17: Effect of Change of Pulse Angle: Pulse Angle=12°(Pink coloured waveshape is a reference from the oscilloscope)

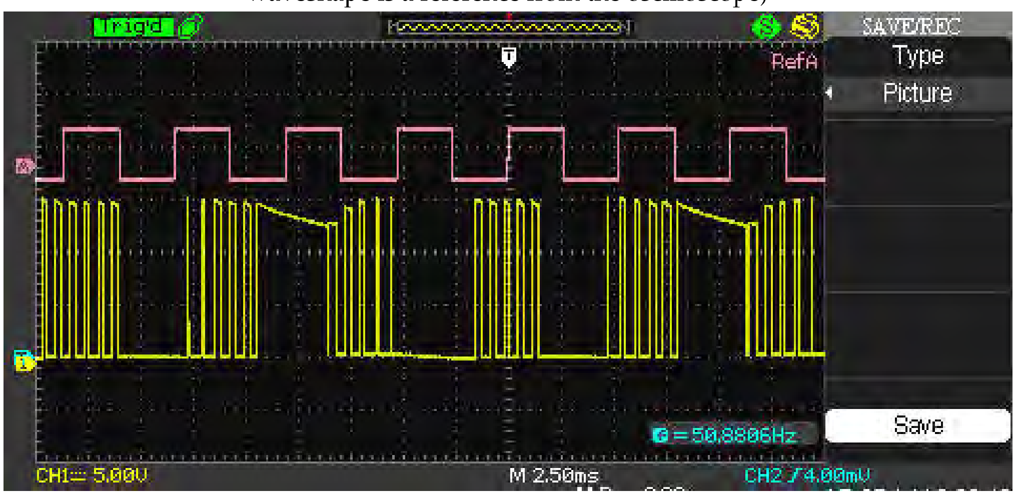

FIGURE 4.18: Effect of Change of Pulse Angle: Pulse Angle=24°

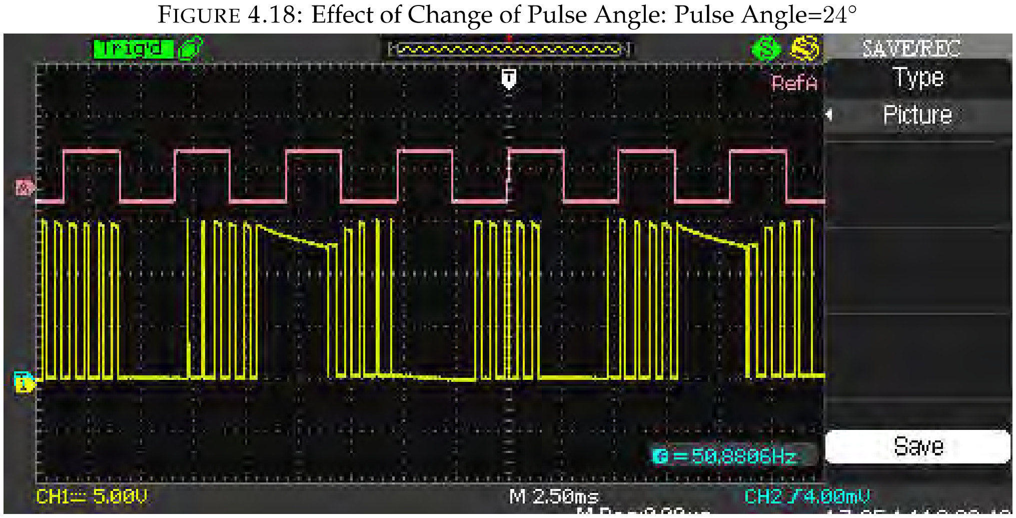

FIGURE 4.19: Effect of Change of Pulse Angle: Pulse Angle=36°(Pink coloured waveshape is a reference from the oscilloscope)

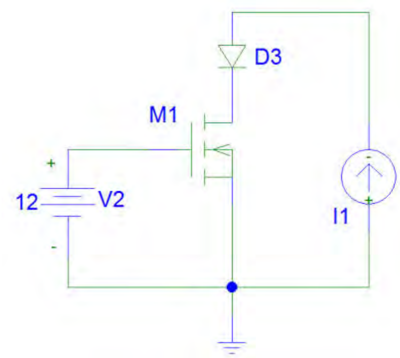

FIGURE 4.20: Circuit for Switch Testing

been very low. According to the datasheets a number of MOSFETs were eligible for this purpose. But practically, most of them do not match with the datasheets in practical behaviour. To test the switches the circuit in Figure 4.20 was built and the MOSFET and diode was replaced with available ones in market. The current of the current was increased and on resistance of the switches was calculated. Also it was observed if the heat dissipation of the switches were compatible. By this procedure MOSFET IRFP250N[39] and diode MBR30H200CT[40] were chosen for this work.

4.6 Circuit Assembly and PCB prototyping

The total circuit was at first built in breadboards. At first the circuit was built part by part and then they were assembled together. The pulse generation circuit and the gate driving circuit built in breadboards can be seen in Figure 4.21 and 4.22.

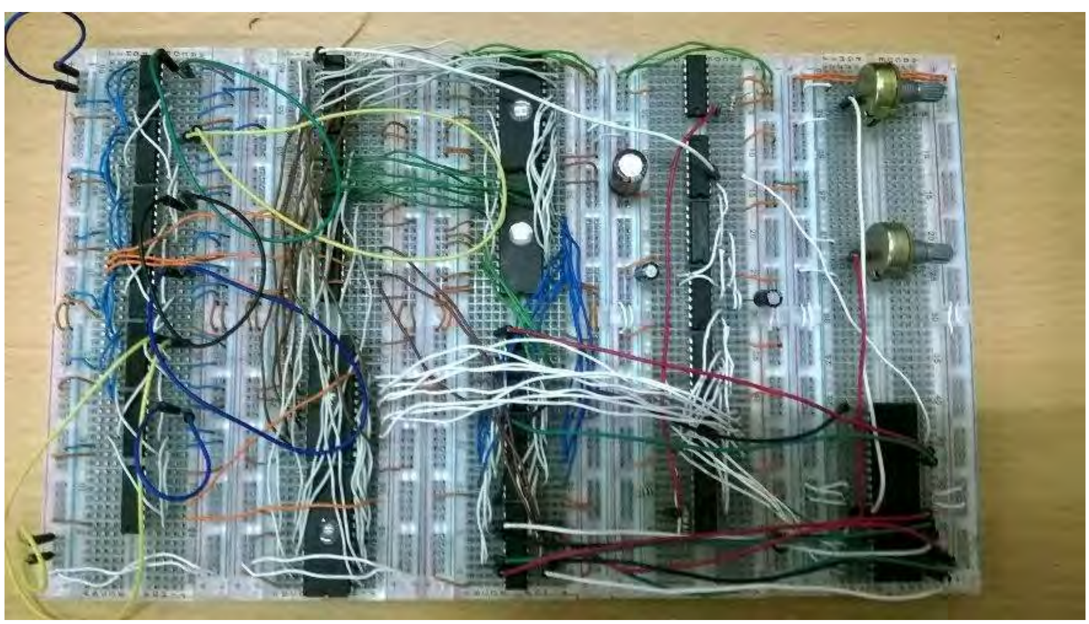

FIGURE 4.21: Built Pulse Generation Circuit in Breadboards

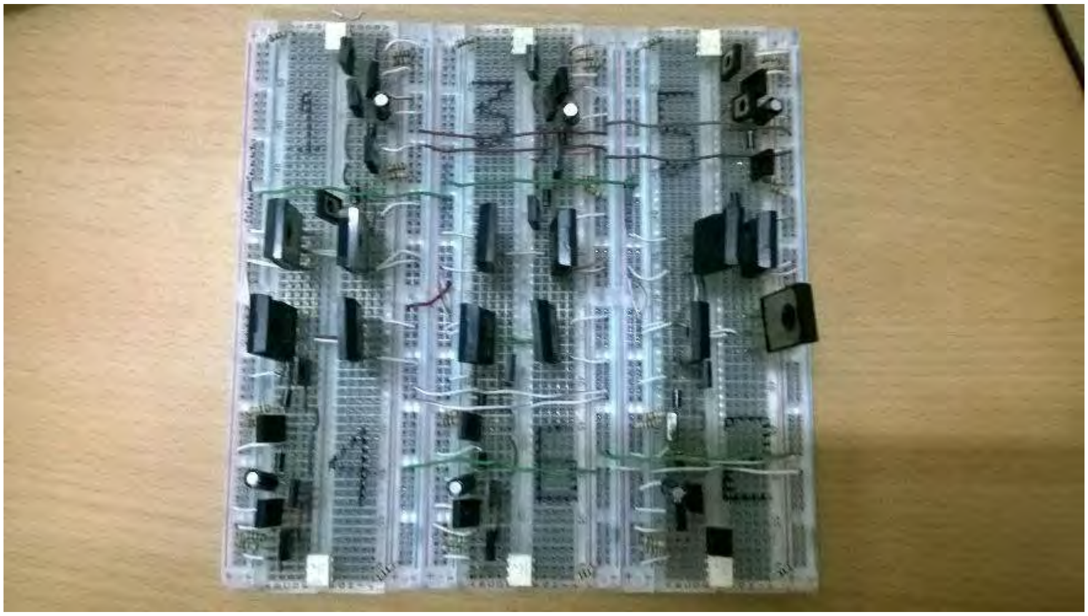

FIGURE 4.22: Built Gate Driving Circuit in Breadboards

After proper testing and verification the circuit was implemented in printed circuit board or PCB. For that purpose, the circuit was built in Proteus(Figure 4.23 to 4.27). Then PCB version of the circuit was then designed(Figure 4.28).

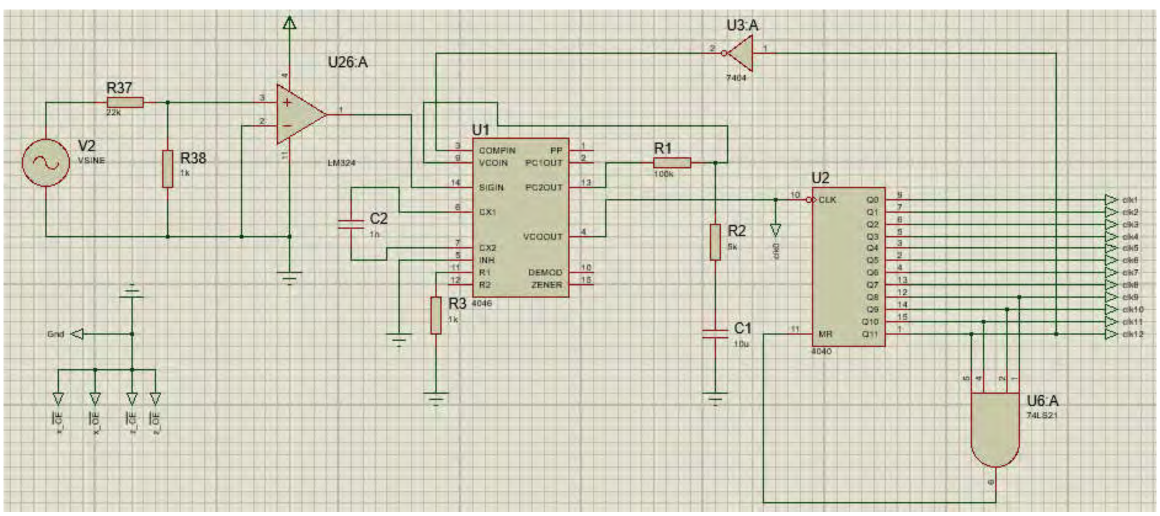

FIGURE 4.23: Phase Locked Loop Circuit built in Proteus

4.7 Outputs

Three small resistors(0.5Ω) was connected in each phase prior to the rectifier to observe the waveshapes of the currents. Current was forced to lead or synchronize with the input voltage(shown in Figure 4.29 and 4.30). Rectified output voltage is also shown in Figure 4.31.

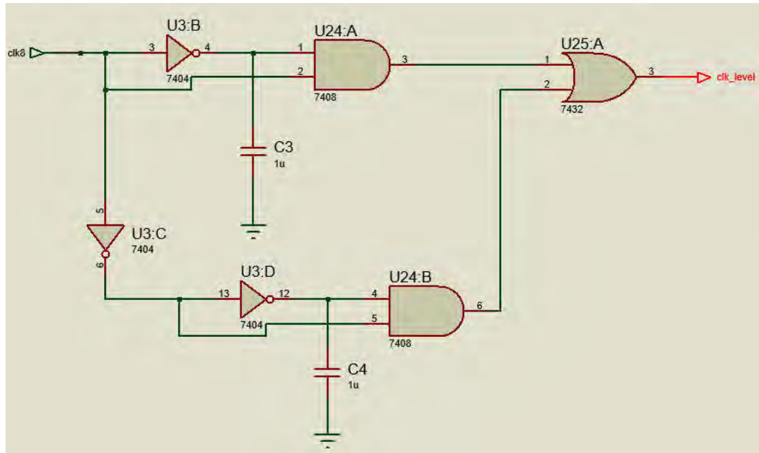

FIGURE 4.24: Edge Detector Circuit built in Proteus

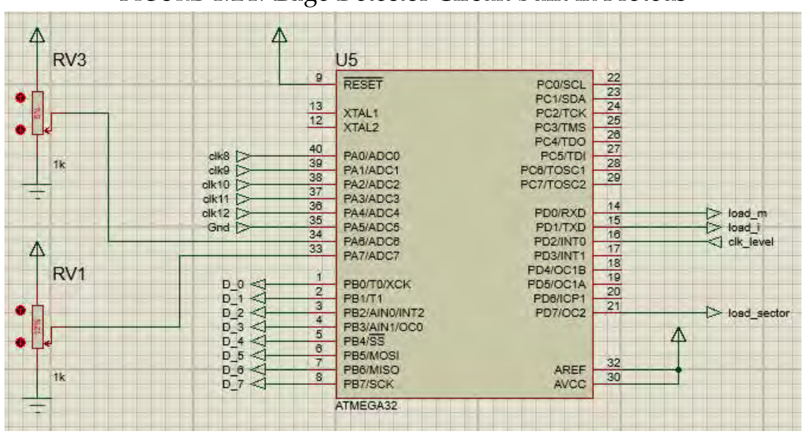

FIGURE 4.25: Atmega32A Microcontroller Connection in Proteus

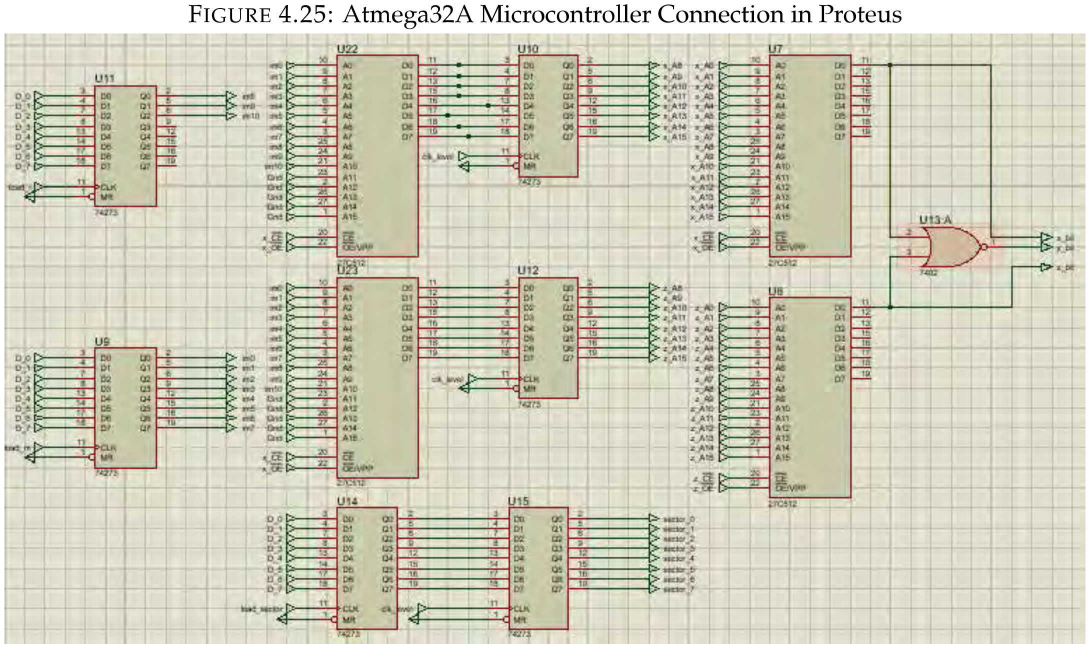

FIGURE 4.26: Double Buffered Circuit with Memory built in Proteus

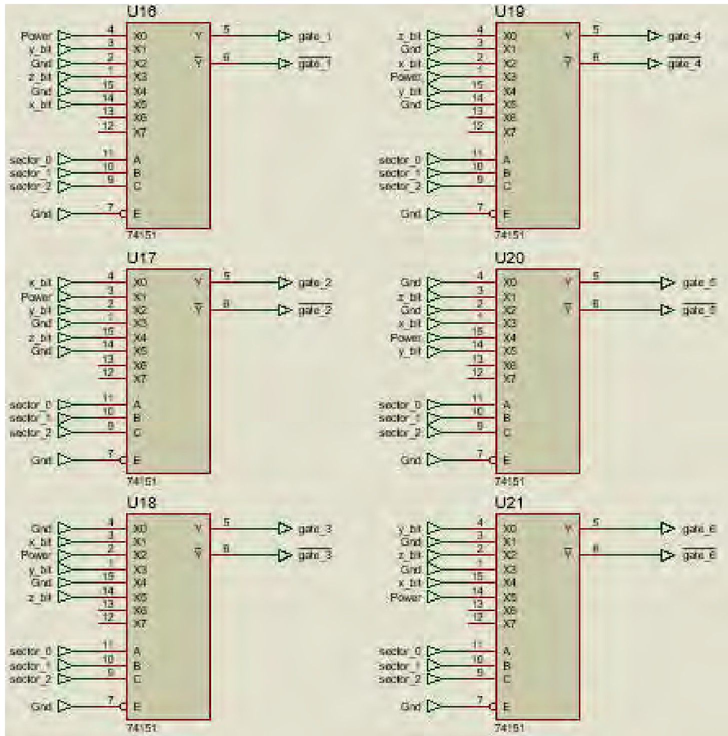

FIGURE 4.27: Six 6 to 1 Multiplexer Circuit built in Proteus

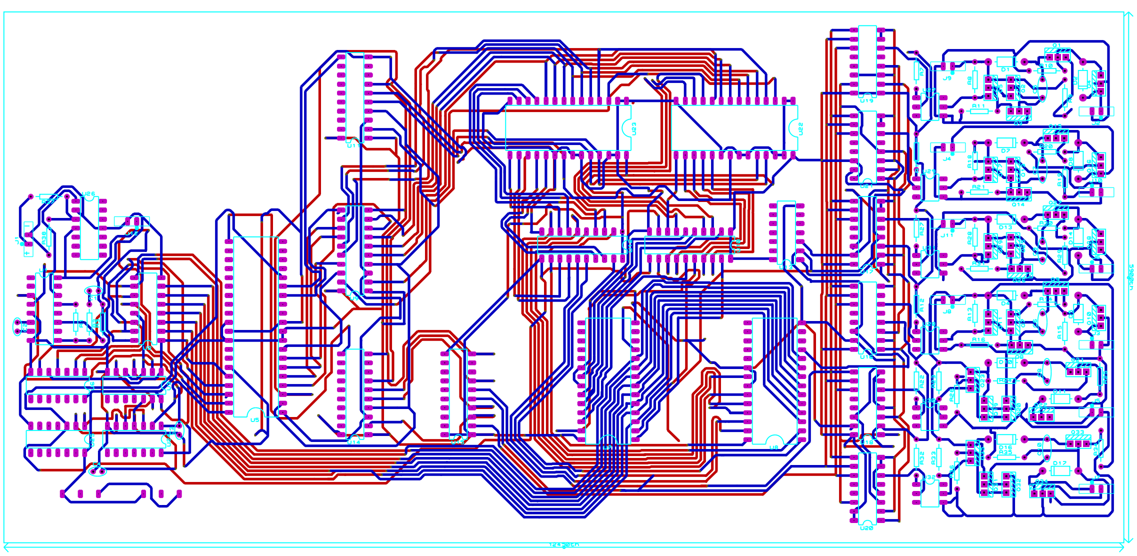

FIGURE 4.28: Designed PCB in Proteus

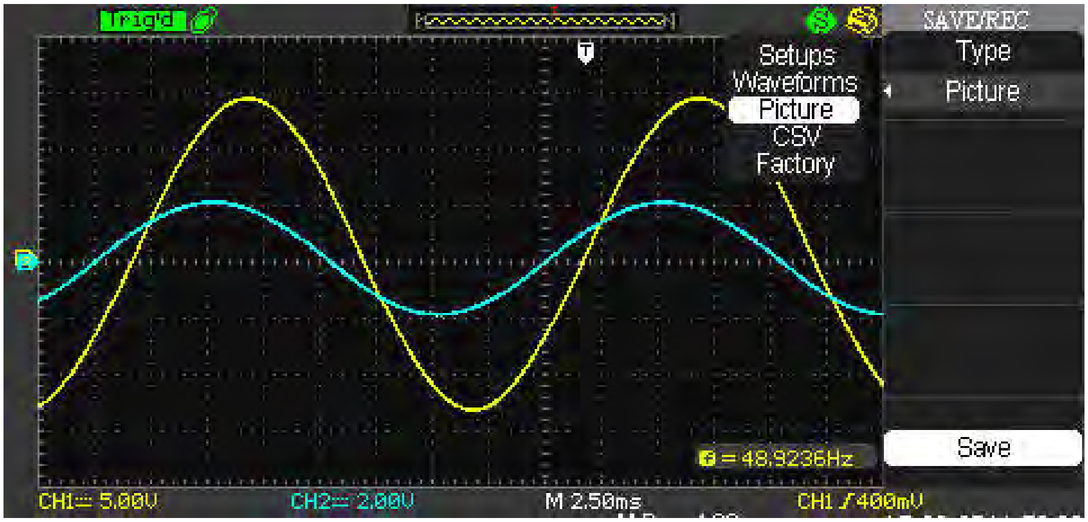

FIGURE 4.29: Input Current leads Voltage(Yellow: Voltage and Blue: Current)

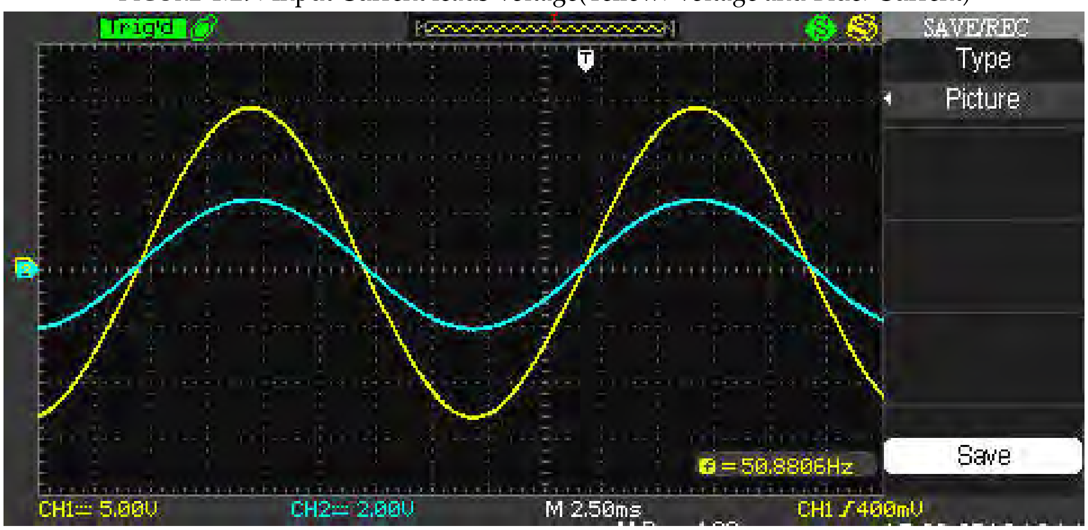

FIGURE 4.30: Input Current and Voltage are synchronized (Yellow: Voltage and Blue: Current)

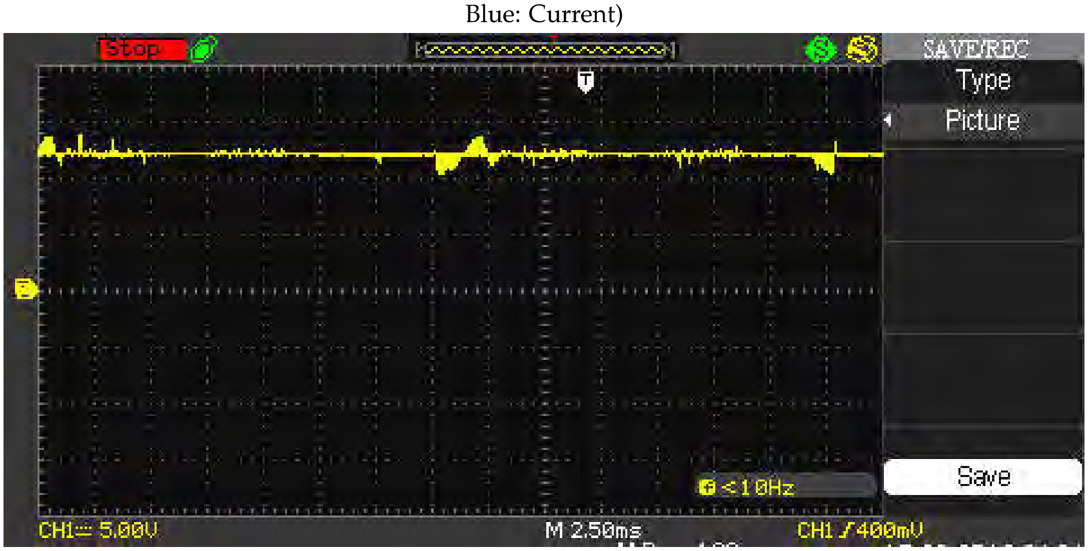

FIGURE 4.31: Rectified Output Voltage

Chapter 5

Conclusion

5.1 Summary and Discussion

In this work, a hardware prototype of three phase variable power factor rectifier has been developed. This has also the capability of compensating reactive power at some extents. At first, on and off time of the switches was calculated by graphical space vector analysis. Calculated times are verified by simulating the rectifier in Matlab Simulink environment. Pulses were generated according to the on and off times. After successful simulation and required voltage, current and power observation, proper circuit components for the work have been selected to implement the rectifier in hardware level. A micro-controller based digital circuit was built to generate the pulses according to the required on and off times. Six MOSFET driver circuits were also built to conduct these pulses to the gates of the MOSFETs of the rectifier. With MOSFETs and diodes with proper voltage, current and power rating, the rectifier circuit was built and tested in laboratory.
Pattern generation by Space Vector reduces hardware complexities comparing other modulation methods such as Sinusoidal Pulse Width Modulation(SPWM). If this work was done using SPWM method, then more than 30 times of memory blocks had to used to store the duty cycles.

5.2 Recommendations

- This system has been designed in a open loop manner with manual control operation for both output voltage and input current angle control. This manual control can be accompanied with close loop feed back control. Two types of feed back will be needed in that case: output voltage or current feedback and condition of grid.
- The control can be made far more sophisticated if real time dq transformation can be done of the voltages and currents. dq transformation will give chance to control real and reactive power separately.
- An LCD display can also be included in the hardware prototype which will show the condition of output voltage/current and input voltage and current.

Bibliography

[1] Yang, T., Bozhko, S. and Asher, G.,"Functional Modeling of Symmetrical Multipulse Autotransformer Rectifier Units for Aerospace Applications," *IEEE Transactions on Power Electronics*, vol. 30, no. 9, pp. 4704-4713, 2015.

[2] Mello, J. P. A., Jacobina, C. B. and Silva, I. R. F. M. D.,"Multilevel Reduced Controlled Switches AC-DC Power Conversion Cells," *IEEE Transactions on Industry Applications*, vol. PP, no. 99, pp. 1-1, 2017.

[3] Wu, J. C., Jou, H. L. and Han, J. J.,"Isolated Battery Charger with Multilevel Rectifier," *IET Power Electronics*, vol. 9, no. 14, pp. 2674-2681, 2016.

[4] Wikipedia, "High-voltage direct current," URL: https://en.wikipedia.org/wiki/ High-voltage_direct_current.

[5] Nicolae, P. M., Nicolae, I. D. and Patru, G. M. I., "Reducing Emissions from an AC-DC- AC Converter to Improve Power Delivery Network Behavior," *2014 IEEE International Symposium on Electromagnetic Compatibility (EMC)*, pp. 138–143, 2014.

[6] Gray, M. K. and Morsi, W. G., "Power Quality Assessment in Distribution Systems EmbeddedWith Plug-InHybrid and Battery Electric Vehicles," *IEEE Transactions on Power Systems*, vol. 30, no. 2, pp. 663–671, 2015.

[7] Pietkiewicz, A. and Tollik, D., "Cost/Performance Considerations for 3-Phase Input Current Shapers," *1st International Telecommunications Energy Special Conference*, Berlin, Germany, pp. 165-170, 1994.

[8] Walther, P., "A New Rectifier System High Efficient, High Dense, Modular, Quick to Install and Superior for Service," *15th International Telecommunications Energy Conference*, Paris, France, vol. 2, pp. 247-250, 1993.

[9] Kolar, J. W. and Friedli, T., "The Essence of Three-Phase PFC Rectifier Systems—Part I," *IEEE Transactions on Power Electronics*, vol. 28, no. 1, pp. 176-198, 2013.

[10] Erickson, R. and Maksimovic, D., "Fundamentals of Power Electronics," Norwell, Mass.: Kluwer Academic, chap. 4, 2001.

[11] Friedli, T., Hartmann, M. and Kolar, J. W., "The Essence of Three-Phase PFC Rectifier Systems—Part II, " *IEEE Transactions on Power Electronics*, vol. 29, no. 2, pp. 543-560, Feb. 2014.

[12] Phillips, K. P., "Current-Source Converter for AC Motor Drives, " *IEEE Transactions on Industry Applications*, vol. 8, no. 6, pp. 679-683, 1972.

[13] Schafmeister, F., Herold, S. and Kolar, J. W., "Evaluation of 1200 V-Si-IGBTs and 1300 V-SiC-JFETs for Application in Three-phase Very Sparse Matrix AC-AC Converter Systems," *18th Annual IEEE Applied Power Electronics Conference and Exposition*, Miami Beach, FL, USA, vol. 1, pp. 241-255, 2003.

[14] Bowes, S. R., "Advanced Regular-sampled PWM Control Techniques for Drives and Static Power Converters," *IEEE Transactions on Industrial Electronics*, vol. 42, no. 4, pp. 367–373, 1995.

[15] Bowes, S. R. and Mount, M. J., "Microprocessor Control of PWM Inverters"," *Pro- ceedings B-Electric Power Applications*, vol. 6, no. 128, pp. 293–305, 1981.

[16] Ziogas, P. D., "The Delta Modulation Technique in Static PWM Inverters," *IEEE Transactions on Industry Applications*, vol. 17, no. 2, pp. 199–204, 1981.

[17] Rahman, K. M., Choudhury, M. A., Khan, M. R. and Rahman, M. A. ,"Dual slope integrator type delta modulator for high performance voltage source inverters," *Proceedings of the Power Conversion Conference*, Nagaoka, Vol. 1,pp 451–455,1997.

[18] Patel, H. S. and Hoft, R. G., "Generalized Techniques of Harmonic Elimination and Voltage Control in Thyristor Inverters: Part I–Harmonic Elimination," *IEEE Transactions on Industry Applications* vol.9, no. 3, pp. 310–317, 1973.

[19] Patel, H. S. and Hoft, R. G., "Generalized Techniques ofHarmonic Elimination and Voltage Control in Thyristor Inverters: Part II — Voltage Control Techniques" *IEEE Transactions on Industry Applications* vol. 10, no. 5, pp. 666–673, 1973.

[20] Bowes, S. R., "Novel Real-time Harmonic Minimized PWM Control for Drives and Static Power Converters," *IEEE Transactions on Power Electronics*, vol. 9, no. 3, pp. 256–262, 1994.

[21] Bowes, S. R. and Clark, P. R. , "Regular-sampled Harmonic-elimination PWM Control of Inverter Drives" *IEEE Transactions on Power Electronics* vol. 10, no. 5, pp. 521–531, 1995.

[22] Coursera, "Converter Circuits," URL: https://www.coursera. org/learn/converter-circuits.

[23] Shah, H. A., Shah, S. K. and Patel, R. "DSP based PWM Generation for High Switching Frequency Voltage Source Inverter," *2015 International Conference on Communications and Signal Processing (ICCSP)* pp. 0517–0520, 2015.

[24] Lakka, M., Koutroulis, E. and Dollas, A., "Development of an FPGA-Based SPWM Generator for High Switching Frequency DC/AC Inverters," *IEEE Transactions on Power Electronics*, vol. 29, no. 1, pp. 356–365, 2014.

[25] Rahman, K. M. and Quamruzzaman, M., "A New Hybrid PWM Scheme for Voltage Source Inverters." *2nd International Conference of Electrical and Computer Engineering*, Dhaka, 2002.

[26] Kwon, B. H., and Min, B., "A Fully Software-controlled PWM Rectifier with Current Link, " *IEEE Transactions on Industrial Electronics*, vol. 40, no. 3, pp. 355-363, 1993.

[27] Bojrup, M., "Advanced Control of Active filters in a Battery Charger Application," Ph. D Dissertation, Department of Industrial Electrical Engineering and Automation (IEA), Lund Institute of Technology, Sweden, 1999.

[28] Rahman, K.M., Choudhury, M. A. and Zulfikar, T. A., "An AT89C51 Microcontroller Based Control Circuit for Dual Three Phase Controlled Rectifier," *International Conference on Electrical and Computer Engineering (ICECE)*, Dhaka, 2004.

[29] Fairchild Semiconductor Corporation, "General Purpose 6-Pin Phototransistor Optocouplers" URL: http://www.futurlec.com/LED/4N25a.shtml.

[30] National Semiconductor Corporation, "Low Power Quad Operational Amplifiers," URL: http: //www.futurlec.com/Linear/LM324N.shtml.

[31] Fairchild Semiconductor Corporation, "Micropower Phase-Locked Loop," URL: http://www. futurlec.com/4000Series/CD4046.shtml.

[32] Fairchild Semiconductor Corporation, "12-Stage Ripple Carry Binary Counters," URL: http: //www.futurlec.com/4000Series/CD4040.shtml.

[33] Fairchild Semiconductor Corporation, "8-bit register with clear," URL: http://www.futurlec. com/74LS/74LS273.shtml.

[34] ST Electronics, "512 Kbit (64Kb x8) UV EPROM," URL: http://www.futurlec.com/ Memory/27C512_Datasheet.shtml.

[35] Fairchild Semiconductor Corporation, "Line Data Selector/Multiplexer," URL: http://www. futurlec.com/74LS/74LS273.shtml.

[36] Atmel Corporation, "8-bit AVRMicrocontroller Atmega32A," URL: http://www.futurlec. com/Atmel/ATMEGA32A-PU.shtml.

[37] Fairchild Semiconductor Corporation, "Complementary low voltage transistor," URL: www. st.com/resource/en/datasheet/CD00001225.pdf.

[38] Motorola Inc., "Standard Lead Recovery Rectifiers," URL: http://www.futurlec.com/ Diodes/1N4007.shtml.

[39] International Rectifier, "N Channel HexFET Transistors," URL: http://www.futurlec. com/Transistors/IRFP250.shtml.

[40] International Rectifier, "Switch-mode Power Rectifier," URL: http://www.onsemi.com/ pub/Collateral/MBR30H200CT-D.PDF.